STUDIES OF BASAL CADMIUM RESISTANCE IN *C. ELEGANS*

A Dissertation

Presented to the Faculty of the Graduate School

of Cornell University

In Partial Fulfillment of the Requirements for the Degree of

Doctor of Philosophy

by

Sungjin Kim

August 2014

STUDIES OF BASAL CADMIUM RESISTANCE IN *C. ELEGANS*

Sungjin Kim, Ph.D

Cornell University 2014

Cadmium (Cd) is a highly toxic transition metal that induces DNA damage, generates reactive oxygen species (ROS), and interferes with the antioxidant system. These effects of Cd toxicity can cause diseases in humans including Alzheimer's and Parkinson's diseases and cancers. For the past decades, Cd has been increasingly emitted into our environment via different industrial products thus threatening human health. Although research to elucidate the molecular basis of Cd toxicity has been actively done, comprehensive study of Cd distribution in tissues and cell types in the organisms, and the effect of Cd on the ionome/metallome is poorly understood. In this regard, the nematode worm *Caenorhabditis elegans* is a perfect multicellular model system to study distribution of Cd and its effect on distribution of other elements in tissues and different cells types, e.g. intestinal cells, neurons, coelomocytes, which are affected by heavy metal poisoning in humans. Furthermore, *C. elegans* shares a high degree of conservation of stress-resistance genes, among which is HMT-1/ABCB6. Therefore, one part of my dissertation aims to establish the effect of Cd on the ionome/metallome in *C. elegans*, while another part is focused on analyses of HMT-1 mediated Cd resistance.

Analyses of the effect of Cd on the *C. elegans* ionome/metallome revealed that dietary Cd reduces the concentrations of biologically important elements such as zinc (Zn), copper (Cu), manganese (Mn), cobalt (Co), sulfur (S), potassium (K), iron (Fe), while it increases concentrations of potentially toxic, non-essential elements such as arsenic (As) and rubidium (Rb). Also, in collaboration with Dr. Lydia Finney, using synchrotron based X-ray fluorescence microscopy (SXRF), I showed that Cd accumulates in the intestinal cells and significantly alters the distribution of Fe. Moreover, in collaboration with Dr. Anuj Sharma I found that Zn homoeostasis is essential for basal Cd resistance in *C. elegans*.

Previous work in the Vatamaniuk's lab has shown that HMT-1 is acutely required for resistance to different heavy metals and is expressed in intestinal cells, head and tail neurons and coelomocytes in *C.*

elegans. Unlike canonical, "full-molecule" ABC transporters, HMT-1 is a half-transporter possessing one TMDs and one NBD. In addition, HMT-1 contains a hydrophobic N-terminal extension (NTE) domain. However, how HMT-1 proteins act and what role the NTE domain plays in their function, are not known. I showed that HMT-1 of *C. elegans* exists as an oligomer, and, at a minimum, homodimerizes. In collaboration with Dr. Vatamaniuk, I showed that HMT-1 localizes to the apical recycling endosomes in intestinal cells. In collaboration with Dr. Anuj Sharma, I established that the NTE domain plays an important structural and functional role: it is essential but not sufficient for the ability of HMT-1 to confer Cd tolerance, HMT-1-HMT-1 protein interactions, and targeting of HMT-1 to apical recycling endosomes

Considering that Cd is not bio-degradable and tends to accumulated in theenvironment and the human body, my thesis research might provide novel avenues for the prevention or treatment of humans diseases caused by toxic heavy metal poisoning.

BIOGRAPHICAL SKETCH

Sungjin Kim was born on March, 12 1982 to the proud parents of Kyung-Moo Kim and Mee-kyung Park in South Korea. Because his father Kyung-Moo Kim was a professor in University he also wanted to work in an academic field. Sungjin likes sports especially baseball. He finished his high school in Kyung-pook high school in Daegu, South Korea. After that, he joined Kyung-pook national University in the department of applied biological chemistry. In August 2008, he received bachelor's degree and eventually joined the lab of Olena K Vatamaniuk in Cornell University. With 5 years of hard work, he eventually lead to this dissertation.

ACKNOWLEDGMENTS

I would like to express deep appreciation to my committee chair, Dr. Olena Vatamaniuk, for guiding me through the 5 years at Cornell with her enthusiasm for research and scholarship and for supporting my work. I would also like to thank my committee members Dr. Kemphues and Dr. Liu for their criticism and encouragement and for helping me through difficult times. I would like to extend my gratitude to the graduate field of environmental toxicology for letting me grow as a scientist through discussions and exchange of ideas. I thank Anuj for being my best friend, peer, and mentor, and soul senior Hail, Sheena who share all the joy and bitterness of graduate life, Jiapei for being wonderful lab member. I am also grateful for my wife, Ah-Reum Jeong, and my parents, Kyung Moo Kim and Mi Kyung Park, for always being at my side with endless support.

TABLE OF CONTENTS

LIST OF FIGURES

LIST OF TABLES

CHAPTER 1

INTRODUCTION

Heavy metals and their toxicity

Heavy metals are metallic elements with densities exceeding 5g/m^3. Some heavy metals (*e.g.*, iron [Fe], copper [Cu], manganese [Mn], and zinc [Zn] serve as micronutrients, but are toxic in excess [1]. Non-essential heavy metals (*e.g.* cadmium [Cd], mercury [Hg], lead [Pb]) are potentially highly toxic [1-3]. At the cellular level, the toxicity of heavy metals results from the displacement of endogenous co-factors such as Cu, Zn, Fe from their binding site, thiol-capping of essential proteins and induction of formation of reactive oxygen species (ROS) and inactivation of essential proteins such as p53, a critical tumor suppressor [4] and [3]. These harmful effects cause dysfunction of vital organs, neurodegenerative diseases, and cancer [1, 3, 5]. The half-molecule ATP-binding cassette (ABC) transporter in the nematode worms *Caenorhabditis elegans*, HMT-1 (**h**eavy **m**etal **t**olerance factor 1), is acutely required for Cd and other metals resistance [6]. However, how it exerts resistance to heavy metals is not known.

Cd is a highly toxic compound and OSHA (Occupational Safety & Health Administration) estimates that about 300,000 workers are exposed to Cd in the United States. Cadmium is a component of earth's crust and is usually present in the environment as molecule complexes with other elements such as oxygen, chlorine, or sulfur (either provide reference or the URL link). Although Cd is a naturally occurring element, it is largely released into our environment as manufacturing and consumer wastes. For example, Cd is used in Ni-Cd battery, plastics, fertilizer, pesticides, insecticide, and cigarettes. Cdis considered as one of 126 priority pollutants by the US Environmental Protection Agency. Also, it is regarded as a potent human carcinogen by the International Agency for Research on Cancer (IARC, 1993)[7]. Either short-term or long-term exposure to cadmium can cause serious defects in cardiovascular, renal, gastrointestinal, neurological, reproductive, and respiratory systems [2, 3]. The typical example of Cd toxicity is Itai-Itai disease caused by Cd-contaminated Jinzu River water, which was used for irrigation of rice fields, drinking

water and washing in Japan. Itai-Itai disease is characterized by severe pain, bone fractures, proteinuria and severe osteomalacia which occurred due to misplacement of Ca [8].

The effect of Cd on the homeostasis of other essential metals.

Itai-itai desease is a classic and one of the first examples of the interference of Cd with homeostasis of essential heavy metals. It occurs due to similar ionic properties of Cd with other metal elements that in addition to Ca also include Fe, and Zn [9-14]. It has been also shown that Cd disrupts Cu homeostasis in *Saccharomyces. cerevisiae* by binding to the transcription factor, Mac1, resulting in reduced expression of Mac1p target, a Cu uptake transorter, CTR1p [15]. Furthermore, cross talk between Cd and Cu homeostasis in *Arabidopsis thaliana* has been revealed by showing that Cu homeostasis is essential for basal Cd resistance in this plant species [16]. Besides Cu, it has been well known that in plants Cd also affects the homeostasis of Fe by inhibiting Fe uptake *via* IRT1 (**i**ron **r**egulated **t**ransporter) [12, 17]. Additionally, over expression of FIT1 a master regulator of Fe homeostasis in dicotyledonous plants rescues Cd sensitivity by facilitating vacuolar sequestration of Cd in roots and improving Fe homeostasis in shoots in plants [18]. While the effect of Cd on homeostasis of essential elements has been recognized in yeast and plants, it is not well studied in animal systems. In this regard, as part of my Ph.D project, I studied the effect of Cd on the ionome/metallome and metal distribution in the multicellular organism, *C. elegans.*

Mechanisms of heavy metal detoxification

Current evidence suggests that several heavy metal detoxification mechanisms are shared among different species. These include: 1) Chelation of heavy metals with cellular ligands such as a tripeptide glutathione (GSH) (in all species) and its derivatives, phytochelatins (PCs, primarily in plants, fungi and nematodes) [19-26]. Chelation with cellular ligands prevents heavy metals from binding to sulfhydryl groups in other proteins. In addition, heavy metal-ligand complexes serve as substrates for transporters involved in heavy metal detoxification. 2) Transport of metal ions or metal-ligand complex across

biological membranes. Heavy metals can be either excreted from the cytosol *via* the plasma membrane into the extracellular space or sequestered into endosomal compartments such as vacuoles in plants and fungi, and their analogs, lysosomes, in animals. In many cases, this process is mediated by ATP-binding cassette (ABC) transporters [21, 27]. Predicted ABC transporter mechanism is illustrated in Figure 1.

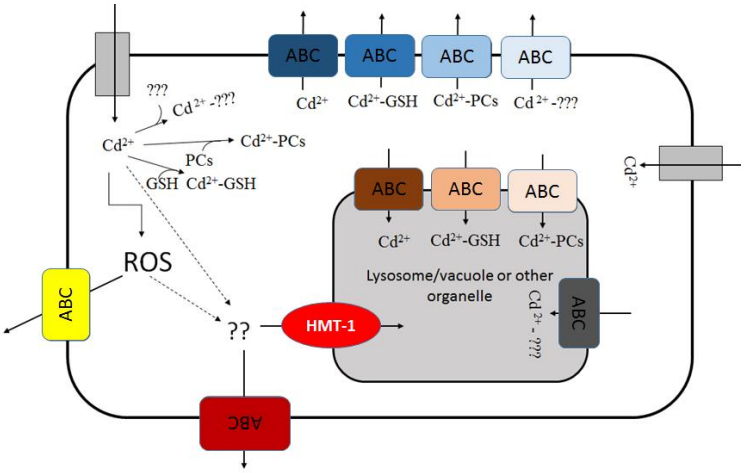

Figure 1. ABC transporter mediated Cd-detoxification. Cd can enter into a cell via unspecific ion channels or transition ions transporters [17]. When Cd enters the cell, it can facilitate formation of reactive oxygen species (ROS), or can be chelated by binding proteins such as cysteine-rich peptide, GSH or GSH derivatives, phytochelatins (PCs), or other unknown metal binding proteins (designated as "???" in the Figure). Detoxification includes ABC transporter-mediated sequestration of Cd ions iand/or Cd-ligand complexes, and/or toxic by-products of Cd toxicity (designated as "??" in the Figure 1) into lysosome/vacuole. Also, Cd can be detoxified by ABC transporter-mediated removal of cytosolic Cd or ROS or Cd-ligand complexes or toxic by-products (??) of Cd toxicity by efflux out of the cell.

3) Scavenging of reactive oxygen species that are by products of heavy metal toxicity. For instance, hydroxyl radicals that are generated by heavy metals such as Cu and Fe *via* Fenton's reaction are removed by the dismutation of superoxide (O_2-) to peroxide (H_2O_2) by superoxide dismutases (SODs), while H_2O_2 is converted to H_2O by glutathione peroxidases or catalases [28]. These molecular mechanisms enable organisms including humans to tolerate heavy metal toxicity, and abnormal cell function will be unavoidable if any of these detoxification mechanisms are disrupted.

ABC transporters are functionally diverse, but share a common structural architecture

HMT-1 belongs to one of the largest membrane protein families, ATP-binding cassette (ABC)

transporters found in most organisms, from microorganisms to humans. Sixty one ABC transporters are found in *C. elegans*, 48 in humans, 57 in *Drosophila*, 103 in *Arabidopsis*, 30 in *Saccharomyces cerevisiae*, and 11 in *Schizosaccharomyces pombe* [29-31]. In *C. elegans,* besides *Ce*HMT-1[32], other ABC transporters, including PGP-5[33] and PGP-1, PGP-3, MRP-1[20] also play roles in Cd resistance.

ABC transporters mediate Mg-ATP-powered translocation of a wide range of substrates across a lipid bilayer and reside on membranes of various cellular organelles [21, 25, 27, 34, 35]. Although ABC transporters are functionally diverse, they share a common architecture. Typically, functional ABC transporters consist of two TMD (transmembrane domains) and two NBD (nucleotide binding domain) are called "full-molecule "ABC transporters. In addition to "full-molecule" ABC transporters, half-molecule ABC transporters contain only one TMD and one NBD. The TMD domains are composed of 4 to 6 membrane-spanning α-helices forming a transmembrane channel for translocation of substances across the lipid bilayer. NBDs are located at the cytosolic surface of the membrane, bind and hydrolyze ATP to energize the transport of substrate molecules. Either full-molecule or half-molecule ABC transporters can possess a hydrophobic N-terminal extension domain termed NTE. The NTE domain consists of 5 to 6 membrane spans (TMD0) and a cytosolic linker (L0), which connects the NTE domain with core domains of ABC transporters (TMDs or NBDs) [26, 30, 32, 35]. However, not all ABC transporters have the NTE domain. In fact, HMT-1-like proteins are the only half-molecule ABC transporters that contains the NTE domain. This feature distinguishes HMTs from other family members and allows the identification of HMT-1 homologs in diverse organisms including humans.

Half-molecule ABC transporters form homo- or hetero-oligomeric protein complexes

Evidence from the X-ray structure analysis of bacterial ABC proteins shows that function of ABC transporters requires at least two NBDs [35, 36]. This configuration appears to be necessary for binding and hydrolysis of ATP to mediate ATP-powered translocation of substrates through the lipid bilayer. [30, 36]. Therefore, two TMD and two NBD are required for the functional ABC transporter. This four-domain

structure of ABC transporters can be formed from a single polypeptide or by the association of two or four separate subunits [30]. In eukaryotes, most full-molecule ABC proteins are encoded as single polypeptides composed of two TMDs and two NBDs [37]. In contrast, half-molecule ABC transporters function by forming homo- or hetero-oligomer complexes with various subunits. For instance, the peroxisomal half transporter, ALDP (ABCD1) can homodimerize or heterodimerize with other half ABC transporters, ALDPR (ABCD2) or PMP70 (ABCD3) [31]. Also, mammalian half-transporters TAP1 and TAP2 form heterodimers to transport peptide degradation products from the cytosol into the lumen of the endoplasmic reticulum [38-40]. The sterol half-transporter ABCG5 and ABCG8 must heterodimerize in order to get to the cell surface [41]. Interestingly, some full-molecule ABC transporters oligomerize as well: for instance, human ABCC1/MRP1, with two TMDs, two NBDs and an NTE, forms functional homodimer regulated by the NTE domain [42]. Whether the half-transporter HMT-1 interacts only with itself or forms functional heterocomplexes with other ABC transporter and cellular proteins, or both, is not known.

HMT-1 confers heavy metal tolerance, but the mechanism of its function is unknown.

HMT-1 was first discovered in *S. pombe* in mutant screens for components of the phytochelatin (PC)-mediated heavy metal resistance [25]. PCs are cysteine-rich peptides derived from GSH, and are synthesized in the cytosol in the presence of heavy metals by phytochelatin synthases (PCSs) [43, 44]. Based on *in vitro* transport assays in *S. pombe*, it has been proposed that HMT-1 proteins are involved in the PC-dependent heavy metal resistance and transport PC-Cd complexes into the vacuole, a lysosomal-like compartment of yeast and plant cells[45, 46]. However, our genetic studies in *C. elegans* showed that *HMT-1* and *PCS-1* do not operate in a linear metal resistance pathway [32]. We also found that HMT-1 of *Drosophila melanogaster*, an organism that lacks a PC synthase homolog in its genome, rescues Cd sensitivity of the *S. pombe hmt1* mutant [29]. Consistently, subsequent studies have shown that *Ce*HMT-1 rescued Cd sensitivity in *S. cerevisiae* cells that are devoid of PC synthase homologs as well [47]. Together, these results suggested that HMT-1 proteins may not transport PCs and contribute to Cd resistance by

another, unknown mechanism.

It has been reported that HMT-1 homologs from human hABCB6 and rat rABCB6 localize to different organelles by different research groups. hABCB6 was shown to localize on the mitochondrial and plasma membrane playing a role in porphyrin homeostasis, whereas rAbcb6 was shown to localize to vesicles and plasma membrane and involved in transitional metal homeostasis.[22, 48] A recent report again challenged a new theory that hABCB6 localize to membrane of mitochondria, lysosomes and plasma membrane [49]. However, the localization of HMT-1 in *C. elegans* is not known.

C. elegans as a model system for studies of Cd toxicity and ion homeostasis.

Although significant progress has been made in analyzing Cd and other heavy metal toxicities and detoxification mechanisms using diverse cellular models, *C. elegans* is a non-mammalian model system that provides the advantage of addressing these questions at a multicellular level. It provides the means for gaining an integrated understanding of subcellular, cell type and tissue distribution pattern of Cd, its effect on the metallome as related to diseases caused by metal imbalance and toxicity, and the roles in these processes of transport proteins with conserved function in heavy metal resistance, such as HMT-1. The advantages of *C. elegans* are: 1) *It* has highly differentiated muscular, nervous, digestive and reproductive systems, which are tissues that are affected by heavy metal poisoning in humans. 2) *It* is comprised of only 959 optically transparent somatic cells, enabling manipulation and observations at a single-cell resolution. 3) HMT-1 function in heavy metal resistance is highly conserved across the species tested. 4) The plethora of powerful genetic resources in *C. elegans* in combination with sophisticated analytical tools such as used here, will allow the full exploitation of the system for discoveries in metal biology.

Based on the above information, the goals of my study were: 1) learn how HMT-1 contributes to Cd resistance by analyzing its oligomeric status and its subcellular localization, 2) learn the function of the NTE domain of HMT-1 and the effect of Cd on the HMT- localization pattern, 3) learn the effect of Cd on the ionome (alias metallome) of *C. elegans*.

Considering that HMTs are highly conserved and the highly toxic effect of Cd in humans a thorough elucidation of the molecular mechanisms of the HMT-1 dependent resistance of Cd in *C. elegans* will provide critical mechanistic insights into the HMT-1-dependent heavy metal resistance pathway in diverse organisms, and will have important implications for future therapeutic developments aiming to alleviate heavy metal-related pathologies in humans.

REFERENCES

1. Waalkes, M.P., T.P. Coogan, and R.A. Barter, *Toxicological principles of metal carcinogenesis with special emphasis on cadmium.* Crit Rev Toxicol, 1992. **22**(3-4): p. 175-201.
2. Waalkes, M.P., *Cadmium carcinogenesis.* Mutat Res, 2003. **533**(1-2): p. 107-20.
3. Waalkes, M.P., *Cadmium carcinogenesis in review.* J Inorg Biochem, 2000. **79**(1-4): p. 241-4.
4. Waisberg, M., et al., *Molecular and cellular mechanisms of cadmium carcinogenesis.* Toxicology, 2003. **192**(2-3): p. 95-117.
5. Waalkes, M.P., S. Rehm, and M.G. Cherian, *Repeated cadmium exposures enhance the malignant progression of ensuing tumors in rats.* Toxicol Sci, 2000. **54**(1): p. 110-20.
6. Schwartz, M.S., et al., *Detoxification of multiple heavy metals by a half-molecule ABC transporter, HMT-1, and coelomocytes of Caenorhabditis elegans.* PLoS One, 2010. **5**(3): p. e9564.
7. Vanchieri, C., *IARC publishes data on worldwide cancer cases. International Agency for Research on Cancer.* J Natl Cancer Inst, 1993. **85**(13): p. 1028-9.
8. Murata, I., et al., *Cadmium enteropathy, renal osteomalacia ("Itai Itai" disease in Japan).* Bull Soc Int Chir, 1970. **29**(1): p. 34-42.
9. Wu, Y., et al., *Biosorption of heavy metal ions (Cu(2+), Mn (2+), Zn (2+), and Fe (3+)) from aqueous solutions using activated sludge: comparison of aerobic activated sludge with anaerobic activated sludge.* Appl Biochem Biotechnol, 2012. **168**(8): p. 2079-93.
10. Bergeron, P.M. and C. Jumarie, *Reciprocal inhibition of Cd(2+) and Ca(2+) uptake in human intestinal crypt cells for voltage-independent Zn-activated pathways.* Biochim Biophys Acta, 2006. **1758**(6): p. 702-12.
11. Clemens, S., et al., *The plant cDNA LCT1 mediates the uptake of calcium and cadmium in yeast.* Proc Natl Acad Sci U S A, 1998. **95**(20): p. 12043-8.
12. Eide, D., et al., *A novel iron-regulated metal transporter from plants identified by functional expression in yeast.* Proc Natl Acad Sci U S A, 1996. **93**(11): p. 5624-8.
13. Vesey, D.A., *Transport pathways for cadmium in the intestine and kidney proximal tubule: focus on the interaction with essential metals.* Toxicol Lett, 2010. **198**(1): p. 13-9.
14. Thevenod, F., *Catch me if you can! Novel aspects of cadmium transport in mammalian cells.* Biometals, 2010. **23**(5): p. 857-75.
15. Heo, D.H., et al., *Cadmium regulates copper homoeostasis by inhibiting the activity of Mac1, a transcriptional activator of the copper regulon, in Saccharomyces cerevisiae.* Biochem J, 2010. **431**(2): p. 257-65.
16. Gayomba, S.R., et al., *The CTR/COPT-dependent copper uptake and SPL7-dependent copper deficiency responses are required for basal cadmium tolerance in A. thaliana.* Metallomics, 2013. **5**(9): p. 1262-75.
17. Vert, G., et al., *IRT1, an Arabidopsis transporter essential for iron uptake from the soil and for plant growth.* Plant Cell, 2002. **14**(6): p. 1223-33.
18. Wu, H., et al., *Co-overexpression FIT with AtbHLH38 or AtbHLH39 in Arabidopsis-enhanced cadmium tolerance via increased cadmium sequestration in roots and improved iron homeostasis of shoots.* Plant Physiol, 2012. **158**(2): p. 790-800.

19. Hanikenne, M., R.F. Matagne, and R. Loppes, *Pleiotropic mutants hypersensitive to heavy metals and to oxidative stress in Chlamydomonas reinhardtii.* FEMS Microbiol Lett, 2001. **196**(2): p. 107-11.
20. Broeks, A., et al., *Homologues of the human multidrug resistance genes MRP and MDR contribute to heavy metal resistance in the soil nematode Caenorhabditis elegans.* EMBO J, 1996. **15**(22): p. 6132-43.
21. Ghosh, M., J. Shen, and B.P. Rosen, *Pathways of As(III) detoxification in Saccharomyces cerevisiae.* Proc Natl Acad Sci U S A, 1999. **96**(9): p. 5001-6.
22. Jalil, Y.A., et al., *Vesicular localization of the rat ATP-binding cassette half-transporter rAbcb6.* Am J Physiol Cell Physiol, 2008. **294**(2): p. C579-90.
23. Leslie, E.M., A. Haimeur, and M.P. Waalkes, *Arsenic transport by the human multidrug resistance protein 1 (MRP1/ABCC1). Evidence that a tri-glutathione conjugate is required.* J Biol Chem, 2004. **279**(31): p. 32700-8.
24. Li, Z.S., et al., *A new pathway for vacuolar cadmium sequestration in Saccharomyces cerevisiae: YCF1-catalyzed transport of bis(glutathionato)cadmium.* Proc Natl Acad Sci U S A, 1997. **94**(1): p. 42-7.
25. Ortiz, D.F., et al., *Heavy metal tolerance in the fission yeast requires an ATP-binding cassette-type vacuolar membrane transporter.* EMBO J, 1992. **11**(10): p. 3491-9.
26. Rea, P.A., *Plant ATP-binding cassette transporters.* Annu Rev Plant Biol, 2007. **58**: p. 347-75.
27. Prasad, R. and A. Goffeau, *Yeast ATP-binding cassette transporters conferring multidrug resistance.* Annu Rev Microbiol, 2012. **66**: p. 39-63.
28. McCord, J.M. and I. Fridovich, *Superoxide dismutase: the first twenty years (1968-1988).* Free Radic Biol Med, 1988. **5**(5-6): p. 363-9.
29. Sooksa-Nguan, T., et al., *Drosophila ABC transporter, DmHMT-1, confers tolerance to cadmium. DmHMT-1 and its yeast homolog, SpHMT-1, are not essential for vacuolar phytochelatin sequestration.* J Biol Chem, 2009. **284**(1): p. 354-62.
30. Higgins, C.F., *ABC transporters: from microorganisms to man.* Annu Rev Cell Biol, 1992. **8**: p. 67-113.
31. Liu, L.X., et al., *Homo- and heterodimerization of peroxisomal ATP-binding cassette half-transporters.* J Biol Chem, 1999. **274**(46): p. 32738-43.
32. Vatamaniuk, O.K., et al., *CeHMT-1, a putative phytochelatin transporter, is required for cadmium tolerance in Caenorhabditis elegans.* J Biol Chem, 2005. **280**(25): p. 23684-90.
33. Kurz, C.L., et al., *Caenorhabditis elegans pgp-5 is involved in resistance to bacterial infection and heavy metal and its regulation requires TIR-1 and a p38 map kinase cascade.* Biochem Biophys Res Commun, 2007. **363**(2): p. 438-43.
34. Mason, D.L. and S. Michaelis, *Requirement of the N-terminal extension for vacuolar trafficking and transport activity of yeast Ycf1p, an ATP-binding cassette transporter.* Mol Biol Cell, 2002. **13**(12): p. 4443-55.
35. Rees, D.C., E. Johnson, and O. Lewinson, *ABC transporters: the power to change.* Nat Rev Mol Cell Biol, 2009. **10**(3): p. 218-27.
36. Smith, P.C., et al., *ATP binding to the motor domain from an ABC transporter drives formation of a nucleotide sandwich dimer.* Mol Cell, 2002. **10**(1): p. 139-49.
37. Jones, P.M. and A.M. George, *Subunit interactions in ABC transporters: towards a functional architecture.* FEMS Microbiol Lett, 1999. **179**(2): p. 187-202.

38. Abele, R. and R. Tampe, *The ABCs of immunology: structure and function of TAP, the transporter associated with antigen processing.* Physiology (Bethesda), 2004. **19**: p. 216-24.
39. Russ, G., et al., *Assembly, intracellular localization, and nucleotide binding properties of the human peptide transporters TAP1 and TAP2 expressed by recombinant vaccinia viruses.* J Biol Chem, 1995. **270**(36): p. 21312-8.
40. Taylor, J.C., et al., *The multidrug resistance P-glycoprotein. Oligomeric state and intramolecular interactions.* J Biol Chem, 2001. **276**(39): p. 36075-8.
41. Graf, G.A., et al., *ABCG5 and ABCG8 are obligate heterodimers for protein trafficking and biliary cholesterol excretion.* J Biol Chem, 2003. **278**(48): p. 48275-82.
42. Yang, Y., et al., *Regulation of function by dimerization through the amino-terminal membrane-spanning domain of human ABCC1/MRP1.* J Biol Chem, 2007. **282**(12): p. 8821-30.
43. Grill, E., E.L. Winnacker, and M.H. Zenk, *Phytochelatins: the principal heavy-metal complexing peptides of higher plants.* Science, 1985. **230**(4726): p. 674-6.
44. Vatamaniuk, O.K., et al., *AtPCS1, a phytochelatin synthase from Arabidopsis: isolation and in vitro reconstitution.* Proc Natl Acad Sci U S A, 1999. **96**(12): p. 7110-5.
45. Vatamaniuk, O.K., et al., *Phytochelatin synthase, a dipeptidyltransferase that undergoes multisite acylation with gamma-glutamylcysteine during catalysis: stoichiometric and site-directed mutagenic analysis of arabidopsis thaliana PCS1-catalyzed phytochelatin synthesis.* J Biol Chem, 2004. **279**(21): p. 22449-60.
46. Ortiz, D.F., et al., *Transport of metal-binding peptides by HMT1, a fission yeast ABC-type vacuolar membrane protein.* J Biol Chem, 1995. **270**(9): p. 4721-8.
47. Kim, S., D.S. Selote, and O.K. Vatamaniuk, *The N-terminal extension domain of the C. elegans half-molecule ABC transporter, HMT-1, is required for protein-protein interactions and function.* PLoS One, 2010. **5**(9): p. e12938.
48. Paterson, J.K., et al., *Human ABCB6 localizes to both the outer mitochondrial membrane and the plasma membrane.* Biochemistry, 2007. **46**(33): p. 9443-52.
49. Kiss, K., et al., *Shifting the paradigm: the putative mitochondrial protein ABCB6 resides in the lysosomes of cells and in the plasma membrane of erythrocytes.* PLoS One, 2012. **7**(5): p. e37378.

CHAPTER 2

CADMIUM ALTERS IONOME AND PROMOTES THE RE-DISTRIBUTION OF IRON IN INTESTINAL CELLS OF *C. ELEGANS*

Introduction

Cadmium (Cd) is a highly toxic transition metal element raising environmental concerns due to its toxicological effects and bioaccumulation features. Although Cd is a component of the earth's crust, it is increasingly emitted into our environment as industrial and consumer wastes, from manufacturing of nickel-Cd batteries, pigments for paints and production of plastic, fertilizers, pesticides, insecticides, etc. [1]. Cd is listed as number seven of 126 priority pollutant by the US Environmental Protection Agency [2], and has been classified as a human carcinogen by International Agency for Research on Cancer (IARC, 1993). Chronic exposure to Cd has been implicated in induction of lung, prostate, kidney and pancreas cancer [1, 3, 4]. Cd enters human body mainly through food, water and air. The classic example of the penetration of Cd into the food chain and associated health disorders is the Itai-Itai disease, characterized by severe pain, bone fractures, proteinuria and severe osteomalacia, that occurred in the Jinzu River basin in Japan [5]. At the cellular level, Cd toxicity results from thiol capping of essential proteins, DNA damage due to interference with function of the DNA repair processes, apoptotic events, and interference with the antioxidant defense system, resulting in the generation of reactive oxygen species (ROS) [1, 3, 4, 6-8]. Further, Cd inactivates essential metalloenzymes through its ability to replace endogenous metal co-factors from their binding sites [2].

Cd absorption can be mediated by transporters and channels for essential elements (*e.g.* iron [Fe], zinc [Zn], calcium [Ca] and manganese [Mn]) due to either the broad substrate specificity of the transporter, or the similar ionic properties of essential and nonessential heavy metals [9-15]. For example in rodents, the intestinal absorption of Cd is mediated by DMT-1, a divalent metal transporter that localizes to the apical membrane of enterocytes lining the small intestine [16] In *Arabidopsis thaliana*, a low specificity

iron transporter from the ZIP family, IRT1, is the main entry point of Cd from the soil into the plant roots [17, 18]. Moreover, it is well established that when different dietary metals exist in a mixture, they may act independently or interact with each other to render synergic or additive, or antagonistic effects. An antagonistic interactions between Zn and Cd with respect to their absorption and accumulation has been reported in plants [19]. It has been also shown that Cd treatment results in increased levels of Zn and Cu in the rat glial cell line C6, and that cells exhibit defects such as increased apoptosis, lipid peroxidation, and DNA damage [20]. Also, Cd disrupts Cu homeostasis *in Saccharomyces cerevisiae* by binding to the transcriptions factor, Mac1 [21]. This result in reduced expression of the MAC1 downstream target *CTR1*, encoding a copper uptake transporter [21]. Studies in plants have shown that Cd alters homeostasis of iron (Fe) and copper (Cu) [22, 23]. Also, Cd mimics the transcriptional response caused by Fe and Cu deficiency [23, 24]. Thus, it is increasingly recognized that Cd competes with the essential elements for the uptake into cells and therefore, Cd toxicity and accumulation could be accompanied by metal imbalance in living organisms [25-30]. It is noteworthy that metal imbalance in cells and tissues is regarded as a cause of a number of diseases, among which the most prominent are Alzheimer's and Parkinson's neurodegenerative disorders [31-33]. How Cd affects the balance and the distribution of essential elements, however, is unknown.

Here, I, in collaboration with Dr. Anuj Sharma, used a nematode worm *Caenorhabditis elegans* (*C. elegans*), as a non-mammalian multicellular model system and inductively-coupled plasma-mass spectrometry (ICP-MS) to study the effect of Cd on the metallome. I also used synchrotron based X-ray fluorescence microscopy (XFM) to determine the distribution of Cd and its effect on the distribution of other elements. I discovered that exposure to Cd decreased the concentration of biologically essential trace elements such as Zn, Mn, Cu, Fe, Co, while it increased the concentration of potentially toxic elements such as As, Rb. Also, using XFM, we found that Cd accumulates in punctate structures throughout the intestinal cells in *C. elegans* and that Cdsignificantly alters distribution pattern of Fe. We also established that Zn homeostasis and Zn uptake are essential for basal Cd resistance in *C. elegans*.

Results

Ionome of wild-type *C. elegans*.

To learn the impact of Cd exposure to the *C. elegans* ionome, we first determined the normal concentration of 20 elements including essential macro- and micronutrients and nonessential, potentially toxic elements in wild-type N2 worms. To allow detection of trace metals (*e.g.* copper [Cu], manganese [Mn], nickel [Ni], cobalt [Co], selenium [Se]) as well as potentially toxic elements (*e.g.* arsenic [As], rubidium [Rb]), we supplemented the nematode growth medium (NGM) with concentrations (500 ppb) that would not affect growth of N2 worms. We refer to this medium as supplemented NGM (sNGM). ICP-MS analysis revealed that accumulation of various elements varied over several orders of magnitude depending on the element and its function as a macro- or micronutrient. For example, worms accumulated 10,883.5 ± 787.9 ppm of the macronutrient P but 72-fold less of the micronutrient Cu (149.7 ± 13.0 ppm) and 9,302-fold less of a micronutrient Co (1.17 ± 0.2 ppm) as compared to P (Table 1).

Table 1. Concentration of elements in wild-type (N2) *C. elegans* grown under control conditions. Data represent mean values ± S.E. from 4 independent experiments.

Element	Concentration, ppm in worm body	Concentration, ppm in media
Al	36.9 ± 4.7	0.500
As	19.4 ± 0.4	1
Ca	2124.8 ± 259.5	75.2
Cd	0.27 ± 0.01	43.2
Cl	623.8 ± 47.6	2104.7
Co	1.17 ± 0.2	0.05
Cu	149.7 ± 13.0	4
Fe	209.4 ± 13.4	2.9
K	7147.7 ± 262.2	1069.6
Mg	1204.9 ± 88.0	90.6
Mn	347.7 ± 39.4	8.3
Mo	0.46 ± 0.02	1
Na	467.7 ± 26.9	1351.2
Ni	1.26 ± 0.17	0.4
P	10883.5 ± 787.9	775
Rb	1.02 ± 0.02	0.4
S	3818.0 ± 200.1	23.55
Se	48.7 ± 5.6	5
Sr	14.2 ± 1.7	0.4
Zn	350.2 ± 34.4	7.26

As would be expected for non- essential and toxic element Cd, its concentration in worms was the lowest (0.27 ± 0.01 ppm). In contrast, the concentration of another non-essential and toxic element As was higher than that of several established micronutrients or beneficial elements such as Ni, Co and Mo (Table 1). The overall accumulation pattern was in the following rank order (from highest to lowest accumulation): P > K > S > Ca > Mg > Cl > Na > Zn > Mn > Fe > Cu > Se > Al > As > Sr > Ni ≥ Co > Rb > Mo > Cd (Table 1).

Comparison of concentrations of these elements in *C. elegans vs*. their levels in the growth medium has shown that Cl, Na and Mo accumulated to only 30%, 35% and 46% of the media levels suggesting that these elements were largely excluded from worms (Table 1). The concentration of other analyzed elements including toxic As and Cd were from 19 to 160-fold higher than in the growth medium, suggesting the existence of mechanisms for their accumulation and intracellular retention in worms.

Cadmium alters accumulation of mineral elements in *C. elegans*.

To determine the effect of Cd on *C. elegans* ionome, accumulation of different elements in wild-type (N2) worms grown on sNGM plates was compared to the ionome of worms grown on medium supplemented with 5 or 50 μM $CdCl_2$. The lower concentration of Cd was chosen because our past studies showed that Cd at 5 μM does not alter growth and development of the wild-type but is the highest concentration that could be tolerated by *hmt-1* mutants [34, 35]. Cadmium at 50 μM was chosen because it is the concentration from which we might obtain the best result of Cd toxicity since it is the highest concentration tolerated by the wild-type worms with minimum signs of toxicity manifested by a 10-20% decrease in the number of worms that have reached the adult stage of development after 3.5 days of growth in the medium with Cd [34, 35].

Dr. Anuj Sharma found that exposure of worms to Cd not only led to its internal accumulation but significantly altered the *C. elegans* ionome. Especially notable was a significant decrease of the concentration of essential elements such as Zn, Mn, Cu, Ca, Co, (Figure 1).

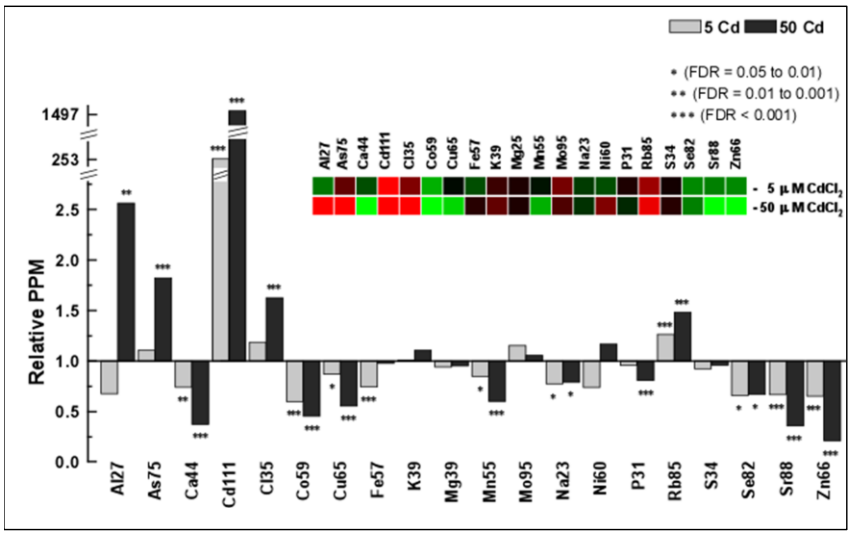

Figure 1. ICP-MS-based analysis of the effect of Cd on accumulation of essential elements in the wild-type (n=4). Worms were grown on NGM-plates supplemented with mineral elements(refer to as sNGM) and with or without $CdCl_2$ at the indicated concentrations. Difference between control *vs.* Cd-treated

conditions is presented as ratio. Control conditions are designated as 1. For generating heat maps (inset), ratio values were log2 transformed and heatmaps were generated using the Matrix2png program [36]. Note that error bars are very small and are not visible.

In contrast, accumulation of potentially toxic elements such as As and Rb significantly increased (Figure 1). I regarded these changes in the internal ion accumulation of Cd-treated worms as an ionomic signature of Cd toxicity. These results provide the first evidence of the effect of Cd on the ionome/metallome in a multicellular organism. I hypothesize that sensitivity of worms to Cd results not only from the increased Cd accumulation but also from its effect on the ion balance.

Zn homeostasis is essential for basal Cd resistance in *C. elegans*.

ICP-MS-based studies described above (Figure 1) suggest that in addition to over-accumulation of Cd, the decreased accumulation of essential elements and increased accumulation of toxic elements in Cd-grown worms might contribute to Cd toxicity. If this suggestion is correct then the additional supplementation of the sNGM medium with essential elements (*e.g.* Zn and/or Cu) might alleviate or decrease Cd toxicity symptoms. To test our predictions Dr. Anuj Sharma and I grew wild-type worms on the medium with increasing levels of added Zn or Cd, or with Zn and Cd added simultaneously. The reason I chose to add Zn and Cu is that both elements are critical micronutrient needed in cells and past studies have been shown to exhibit synergic or additive, or antagonistic effects with Cd [19, 20, 37, 38]. Cd toxicity was evaluated by the ability of worms to reach the adult stage and internal morphological changes as previously described [35]. Dr Anuj Sharma and I found that while 100% of wild-type worms have reached the adult stage after 3.5 days of growth on NGM plates without Cd, their development was significantly delayed in the presence of Cd with only 82 ± 1.5% and 30 ± 5.4% of worms reaching the adult stage by 3.5 days on plates supplemented with 50 µM or 75 µM $CdCl_2$, respectively. It is noteworthy that prolonged incubation of worms at higher (75 µM) concentration of $CdCl_2$ led to development of necrotic lesions in intestinal cells (Figure 2 D).

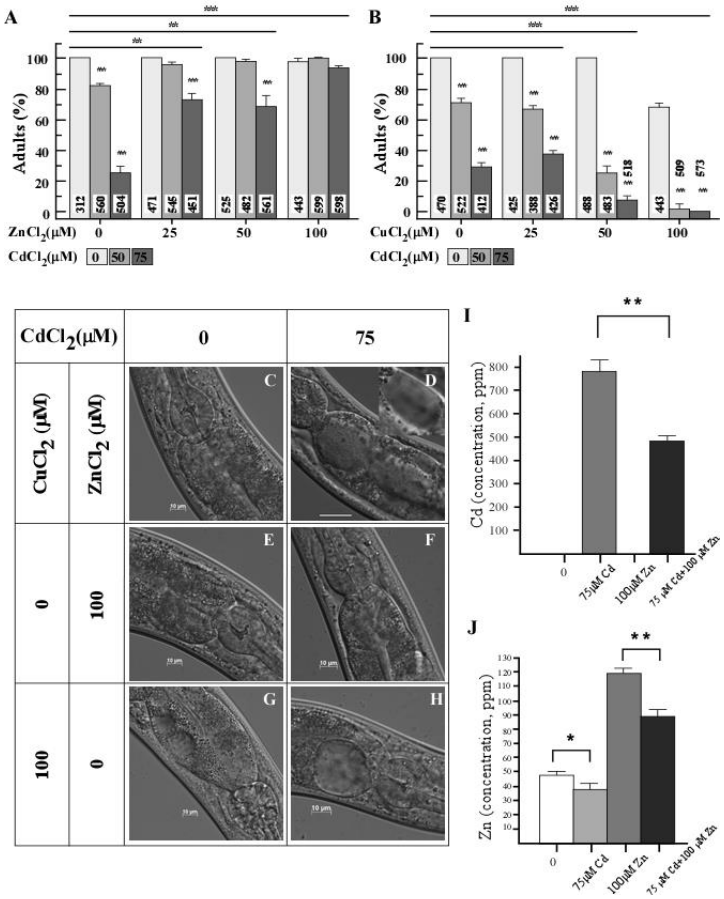

Figure 2. Zn rescues while Cu increases Cd toxicity of worms. A. Percentage of worms that reached the adult stage after 3.5 days of growth in the presence of the indicated concentrations of $CdCl_2$ and $ZnCl_2$ in the NGM medium. **B.** Percentage of worms that reached the adult stage after 3.5 days of growth in the presence of the indicated concentrations of $CdCl_2$ and $CuCl_2$ in the NGM medium. (**C** to **H)** Differential interference contract (DIC) micrographs of intestinal cells of 5-day-old worms grown as described in **A** and **B** under indicated concentrations of $CdCl_2$, $ZnCl_2$ or $CdCl_2$. Concentration of Cd (**I**) and Zn (**J**) was analyzed by ICP-MS in worms grown as described in the Figure **A**. "75μM Cd" on X-axis of the graph(I and J) indicates the worms grown on NGM supplemented with 75 μM Cd, "100 μM Zn" on X-axis of the graph (I and J) indicates the worms grown on NGM supplemented with 100μM Zn,"75 μM Cd+100 μM Zn" on X-axis of the graph (I and J) means worms were grown on NGM supplemented with 75 μM Cd and 100 μM Zn Statistically significant differences are indicated with asterisks (*, $p \leq 0.05$; ** $p \leq 0.01$).

In contrast to Cd, the supplementation of the NGM medium with $ZnCl_2$ at 25, 50 or 100 μM did not affect growth or morphology of worms (Figure 2A, E). Importantly, Zn, added to the medium simultaneously with Cd rescued Cd-caused growth and morphology defects of worms (Figure 2 F). The most effective concentration of zinc that fully rescued 75 μM Cd-caused growth defects was 100 μM. The ability of Zn to rescue Cd sensitivity phenotypes of worms can be interpreted using two scenarios: 1) Extra Zn competes

with Cd for the uptake and thus, Zn decreases the internal concentration of Cd while increasing the internal concentration of Zn; 2) Zn and Cd are taken up independently and extra Zn is needed for the protection of Zn-requiring cellular functions (*e.g.* enzymes that use Zn as a cofactor) from Cd. To test, which of these, not mutually exclusive scenarios, operate in *C. elegans*, I analyzed Zn and Cd concentrations in worms that were grown with Cd, or Zn, or with both transition metals simultaneously. Consistent with our previous findings (Figure 1), Cd accumulation in worms was accompanied by the decrease in the internal concentration of Zn (Figure 2 J). I also found that Zn supplementation decreased Cd accumulation in worms by 0.62-fold in comparison with worms that were grown only in the presence of Cd, suggesting that Zn and Cd uptake pathways, in part, overlap (Figure 2 I). Consistent with this suggestion, Zn concentration in Cd treated worms was 0.74-fold lower than in worms grown in the presence of Zn without Cd (Figure 2 J). Nevertheless, Zn concentration was 1.85-fold higher in worms grown with Zn and Cd simultaneously than in worms grown under control conditions (Figure 2 J). These results favor the conclusion that Zn homeostasis is important for basal Cd resistance in *C. elegans* through the ability of Zn to decreased internal Cd concentration due to competition for the uptake but also through the protection of the internal Zn-requiring cellular functions (*e.g.* enzymes that use Zn as a cofactor).

Cu increases Cd-caused toxicity symptoms in *C. elegans*

Dr. Anuj Sharma and I then tested if supplementing the NGM medium with Cu would also rescue Cd-caused toxicity. We grew worms either with increasing concentrations of Cu, or Cd or with both transition elements simultaneously. We found that while supplementing NGM medium with lower concentrations of Cu (25 and 50 µM) did not affect growth and cellular morphology of worms, higher concentration of Cu (100 µM) delayed their development and caused necrosis of intestinal cells even in medium devoid of Cd (Figure 2B, G). Furthermore, when Cu and Cd were added simultaneously, Cu exacerbated Cd toxicity; significantly decreased numbers of worms reached the adult stage and we observed more severe necrosis of intestinal cells (Figure 2B, H). Our finding that the supplementation of the NGM

medium with Cu exacerbates Cd toxicity was not entirely surprising since excess Cu is toxic to cells due to its ability to promote the formation of free radicals [8]. It is likely that the increased Cd sensitivity of worms treated with Cu (Figure 2B, G, H) results from damaging effect of excess Cu ions. Based on these results I suggest that the decreased Cu accumulation in Cd-cultured worms (Figure 1) serves a protective function.

Cd not only affects the concentration but also changes the distribution pattern of trace elements

The ICP-MS-based study descried above enabled us to quantify concentrations of different elements, including Cd, and the effect of Cd on the balance of physiologically relevant, as well as potentially toxic metals. While these analyses are very informative, they do not provide information about the spatial distribution of Cd and its effect on the spatial distribution of other elements. It is possible, however, that spatial distribution of Cd and its effect on the distribution of other elements might be among the underappreciated bases for Cd-caused diseases. In this regard, it is noteworthy that Alzheimer's and Parkinson's neurodegenerative disorders involve abnormal accumulation of transition metals in brain tissue [31].

To analyze the spatial distribution of Cd and other elements in worms I employed X-ray fluorescence microscopy (XRFM), which has become a method of choice for visualizing the distribution of transition metals *in situ* [39-43]. XFM based techniques have the unique advantage of combining great elemental sensitivity, the ability to analyze nearly all elements of the periodic table simultaneously with the ability to image whole, unsectioned cells, as well as comparatively thick tissue sections, at high sensitivity and high spatial resolution [39-42]. This is particularly well suited for analyses of elemental distribution in worms since they are quite thick (the adult worm is ~200 nm in diameter). I grew wild-type N2 worms for 24h with or without 50 μM Cd and subjected them to XFM analyses. In collaboration with Dr. Lydia Finney I found that in both control worms and worms expose to high levels of Cd the bulk of Cd was localized in intestinal cells where it exhibited a punctate distribution with peaks in the vicinity of nucleus-like structures (Figure 3 A).

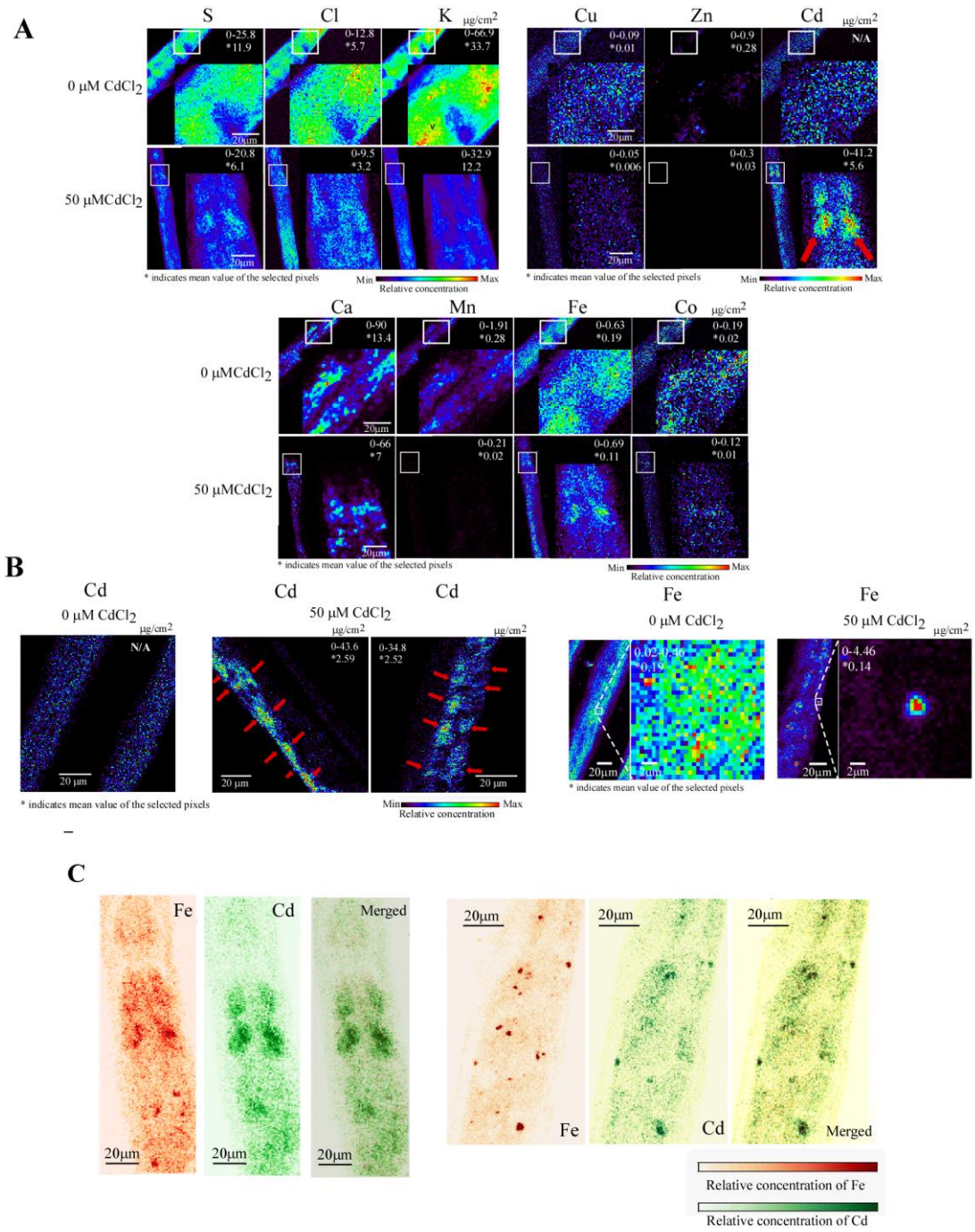

Figure 3. X-ray fluorescence microscopy (XRFM) shows that Cd alters the concentration and the distribution of essential elements. A. The first two intestinal cells near the pharynx were selected to visualize the concentration and the distribution of Cd and its effect on the concentration and spatial distribution of other elements including sulfide (S), chloride (Cl), potassium (K) , copper (Cu), zinc (Zn), calcium (Ca), manganese (Mn), iron (Fe), Cobalt (Co). The value indicated on the top right corner represents the minimum to maximum concentration (μg/cm^2) of the selected area. The asterisk (*)

represents the average concentration of the selected pixels of the indicated element. The scale bar in the lower right corner represents 20 µm. **B.** The magnified view of the distribution of Fe and Cd so that the scale bar is 2µm. **C.** Individual and merged images of Fe, Cd.

Consistent with the results from the ICP-MS study (Figure 1), Cd exposure correlated with a decreased concentration of biologically essential elements Ca, Cu, Zn, Mn, Co (Figure 3 A). In addition, concentration of S, K, Cl was also reduced in Cd grown, *vs.* control worms (Figure 3 A). While Cd did not alter the spatial distribution of the majority of analyzed elements, profound differences were found in the spatial distribution of Fe (Figure 3 B). While Fe was localized evenly at low concentrations through the entire intestine in worms grown under control conditions, Fe accumulated to a high concentration in discrete structures resembling the nucleus of intestinal cells (Figure 3 B). Furthermore, large portion of Fe and Cd co-accumulated in intestinal cells. Considering the thiophilicity of Cd, it is possible that Cd attack proteins which utilize Fe-S cluster as a co-factor such as dehydratases and this may be an unknown aspect of Cd toxicity[44] (Figure 3 C).

Cd upregulates expression of genes encoding putative Zn transporters in *C. elegans*.

Members of two major families of transporters are involved in Zn homeostasis in animals: the Cation Diffusion Facilitator (CDF/SLC30) family and the Zrt, Irt-like proteins (Zips/SLC39) family [45-48]. The *C. elegans* genome encodes 14 ZIP and 13 CDF family members of which, only four are CDF transporters. These four, CDF-1, CDF-2, TTM-1 and SUR-7 have been characterized and have been shown to respond transcriptionally to Zn deficiency or excess and have been suggested to mediate Zn efflux to maintain optimal internal Zn concentrations during Zn deficiency or Zn excess [49-51]. Further, expression of *TTM-1* was shown to be upregulated by Cd as well [52, 53] further emphasizing a link between Zn homeostasis and Cd. Therefore, here Dr. Anuj Sharma tested whether expression of other Zn transporters, *CDF-1*, *CDF-2* and *SUR-7* is altered by Cd in worms. Quantitative real-time PCR (qRT-PCR) analysis of the population of worms synchronized at the adult stage revealed that expression of *CDF-1, CDF-2,* as well as *TTM-1,* was upregulated by 2-, 4- and 8.5-fold respectively, in Cd-grown worms *vs.* worms grown under

control conditions. The level of the *SUR-7* transcript, in contrast, was not altered by Cd exposure (Figure 4A). These suggest that *CDF-1*, *CDF-2* and *TTM-1* might be involved in crosstalk between Zn homeostasis and basal Cd resistance.

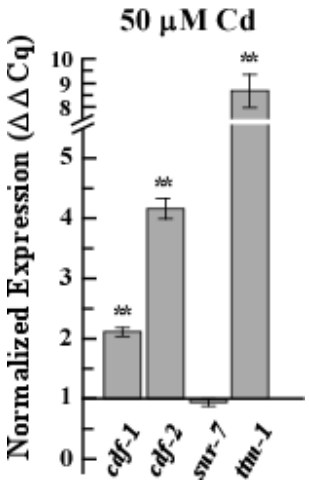

Figure 4. Cd upregulates mRNA expression of Zn transporters. qRT-PCR analysis of transcript abundance of *CDF-1*, *CDF-2*, *TTM-1* and *SUR-7* in adult worms grown from the L1 stage on 50 µM of $CdCl_2$. Results are normalized to expression of *ACT-1* and are presented relative to expression of genes in worms grown under control condition, which is designated as 1. Error bars indicate S.E. (n = 6). Asterisks indicate statistically significant differences (* $p \leq 0.05$ and ** $p \leq 0.001$, respectively).

Zn transporters are involved in Cd detoxification

I next tested whether function of CDF-1, CDF-2 or TTM-1 is required for basal Cd resistance in *C. elegans*. To do so Dr. Anuj Sharma and I tested Cd sensitivity of worms that lack one or more of these transporters. We found that, *cdf-1*, *sur-7* and *ttm-1* mutants but not *cdf-2* mutant, were more sensitive to Cd that was manifested by the delay in the ability of mutant vs. wild-type worms to reach the adult stage (Figure 5).

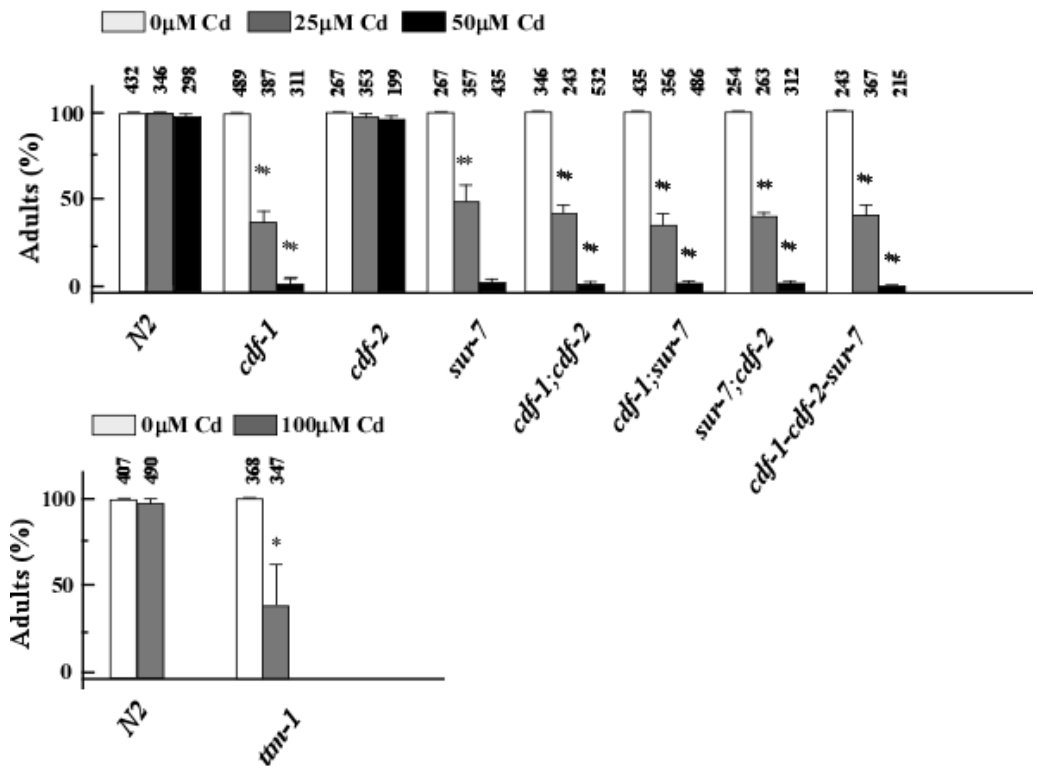

Figure 5. Zn transporters are involved in basal Cd resistance in *C. elegans*. *cdf-1, cdf-2, sur-7* single mutants, *cdf-1;cdf-2, cdf-1;sur-7, cdf-2;sur-7* double and *cdf-1;cdf-2;sur-7* triple mutants were grown on the NGM media supplemented with indicated concentration of $CdCl_2$. The total number of worms tested is written above each bar. The asterisks represent statistically significant differences between mean values of positive control, at 0 μM $CdCl_2$ and Cd treated conditions (*$p \leq 0.05$, **$p \leq 0.01$).

Since double (*cdf-1cdf-2, cdf-1sur-7, cdf-2sur-7*) and triple (*cdf-1cdf-2sur-7*) mutants were as sensitive to Cd as either of the single mutants, except for *cdf-2*, we concluded that these genes might function together in the basal Cd resistance pathway.

Discussion

Cd has been at center stage of heavy metal toxicity research since Pb containing petrol was banned and Hg/As containing products are restricted in developed countries due to their high toxicity [54]. Cd is emerging as a big threat to human health as it resides as an impurity of the dietary and essential element Zn; it mimics many essential elements in biological system and tends to bioaccumulate [55-59]. Therefore, efforts have been made to understand the mechanism of uptake, toxicity and detoxification of Cd [52, 56-

58, 60-80]. Specially, the roles of Zn, Ca, Fe and Mg have been extensively studied as transporters of these elements are commonly exploited by Cd in biological systems [13, 14, 81-85]. In the present study, I further extended the understanding of Cd and Zn interaction in biological system using the *C. elegans* system. I in collaboration with Dr. Anuj Sharma identified the elemental accumulation pattern in worms and how Cd affected this pattern providing an exclusive signature of Cd toxicity. Further, significance of Zn supplement in reverting Cd toxicity was evaluated comparing with additive toxic effect of Cu fortification. Simultaneously, I also concluded that not only accumulation but also the cellular distribution pattern of different elements changed significantly in Cd treated worms. Specially, Fe distribution pattern changed drastically showing a specific pattern which could be an additional factor contributing towards toxic phenotype.

As reported previously we found that at high levels, Cd competes with Zn in worms and further affects the accumulation and distribution of elements in a Zn dependent manner [22, 81]. In earlier studies, Cd is transported by different ways, for instance, Cd uptake by mammalian cultured cells was shown to use Ca^{2+} channels [81, 84, 86]. SLC11A2 (DMT1) shows a preference for Fe^{2+} but also transports Pb^{2+} and Cd^{2+}[86], similarly Zn transporters were also shown to transport Cd in different human cell lines [13, 37]. Altogether, the decrease in essential element accumulation could be explained due to competition by Cd uptake/transport of Cd by other essential element associated transporters. Also during Cd-exposure Zn and Cu transporters are considered the first choice; competition for uptake of Cd vs Zn/Cu/Mn/Fe/Pb/Hg using *Xenopus* oocytes showed that Zn is the most efficient competitor of Cd even with lower Zn/Cd ratio [37]. In plants, it has been reported that the interaction between Zn and Cd is either antagonistic or synergistic depending on the plant tissue [19]. Furthermore, lower concentration of Zn decreased Cd-induced oxidative stress while high concentration of Zn caused accumulation of oxidative stress in plant [19].

Dr. Anuj Sharma and I also showed that new Zn transporters (Cdfs) play very significant role in Cd detoxification and their up regulation may be a direct reason for Zn deficiency in Cd treated worms. We cannot explain at present, what triggers their expression under these circumstances exactly, but it may be

due to over accumulation of Cd which triggers the higher Zn response (over expression of *cdf-1* and *ttm-1*) by cells.

Using ICP-MS, I and Dr. Anuj Sharma established the ionome signature of Cd toxicity. Base sensitivity of worms to Cd is due to not only increased Cd accumulation but also the decreased amounts of essential element such as Zn, Fe, Mn, Co, Cu and increased accumulation of toxic elements such as As, Rb. Fe, Zn and Cu are such essential elements which are required by different enzymes and transcriptional factors as co-factors. In addition these elements are harmful to our system both in excess and in deficit. Fe, Zn and Cu deficiency have been associated with multiple disease conditions in humans [87-90]. ICP-MS data of Zn-Cd supplemented worms (Figure 2-I & J) also support our hypothesis, this showed that even in the presence of Zn, Cd accumulate in high concentration comparing to control yet exhibit no toxic symptoms in worms.

Moreover, in collaboration with Dr. Lydia Finney I discovered that distribution of Fe was dramatically changed upon a short-term exposure of 50 μM Cd. As shown in the Figure 3B, it seems that Fe which were spread throughout the entire worm intestine without Cd gathered and hyper-accumulated in numerous spots. However, we don't know whether this phenomena is a defense mechanism the animal exerts to prevent Cd toxicity or is one of the reasons of Cd toxicities. I speculate this Fe- accumulating spots might be localized to the nucleus since each cell can possess only one nucleus. If the Fe-accumulated spots are other subcellular organelle such as lysosome, various endosome, mitochondria, then the spots would be hundreds or thousands but in our result it was numerable. Furthermore regarding the fact that Cd could induce abnormal Fe homeostasis I could reveal the connection between Cd toxicity and neurodegenerative disease. Because abnormal homeostasis of Fe, which is described by accumulation of Fe in nucleus was also manifested in the brain neurons of Alzheimer patient [32, 33]. Our finding that Cd promoted redistribution of Fe in the cell is quite intriguing because trace elements such as Fe were traditionally regarded as static due to their roles as cofactors in cellular enzymes. This concept, however, was recently challenged by finding that another trace element, Cu, is not static but moves in neuronal cells from cell

bodies to peripheral processes upon neuron activation [91]. Further, the dynamic Cu redistribution is dependent on Ca release, suggesting a link between mobile Cu and the major cell signaling pathway [91]. Our finding that Cd triggers redistribution of Fe in the intestinal cells that, among other cell types, are affected by Cd poisoning in human [3, 4], suggests that mobility of transition metals might contribute to cell physiology and pathology.

Material and Methods

C. elegans strains and growth conditions

C. elegans strains routinely were maintained at 20° C on solid Nematode Growth medium (NGM) using the *Escherichia coli* OP50 strain as a food source as described [92]. For ICP-MS analyses NGM medium was supplemented with other trace elemenst as detailed below and was regarded as supplemental NGM (sNGM). *cdf-1, cdf-2, sur-7, ttm-1* single mutants, *cdf-1;cdf-2, cdf-1;sur-7, cdf-2;sur-7* double and *cdf-1;cdf-2;sur-7* triple mutants alleles were the generous gift of Dr. Kornfeld (Washington University in St. Louis).

Cadmium sensitivity assays

Adult worms (2 adults/plate) were placed on OP50 seeded NGM agar plates supplemented with or without $CdCl_2$ at the indicated concentration. Worms were incubated for 5 h at 20°C to lay eggs, before adult worms were removed. The effect of heavy metals on hatching was analyzed after 24 h. Cd in concentrations used did not appear to affect hatching of wild-type or mutant strains. Instead, heavy metal sensitivity of mutant strains was manifested as larval arrest or delay in larval stages. Therefore, I evaluated heavy metal sensitivity by assessing the percentage of arrested worms from the total number of hatched worms that have reached the adult stage in media with or without heavy metals. I assessed heavy metal sensitivity on 4^{th} day of culturing, when hatched worms have reached the adult stage in control (without heavy metal) condition. Since I started these assays with semi-synchronous population (eggs), all N2 worms

and most of mutant worms were adults after 4 days of culturing on control plates. For metal competition assays, N2 worms were scored when control worms just reached the young adult stage.

The results represent mean values (±S.D.) of at least three independent experiments each of which had three experimental replicates. Statistical significance of measurements for cadmium sensitivity analysis was determined using Kolmogorov Smirnov Test (with Dallal-Wilkinson Lilliefor p value). The absence of standard error (±S.E.) bars in some parts of some Figures indicates that either all of worms had reached the adult stage or survived at the particular condition or that the S.E. values were very low and thus S.E. bars are invisible.

Sample preparation for SXFM-

Synchronized population of the L1 stage worms were grown on NGM plates to adult stage. For Cd treatment, synchronized young adult worms were collected and transfered to the multiple 60mm NGM plates supplemented with 50 μM $CdCl_2$ and grown for 24 hours. After 24 hours worms were collected and washed with excess S-basal for 3 times. Each time, worms were incubated in S-basal for 15mins before centrifuge to remove bacteria from worm gut. Then worms were finally filtered out with Ultrafree-Cl Centrifugal Filter Units (MILLIPORE) at 30g for 1 min to remove remaining bacteria. Worms were then anesthetized with ice-cold 0.2% (w/v) NaN_3 for 2mins. After all the worms were completely immobilized, they were washed twice with de-icing agent, ice-cold 1.5% (w/v) CH_3COONH_4. Immobilized animals were transferred to 200nm thick silicon nitrite window (SiMPore, Inc) and straighten using an eyelash. Excess of liquid was removed using fine papered paper wicks (MiTeGen, USA). Then the window with straighten worms were plunge frozen in liquid N2 slush and dried overnight using a Balzers High Pressure Freezer. Freeze-dried worms were stored in cryovial at room temperature with desiccants.

SXRF

Dehydrated samples were analyzed by XFM using the X-ray microprobe at 2-ID-E beamline in the

Advanced Photon Source (Argonne, IL). An incident energy of 10.5 KeV with a dewell time of 0.1 sec for stepsize of 0.5 µm, to excite the Cd L-edge. Full X-ray emission spectra was collected by Vortex 4-element silicon drift detector (SII, Inc) to obtain the information of S, Cl, K, Ca, Mn, Cu, Fe, Zn, Co as well as Cd. Elemental maps were obtained and peak fitting and quantified using MAPS software

RNA Isolation and qRT-PCR

N2 wild-type worms were synchronized in the L1 stage and ~2000 L1s were placed on seeded 100 mm NGM agar plates seeded with *Escherichia coli* OP50 and supplemented with or without 50 µM $CdCl_2$. After 48h young adult hermaphrodites were collected from plates with M9 medium and washed free from *E. coli* OP50 by two rounds of centrifugation (3,500× *g* for 2 min) and resuspension in M9 medium. Worms were concentrated using Ultrafree-Cl Centrifugal Filter Units (MILLIPORE). Total RNA was isolated from worms with TRIZOL reagent (Invitrogen) according to manufacturer's recommendations. DNAse *I* (Roche) digestion of gDNA prior to first strand cDNA synthesis and qRT-PCR thermocycling procedures were as described [23, 93]. Data were normalized to the expression of *ACT1*. The fold-difference ($2^{-\Delta\Delta Ct}$) or relative quantities were calculated using the CFX Manager Software, version 1.5 (BioRad).

Worm preparation and elemental analysis

Elemental analyses was performed using ICP-MS., Worms were grown on OP50 seeded NGM plates containing 1x mineral mix [94] (to make sure detectable amount of each element) and thus the medium is referred as sNGM. The sNGM was also supplemented with the indicated concentrations of $CdCl_2$. Worms were harvested on 4th day of growth and washed free from *E. coli* OP50 by several rounds of washing and centrifugation as described above. The worm culture was thoroughly mixed and transferred into plastic reservoirs so that they could be pipetted using multichannel pipettes. Meanwhile, a 350 µL AcroPrep™ 96 filter plate with prefilter material/1.2 µm Supor® membrane (Pall Life Sciences) was wetted with methanol (300 µL/well) and washed with DI water (400 µL/well). The *C. elegans* cultures were then

pipetted into the filter membrane plate (100 µL/well, four replicates per mutant line, *i.e.* ~1000 worms per well), and washed and rinsed with EDTA solution (1 mM, pH 8.0) and DI water, respectively. A total of four such wash and rinse steps were performed (350 µL/well). Note that the filtration step separates the worms from the bacteria feed as the bacteria go through the membrane pores as well. Further, the filter membrane plate was dried (150 minutes) in an oven at 88 ˚C. Nitric acid (45 µL/well) was added to the dried worms in the filter plate and the samples digested in a heating block set at 88 ˚C for about 60 minutes. The digested samples were drawn into a deep-well collection plate containing 0.025 % Triton X-100 solution (95 µL/well using vacuum manifold). Deionized water (135 µL/well, 3 times) was then drawn through the filter membrane and also into the collection plate; thus the final solution volume per well in the plate was 500 µL (with final Triton X-100 concentration of 0.005%). Sample solutions were thoroughly mixed and analyzed using a Perkin Elmer DRC II ICP-MS (inductively coupled plasma- mass spectrometry) with the ESI (Elemental Scientific, Inc) SC-2 auto-sampler and the Apex Q sample introduction system. Calibration standards were prepared from single elemental stock solutions containing all the elements of interest (Na, Mg, Al, P, S, Cl, K, Ca, Mn, Fe, Co, Ni, Cu, Zn, As, Se, Mo, Cd, Rb, and Sr). The standards were matrix-matched (i.e., contain Triton X-100 and nitric acid). Note that the Triton X-100 was added to enable smooth self-aspiration of the PFA nebulizer of the Apex Q. The instrument software uses the linear calibration to determine the concentrations of the individual elements in the digested *C. elegans* samples. These concentrations were used together with the dilution factor and the calculated sample weights to determine the elemental concentrations (ppm or molarity) in the original *C. elegans* samples.

Statistical Analysis

Statistical analyses of the majority of experimental data were performed using the ANOVA Single Factor Analysis. Statistical analysis of qRT-PCR data was determined by paired *t*-test.

This is a manuscript in preparation.

*Anuj K Sharma[a], *Sungjin Kim[a,b], John Danku[c], David E. Salt[c], Lydia Finney[d], Stefan Vogt[e], Eric Craft[f], Olena K Vatamaniuk[a]

[a]Department of Crop and Soil Sciences, Cornell University, Ithaca, New York 14853

[b]Graduate Field of Environmental Toxicology, Cornell University, Ithaca, New York 14853

[c]Institute of Biological and Environmental Sciences, University of Aberdeen, AS24 3UU Scotland, United Kingdom

[d]X-ray Science Division, Advanced Photon Source, Argonne National Laboratory, Lemont, IL 60439,USA

[e]Experimental Facilities Division, Advanced Photon Source, Argonne National Laboratory, Argonne, IL60439

[f]Robert W. Holley Center for Agriculture and Health, U.S. Department of Agriculture–Agricultural Research Service, Ithaca, New York 14853

* These authors contributed equally to this work

REFERENCE

1. Waalkes, M.P., T.P. Coogan, and R.A. Barter, *Toxicological principles of metal carcinogenesis with special emphasis on cadmium.* Crit Rev Toxicol, 1992. **22**(3-4): p. 175-201.
2. Waisberg, M., et al., *Molecular and cellular mechanisms of cadmium carcinogenesis.* Toxicology, 2003. **192**(2-3): p. 95-117.
3. Waalkes, M.P., *Cadmium carcinogenesis.* Mutat Res, 2003. **533**(1-2): p. 107-20.
4. Waalkes, M.P., *Cadmium carcinogenesis in review.* J Inorg Biochem, 2000. **79**(1-4): p. 241-4.
5. Murata, I., et al., *Cadmium enteropathy, renal osteomalacia ("Itai Itai" disease in Japan).* Bull Soc Int Chir, 1970. **29**(1): p. 34-42.
6. Clemens, S., *Toxic metal accumulation, responses to exposure and mechanisms of tolerance in plants.* Biochimie, 2006. **88**(11): p. 1707-1719.
7. Stadtman, E.R., *Metal ion-catalyzed oxidation of proteins: biochemical mechanism and biological consequences.* Free Radic Biol Med, 1990. **9**(4): p. 315-25.
8. Valko, M., H. Morris, and M.T. Cronin, *Metals, toxicity and oxidative stress.* Curr Med Chem, 2005. **12**(10): p. 1161-208.
9. Clemens, S., et al., *The plant cDNA LCT1 mediates the uptake of calcium and cadmium in yeast.* Proc Natl Acad Sci U S A, 1998. **95**(20): p. 12043-8.
10. Eide, D., et al., *A novel iron regulated metal transporter from plants identified by functional expression in yeast.* Proc Natl Acad Sci USA, 1996. **93**: p. 5624 - 5628.
11. Cohen, C.K., et al., *The role of iron-deficiency stress responses in stimulating heavy-metal transport in plants.* Plant Physiol, 1998. **116**(3): p. 1063-72.
12. Sasaki, A., et al., *Nramp5 Is a Major Transporter Responsible for Manganese and Cadmium Uptake in Rice.* The Plant Cell Online, 2012. **24**(5): p. 2155-2167.
13. Thevenod, F., *Catch me if you can! Novel aspects of cadmium transport in mammalian cells.* Biometals, 2010. **23**(5): p. 857-75.
14. Levesque, M., et al., *Characterization of cadmium uptake and cytotoxicity in human osteoblast-like MG-63 cells.* Toxicol Appl Pharmacol, 2008. **231**(3): p. 308-17.
15. Vesey, D.A., *Transport pathways for cadmium in the intestine and kidney proximal tubule: focus on the interaction with essential metals.* Toxicol Lett, 2010. **198**(1): p. 13-9.
16. Bressler, J.P., et al., *Divalent metal transporter 1 in lead and cadmium transport.* Ann N Y Acad Sci, 2004. **1012**: p. 142-52.
17. Eide, D., et al., *A novel iron-regulated metal transporter from plants identified by functional expression in yeast.* Proc Natl Acad Sci USA, 1996. **93**(11): p. 5624-5628.
18. Korshunova, Y.O., et al., *The IRT1 protein from Arabidopsis thaliana is a metal transporter with a broad substrate range.* Plant Mol Biol, 1999. **40**(1): p. 37-44.
19. Tkalec, M., et al., *The effects of cadmium-zinc interactions on biochemical responses in tobacco seedlings and adult plants.* PLoS One, 2014. **9**(1): p. e87582.
20. Nzengue, Y., et al., *Oxidative stress induced by cadmium in the C6 cell line: role of copper and zinc.* Biol Trace Elem Res, 2012. **146**(3): p. 410-9.
21. Heo, D.H., et al., *Cadmium regulates copper homoeostasis by inhibiting the activity of Mac1, a transcriptional activator of the copper regulon, in Saccharomyces cerevisiae.* Biochem J, 2010. **431**(2): p. 257-65.

22. Wu, Y., et al., *Biosorption of heavy metal ions (Cu(2+), Mn (2+), Zn (2+), and Fe (3+)) from aqueous solutions using activated sludge: comparison of aerobic activated sludge with anaerobic activated sludge.* Appl Biochem Biotechnol, 2012. **168**(8): p. 2079-93.
23. Gayomba, S.R., et al., *The CTR/COPT-dependent copper uptake and SPL7-dependent copper deficiency responses are required for basal cadmium tolerance in A. thaliana.* Metallomics, 2013. **5**(9): p. 1262-75.
24. Besson-Bard, A., et al., *Nitric oxide contributes to cadmium toxicity in Arabidopsis by promoting cadmium accumulation in roots and by up-regulating genes related to iron uptake.* Plant Physiol, 2009. **149**(3): p. 1302-15.
25. Vert, G., et al., *IRT1, an Arabidopsis Transporter Essential for Iron Uptake from the Soil and for Plant Growth.* The Plant Cell Online, 2002. **14**(6): p. 1223-1233.
26. Korshunova, Y.O., et al., *The IRT1 protein from Arabidopsis thaliana is a metal transporter with a broad substrate range.* Plant Mol Biol, 1999. **40**(1): p. 37-44.
27. Eide, D., et al., *A novel iron-regulated metal transporter from plants identified by functional expression in yeast.* Proceedings of the National Academy of Sciences of the United States of America, 1996. **93**(11): p. 5624-5628.
28. Park, J.D., N.J. Cherrington, and C.D. Klaassen, *Intestinal Absorption of Cadmium Is Associated with Divalent Metal Transporter 1 in Rats.* Toxicological Sciences, 2002. **68**(2): p. 288-294.
29. Gunshin, H., et al., *Cloning and characterization of a mammalian proton-coupled metal-ion transporter.* Nature, 1997. **388**(6641): p. 482-488.
30. Hoch, E., et al., *Histidine pairing at the metal transport site of mammalian ZnT transporters controls Zn2+ over Cd2+ selectivity*. Proc Natl Acad Sci U S A, 2012. **109**(19): p. 7202-7.
31. Bush, A.I., *Metals and neuroscience.* Current Opinion in Chemical Biology, 2000. **4**(2): p. 184-191.
32. Honda, K., et al., *Ribosomal RNA in Alzheimer disease is oxidized by bound redox-active iron.* J Biol Chem, 2005. **280**(22): p. 20978-86.
33. Muhoberac, B.B. and R. Vidal, *Abnormal iron homeostasis and neurodegeneration.* Front Aging Neurosci, 2013. **5**: p. 32.
34. Schwartz, M.S., Benci, J. L., Selote, D. S., Sharma, A. K., Chen, A. G., Dang, H., Fares, H., Vatamaniuk, OK, *Detoxification of multiple heavy metals by a half-molecule ABC transporter, HMT-1, and coelomocytes of Caenorhabditis elegans.* PLoS One, 2010. **5**(3): p. e9564.
35. Vatamaniuk, O.K., et al., *CeHMT-1, a putative phytochelatin transporter, is required for cadmium tolerance in Caenorhabditis elegans.* J Biol Chem, 2005. **280**(25): p. 23684-90.
36. Pavlidis, P. and W.S. Noble, *Matrix2png: a utility for visualizing matrix data.* Bioinformatics, 2003. **19**(2): p. 295-296.
37. Liu, Z., et al., *Cd2+ versus Zn2+ uptake by the ZIP8 HCO3--dependent symporter: kinetics, electrogenicity and trafficking.* Biochem Biophys Res Commun, 2008. **365**(4): p. 814-20.
38. Pence, N.S., et al., *The molecular physiology of heavy metal transport in the Zn/Cd hyperaccumulator Thlaspi caerulescens.* Proc Natl Acad Sci U S A, 2000. **97**(9): p. 4956-60.
39. Ascone, I. and R. Strange, *Biological X-ray absorption spectroscopy and metalloproteomics.* Journal of Synchrotron Radiation, 2009. **16**(3): p. 413-421.

40. Finney, L., et al., *X-ray fluorescence microscopy reveals large-scale relocalization and extracellular translocation of cellular copper during angiogenesis.* Proceedings of the National Academy of Sciences, 2007. **104**(7): p. 2247-2252.
41. Finney, L.A. and T.V. O'Halloran, *Transition Metal Speciation in the Cell: Insights from the Chemistry of Metal Ion Receptors.* Science, 2003. **300**(5621): p. 931-936.
42. Paunesku, T., et al., *X-ray fluorescence microprobe imaging in biology and medicine.* Journal of Cellular Biochemistry, 2006. **99**(6): p. 1489-1502.
43. Tian, S., et al., *Cellular Sequestration of Cadmium in the Hyperaccumulator Plant Species Sedum alfredii.* Plant Physiology, 2011. **157**(4): p. 1914-1925.
44. Xu, F.F. and J.A. Imlay, *Silver(I), mercury(II), cadmium(II), and zinc(II) target exposed enzymic iron-sulfur clusters when they toxify Escherichia coli.* Appl Environ Microbiol, 2012. **78**(10): p. 3614-21.
45. Eng, B.H., et al., *Sequence analyses and phylogenetic characterization of the ZIP family of metal ion transport proteins.* J Membr Biol, 1998. **166**(1): p. 1-7.
46. Guerinot, M.L., *The ZIP family of metal transporters.* Biochim Biophys Acta, 2000. **1465**(1-2): p. 190-8.
47. Eide, D.J., *The SLC39 family of metal ion transporters.* Pflugers Arch, 2004. **447**(5): p. 796-800.
48. Bruinsma, J.J., et al., *Identification of mutations in Caenorhabditis elegans that cause resistance to high levels of dietary zinc and analysis using a genomewide map of single nucleotide polymorphisms scored by pyrosequencing.* Genetics, 2008. **179**(2): p. 811-28.
49. Gaither, L.A. and D.J. Eide, *Eukaryotic zinc transporters and their regulation.* Biometals, 2001. **14**(3-4): p. 251-70.
50. Davis, D.E., et al., *The cation diffusion facilitator gene cdf-2 mediates zinc metabolism in Caenorhabditis elegans.* Genetics, 2009. **182**(4): p. 1015-33.
51. Roh, H.C., et al., *ttm-1 encodes CDF transporters that excrete zinc from intestinal cells of C. elegans and act in a parallel negative feedback circuit that promotes homeostasis.* PLoS Genet, 2013. **9**(5): p. e1003522.
52. Cui, Y., et al., *Toxicogenomic analysis of Caenorhabditis elegans reveals novel genes and pathways involved in the resistance to cadmium toxicity.* Genome Biol, 2007. **8**(6): p. R122.
53. Huffman, D.L., et al., *Mitogen-activated protein kinase pathways defend against bacterial pore-forming toxins.* Proc Natl Acad Sci U S A, 2004. **101**(30): p. 10995-1000.
54. Tchounwou, P.B., et al., *Heavy metal toxicity and the environment.* EXS, 2012. **101**: p. 133-64.
55. Bridges, C.C. and R.K. Zalups, *Molecular and ionic mimicry and the transport of toxic metals.* Toxicol Appl Pharmacol, 2005. **204**(3): p. 274-308.
56. *Occupational Medicine Forum. What are the major points to consider for review of heavy metal toxicity? Part 1.* J Occup Environ Med, 2006. **48**(9): p. 988-90.
57. Akesson, A., B. Julin, and A. Wolk, *Long-term dietary cadmium intake and postmenopausal endometrial cancer incidence: a population-based prospective cohort study.* Cancer Res, 2008. **68**(15): p. 6435-41.
58. Bin, Q.H. and D. Garfinkel, *The cadmium toxicity hypothesis of aging: a possible explanation for the zinc deficiency hypothesis of aging.* Med Hypotheses, 1994. **42**(6): p. 380-4.

59. Carruthers, M. and B. Smith, *Evidence of cadmium toxicity in a population living in a zinc-mining area. Pilot survey of Shipham residents.* Lancet, 1979. **1**(8121): p. 845-7.
60. Vatamaniuk, O.K., et al., *CeHMT-1, a putative phytochelatin transporter, is required for cadmium tolerance in Caenorhabditis elegans.* J Biol Chem, 2005. **280**(25): p. 23684-23690.
61. Al Khateeb, W. and H. Al-Qwasemeh, *Cadmium, copper and zinc toxicity effects on growth, proline content and genetic stability of Solanum nigrum L., a crop wild relative for tomato; comparative study.* Physiol Mol Biol Plants, 2014. **20**(1): p. 31-9.
62. Aquino, N.B., et al., *The role of cadmium and nickel in estrogen receptor signaling and breast cancer: metalloestrogens or not?* J Environ Sci Health C Environ Carcinog Ecotoxicol Rev, 2012. **30**(3): p. 189-224.
63. Awasthi, M. and L.C. Rai, *Toxicity of nickel, zinc, and cadmium to nitrate uptake in free and immobilized cells of Scenedesmus quadricauda.* Ecotoxicol Environ Saf, 2005. **61**(2): p. 268-72.
64. Barrett, J.R., *Cadmium and breast cancer: exposure associated with Basal-like phenotype.* Environ Health Perspect, 2009. **117**(12): p. A552.
65. Goyer, R.A., J. Liu, and M.P. Waalkes, *Cadmium and cancer of prostate and testis.* Biometals, 2004. **17**(5): p. 555-8.
66. Hartwig, A., *Cadmium and cancer.* Met Ions Life Sci. **11**: p. 491-507.
67. Il'yasova, D. and G.G. Schwartz, *Cadmium and renal cancer.* Toxicol Appl Pharmacol, 2005. **207**(2): p. 179-86.
68. Lemen, R.A., et al., *Cancer mortality among cadmium production workers.* Ann N Y Acad Sci, 1976. **271**: p. 273-9.
69. Luckett, B.G., et al., *Cadmium exposure and pancreatic cancer in south Louisiana.* J Environ Public Health. **2012**: p. 180186.
70. Marchetti, C., *Role of calcium channels in heavy metal toxicity.* ISRN Toxicol. **2013**: p. 184360.
71. Matovic, V., et al., *Cadmium toxicity revisited: focus on oxidative stress induction and interactions with zinc and magnesium.* Arh Hig Rada Toksikol, 2011. **62**(1): p. 65-76.
72. Meshitsuka, S., M. Ishizawa, and T. Nose, *Uptake and toxic effects of heavy metal ions: interactions among cadmium, copper and zinc in cultured cells.* Experientia, 1987. **43**(2): p. 151-6.
73. Moulis, J.M., *Cellular mechanisms of cadmium toxicity related to the homeostasis of essential metals.* Biometals. **23**(5): p. 877-96.
74. Perfus-Barbeoch, L., et al., *Heavy metal toxicity: cadmium permeates through calcium channels and disturbs the plant water status.* Plant J, 2002. **32**(4): p. 539-48.
75. Person, R.J., et al., *Chronic cadmium exposure in vitro induces cancer cell characteristics in human lung cells.* Toxicol Appl Pharmacol. **273**(2): p. 281-8.
76. Schwartz, M.S., et al., *Detoxification of multiple heavy metals by a half-molecule ABC transporter, HMT-1, and coelomocytes of Caenorhabditis elegans.* PLoS One, 2010. **5**(3): p. e9564.
77. Sooksa-Nguan, T., et al., *Drosophila ABC transporter, DmHMT-1, confers tolerance to cadmium. DmHMT-1 and its yeast homolog, SpHMT-1, are not essential for vacuolar phytochelatin sequestration.* J Biol Chem, 2009. **284**(1): p. 354-62.
78. Cui, Y., et al., *Toxicogenomic analysis of Caenorhabditis elegans reveals novel genes and pathways involved in the resistance to cadmium toxicity.* Genome Biol, 2007. **8**(6).

79. Hall, J., K.L. Haas, and J.H. Freedman, *Role of MTL-1, MTL-2, and CDR-1 in mediating cadmium sensitivity in Caenorhabditis elegans.* Toxicol Sci. **128**(2): p. 418-26.
80. Tvermoes, B.E., G.S. Bird, and J.H. Freedman, *Cadmium induces transcription independently of intracellular calcium mobilization.* PLoS One. **6**(6): p. e20542.
81. Bergeron, P.M. and C. Jumarie, *Reciprocal inhibition of Cd(2+) and Ca(2+) uptake in human intestinal crypt cells for voltage-independent Zn-activated pathways.* Biochim Biophys Acta, 2006. **1758**(6): p. 702-12.
82. Bouckaert, J., R. Loris, and L. Wyns, *Zinc/calcium- and cadmium/cadmium-substituted concanavalin A: interplay of metal binding, pH and molecular packing.* Acta Crystallogr D Biol Crystallogr, 2000. **56**(Pt 12): p. 1569-76.
83. Cui, Y., Y. Zhu, and Z. Zhao, *[Effect of calcium content in diet on the accumulation and toxicity of cadmium in organisms]*. Wei Sheng Yan Jiu, 2004. **33**(3): p. 361-4.
84. Hinkle, P.M. and M.E. Osborne, *Cadmium toxicity in rat pheochromocytoma cells: studies on the mechanism of uptake.* Toxicol Appl Pharmacol, 1994. **124**(1): p. 91-98.
85. Ohana, E., et al., *Silencing of ZnT-1 expression enhances heavy metal influx and toxicity.* J Mol Med (Berl), 2006. **84**(9): p. 753-63.
86. Bressler, J.P., et al., *Divalent metal transporter 1 in lead and cadmium transport.* Ann N Y Acad Sci, 2004. **1012**: p. 142-152.
87. Camaschella, C. and P. Strati, *Recent advances in iron metabolism and related disorders.* Intern Emerg Med, 2010. **5**(5): p. 393-400.
88. Chasapis, C.T., et al., *Zinc and human health: an update.* Arch Toxicol, 2012. **86**(4): p. 521-34.
89. Hansch, R. and R.R. Mendel, *Physiological functions of mineral micronutrients (Cu, Zn, Mn, Fe, Ni, Mo, B, Cl).* Curr Opin Plant Biol, 2009. **12**(3): p. 259-66.
90. Mocchegiani, E., et al., *Micronutrient (Zn, Cu, Fe)-gene interactions in ageing and inflammatory age-related diseases: implications for treatments.* Ageing Res Rev, 2012. **11**(2): p. 297-319.
91. Dodani, S.C., et al., *Calcium-dependent copper redistributions in neuronal cells revealed by a fluorescent copper sensor and X-ray fluorescence microscopy.* Proceedings of the National Academy of Sciences, 2011. **108**(15): p. 5980-5985.
92. Brenner, S., *The genetics of Caenorhabditis elegans.* Genetics, 1974. **77**(1): p. 71-94.
93. Jung, H.I., et al., *COPT6 is a Plasma Membrane Transporter that Functions in Copper Homeostasis in Arabidopsis and is a Novel Target of SQUAMOSA Promoter Binding Protein-Like 7.* J Biol Chem, 2012. **287**: p. 33252-33267.
94. Nass, R. and I. Hamza, *The nematode C. elegans as an animal model to explore toxicology in vivo: solid and axenic growth culture conditions and compound exposure parameters.* Curr Protoc Toxicol, 2007. **Chapter 1**: p. Unit1 9.

CHAPTER 3

THE N-TERMINAL EXTENSION DOMAIN OF THE *C. ELEGANS* HALF-MOLECULE ABC TRANSPORTER, HMT-1, IS REQUIRED FOR PROTEIN-PROTEIN INTERACTIONS AND FUNCTION

Introduction

Increasing emission of heavy metals and metalloids such as cadmium (Cd), mercury (Hg), lead (Pb) and arsenic (As) into food, water and air poses major health and environmental problems. Members of the heavy metal tolerance factor 1 (HMT-1) transporter family are acutely required for detoxification of heavy metals and belong to the ‘‘B’’ branch of the ATP-bindings cassette (ABC) transporters superfamily [1–7]. It has been proposed that HMTs transport heavy metals coordinated to glutathione (GSH) derivatives named phytochelatins (PC) [8]. Recent genetic and biochemical studies have shown that HMTs act independently of PC, but how they function and their physiological substrates are not known [2, 7, 9, 10]. HMT-1 proteins share a conserved architecture that distinguishes them from other ABC transporters in diverse species including *Schizosaccharomyces pombe, Chlamydomonas reinhardtii, Caenorhabditis elegans, Drosophila melanogaster, Rattus norvegicus*, and *Homo sapiens* [2,4,5,9,11]. HMTs are half-molecule ABC transporters containing one polytopic membrane domain (TMD1) and one ATP-binding domain (NBD1) and are the only half-transporters that, in addition to TMD1 and NBD1, possess a hydrophobic NH2-terminal extension (NTE) [2,3,12]. Based on solved crystal structures of ABC transporters from prokaryotes, formation of at least a four domain structure (two TMDs and two NBDs) is a prerequisite to mediate the Mg-ATP-powered translocation of substances across a lipid bilayer [13]. The four-domain structure of ABC transporters can be formed from a single polypeptide or by the association of two or four separate subunits [14]. In eukaryotes, most ABC proteins are encoded as single polypeptides containing two TMDs and two NBDs [15]. In contrast, half-molecule ABC transporters function by forming homo- or heterooligomers and/or complexes with other cellular components [15–20]. For instance, the peroxisomal halftransporter

ALDP (ABCD1) can homodimerize or heterodimerize with related ABC half-transporters ALDPR (ABCD2) or PMP70 (ABCD3) and interfering with dimerization disrupts ALDP function [18]. Mammalian half-transporters TAP1 and TAP2 form heterodimers to transport peptide degradation products from the cytosol into the lumen of the endoplasmic reticulum [16, 19, 20]. The sterol half-transporters ABCG5 and ABCG8 must heterodimerize in order to get to the cell surface [21]. Interestingly, some full- molecule ABC transporters oligomerize as well: for instance, human ABCC1/MRP1, with two TMDs, two NBDs and an NTE, forms functional homodimer and homodimerization is regulated through the NTE domain [22]. Whether HMTs form higher order complexes and the role of their NTE domain have not been investigated. Because *C. elegans* HMT-1 (*Ce*HMT-1) is expressed in liver-like cells, the coelomocytes, as well as head neurons and intestinal cells, which are the cell types that are affected by heavy metal poisoning in humans [7], we have used *C. elegans* as a model system for identifying functional domains of HMT-1 expecting that our studies will provide insights into the function of equivalent domains in HMTs in higher animals. We now show that HMT-1 exists as an oligomer in vivo, can self-associate in yeast and that oligomerization is required for the ability of HMT-1 to detoxify cadmium. We also show that the NTE domain is essential for HMT-1 self-association and function. However, unlike the NTE of ABCC1/MRP1, the NTE of HMT-1 is not sufficient for self-association suggesting that multiple regions of HMT-1 must associate with one another to form an active transporter.

Results

HMT-1 exists in a protein complex in *C. elegans*

We first sought to test whether HMT-1 exists as an oligomer in *C. elegans*. Towards this goal, we generated transgenic worms expressing functional translational HMT-1::GFP fusions and analyzed the HMT-1::GFP in fractioned worm lysates. As would be expected for integral membrane protein, SDS-PAGE and immunoblot analyses of fractionated lysates from *phmt-1-hmt- 1::GFP* worms identified HMT-1::GFP among total and membrane proteins, but not among soluble proteins (Figure 1 A).

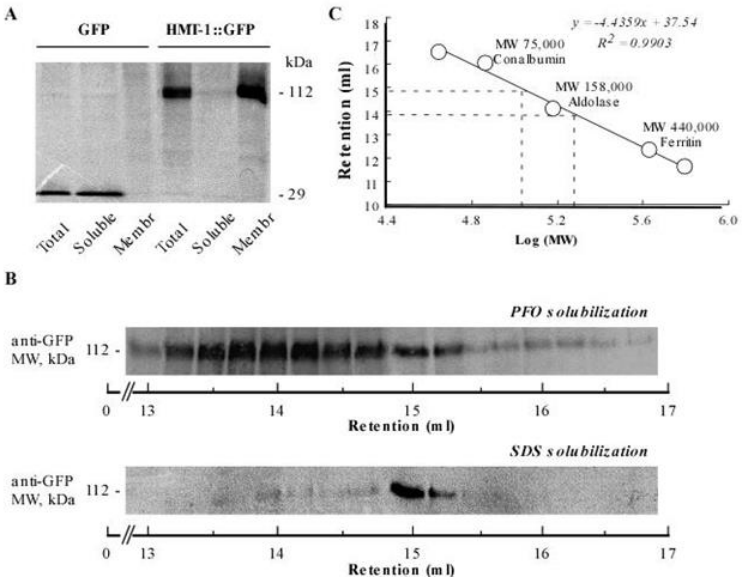

Figure 1. HMT-1 forms an oligomeric complex. A. SDS/PAGE and Western blot analyses of HMT-1::GFP. Aliquots (30 µg/lane) of total (Total), soluble (Soluble) or microsomal membrane proteins (Membr) isolated from worms expressing either HMT-1::GFP (HMT-1::GFP) or GFP alone (GFP)under the control of the hmt-1 promoter were subjected to SDS-PAGE and immunoblot analysis. **B.** Membrane proteins isolated from HMT-1::GFP expressing worms were solubilized either with PFO (PFO-solubilization) or with SDS (SDS-solubilization) and separated by FPLC on Superose 6HR column. Fractions (250 ml) were collected, proteins were precipitated with TCA, and HMT-1::GFP was detected by SDS/PAGE and Western analysis. **C.** The apparent molecular masses of PFO- or SDS- extracted HMT-1::GFP after FPLC analysis were estimated based on the linear regression of the retention time of molecular mass markers.

We also fractioned transgenic worms that express transcriptional phmt-1::GFP fusions. Since the GFP polypeptide does not possess membrane-spanning domains, it localized only in the total and soluble, but not in the membrane fraction of proteins (Figure 1 A). We next performed a gel-filtration separation of HMT-1::GFP by fast protein liquid chromatography (FPLC) on a Superose 6HR column (GE Healthcare). We solubilized HMT-1::GFP with perfluorooctanoate (PFO), a mild detergent that preserves interactions between protein subunits and has been successfully used in studies of ABC transporters [23,24]. We also extracted HMT-1::GFP with SDS, a strong ionic detergent, which disrupts protein interactions [25]. If HMT-1::GFP exists as a monomer in vivo, PFO- and SDS-extracted HMT-1::GFP would have identical migration properties. However, if HMT-1::GFP forms higher oligomeric states, the migration properties

would be distinct. We established that the elution peak of SDS-extracted HMT- 1::GFP was at 15 ml, corresponding to an estimated Mr of 125,000 (Figure 1B, C). Since the calculated molecular mass of HMT-1::GFP is 117,000, the observed elution profile (Figure 1B,C) is consistent with the migration of an HMT-1::GFP monomer. In contrast, PFO-extracted HMT-1::GFP was eluted as a broad peak at 13-15.25 ml (Figure 1B, C). The highest the anti-GFP antibody immunoreactivity was observed in fractions 13.75–14.25 ml, corresponding to estimate molecular masses of 340–269 kDa (Figure 1B, C). These estimated molecular masses suggest that HMT- 1::GFP is present almost exclusively in a protein complex either with itself or/and with other proteins in *C. elegans*.

Detection of HMT-1–HMT-1 interactions using Mating- Based Split-Ubiquitin Yeast-Two-Hybrid System (mbSUS)

The simplest explanation of the gel-filtration data is that HMT-1 homomerizes. To test this we used a mbSUS that detects binary interactions of membrane proteins in vivo [26, 27]. To do so, different HMT-1 fusions with ubiquitin were constructed (Figure 2A, B, 3A), and interactions were monitored by the release of the artificial transcriptional factor PLV that activated the expression of lexA-driven reporter genes, ADE2, HIS3 and lacZ. Based on the predicted membrane topology (TMHMM software, version 2.0 (http://www.cbs.dtu.dk/services/TMHMM-2.0/), the HMT-1 NH2-terminus is located outside (Lumen), whereas the COOH terminus is inside (Cytosol) (Figure 2 A).

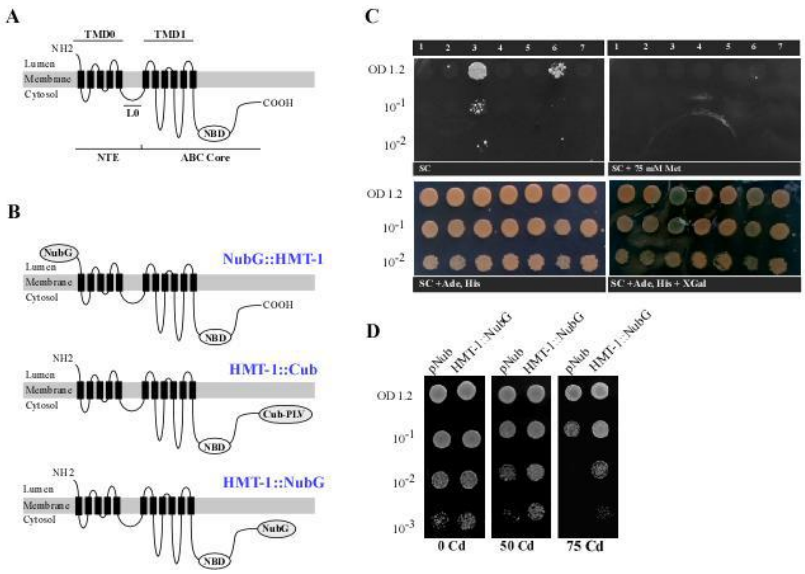

Figure 2. **HMT-1 interacts with itself. A.** Schematic representation of the topology of the full-length HMT-1 polypeptide. Based on the predicted topology (TMHMM software, version 2.0), the NH2-terminus is located outside (Lumen), whereas the COOH-terminus is inside (Cytosol). Also shown are the HMT-1 core region (ABC core) consisting of a single transmembrane domain (TMD1) with six transmembrane spans and a single nucleotide binding domain (NBD1). In addition to a core region, HMT-1 possesses the N-terminal extension (NTE), comprised of a membrane spanning domain (TMD0) and a linker domain (L0). **B.** Full-length HMT-1 was fused at the C-terminus with CubPLV (HMT-1::Cub) or with NubG at the C- or N-termini (NubG::HMT-1 and HMT-1::NubG, respectively). **C.** Only the yeast expressing HMT-1::Cub and HMT-1::Nub grow on selective medium along with positive control (KAT1::Cub + KAT1::NubG) among various negative controls. **D.** HMT-1::NubG confers Cd tolerance in yeast while yeast with empty vector, indicated as pNub is sensitive in Cd.

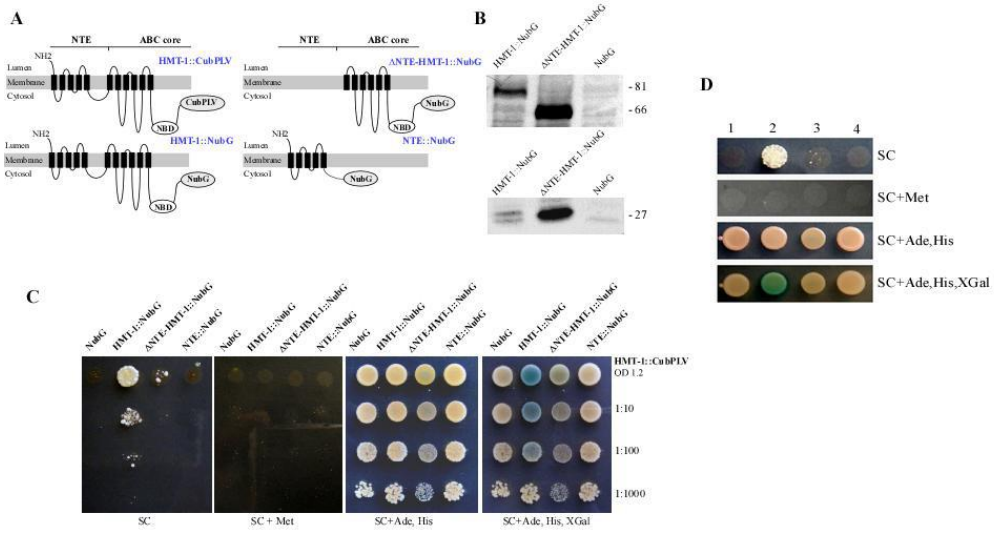

Figure 3. NTE is essential, but not sufficient for protein-protein interactions of HMT-1. A. Full-length HMT-1 was fused at the C-terminus with CubPLV (HMT-1::Cub) or with NubG (HMT-1::NubG). HMT-

1 lacking NTE was fused at the C terminus with NubG (ΔNTE-HMT-1::NubG). **B.** SDS-PAGE and immunoblot analysis of microsomal membranes prepared from THY.AP5 cells expressing the NubG-fused full-length HMT-1 (HMT-1::NubG), NubG-fused HMT-1 lacking NTE (ΔNTE-HMT-1::NubG), NTE-fused to NubG (NTE::NubG), or empty NubG vector (NubG). **C.** Interactions were manifested by the ability of cells to grow on SC media without adenine and histidine (SC), but not in SC media with methionine (SC + Met). Minimal growth relative to the negative controls (co-expression with vector alone, NubG) was observed when HMT-1::NubG prey construct lacking NTE (ΔNTE-HMT-1::NubG) was co-expressed with the full-length HMT-1::CubPLV bait (HMT-1::Cub). Diploid cells did not grow when the NTE domain fused to NubG (NTE::NubG) was co-expressed with HMT-1::CubPLV bait (HMT-1::Cub). Interactions were also visualized by the presence of β-galactosidase activity. **D.** mbSUS analysis of ΔHMT-1 self-association. Numbers across the top represent experiments and controls as follows: 1. HMT-1::CubPLV + NubG; 2. HMT-1::CubPLV + HMT-1::NubG; 3. HMT-1::CubPLV + ΔNTE-HMT-1::NubG; 4. ΔNTE-HMT-1::CubPLV + ΔNTE-HMT-1::NubG. Note the presence of cell growth and β-galactosidase activity in cells co-expressing the full-length HMT-1::NubG with HMT-1::CubPLV, but not ΔNTE-HMT-1::NubG with ΔNTE-HMT-1::CubPLV, or the full length HMT-1::CubPLV with ΔNTE-HMT-1::NubG, or NubG only.

HMT-1 ‘‘bait’’ vector was generated by fusing the C-terminus of the full-length of HMT-1 with a CubPLV fusion peptide (Figure 2 B). Since interactions can be detected only when CubPLV fusion and NubG fusions are in the cytosol [26,27], we generated two HMT-1 prey constructs by fusing NubG at NH2- or COOH-termini (‘‘NubG::HMT-1’’ and ‘‘HMT-1::NubG,’’ respectively (Figure 2 B). Therefore, if the topology prediction is correct, NubG of HMT-1::NubG -prey fusions would be localized in the cytosol (Figure 2 B) and would promote detection of interactions. In contrast, NubG of the NubG::HMT-1-prey construct will be localized intra-organellarly that will prevent interaction read-out (Figure 2 B). This experimental design assessed the membrane topology of HMT-1 and provided a negative control for spurious interactions. For other controls we co-expressed the following constructs: for detecting false positives due to self-activation, HMT-1::NubG or HMT-1::CubPLV were coexpressed with the empty pMetYCgate or pXNgate vectors respectively; as a positive control of interactions, the potassium channel, KAT1, from Arabidopsis thaliana, was used (KAT1::Cub- PVL bait and KAT1::NubG prey [27]); finally KAT1 was used as bait or prey for showing the specificity of HMT-1 interactions. The interactions were visualized in diploid cells by their ability to grow on SC medium lacking adenine and histidine, and by β-galactosidase activity assays. We ascertained that interactions occur only due to expression of HMT-1::CubPLV, or in case of the positive control, KAT1-CubPLV, by suppressing their expression with methionine (Figure 2 C). Our data show that

regardless of whether interactions were monitored as colony formation on selective media or by β-galactosidase activity, interactions did not occur between HMT-1:: CubPLV and NubG lacking the HMT-1 insert (Figure 2 C). As would be expected for membrane proteins participating in different biological processes, interactions did not occur between *C. elegans* HMT-1 and *A. thaliana* KAT-1, regardless of the vector combination used in the study (Figure 2 C). Furthermore, HMT-1- HMT-1 interactions were not detected when NubG was placed at the HMT-1 amino terminus. Instead, we detected interactions only when NubG was placed on the carboxyl terminus. Based on these results we propose that: first, HMT-1 at a minimum can form homodimers; second, the COOH-terminus of HMT-1 localizes in the cytosol since interactions were detected only when CubPLV and NubG were fused at the C-termini. Our data also suggest that the NH2-terminus of HMT-1 may be in the lumen. However, it is also possible that the amino terminal fusion is on the same side of the membrane but is not accessible to the Cub-PLV bait. Additional studies will determine the precise topology of HMT-1.

HMT-1 of *C. elegans* increases Cd tolerance of *S. cerevisiae*

We showed previously that HMT-1 functions independently of PC synthases in heavy metal detoxification [2, 7, 9]. Therefore, HMTs are expected to increase heavy metal tolerance of organisms that lack the capacity to produce PC. Consistent with this, Preveral and colleagues showed that *Sp*HMT-1 increases heavy metal tolerance of *E. coli* and *S. cerevisiae*, whose genomes lack PC synthase homologs [10]. Here we tested whether *Ce*HMT-1 is able to increase Cd tolerance of *S. cerevisiae*, and in doing so, test if the interacting construct, HMT-1::NubG, is functional. In this assay, we compared Cd sensitivity of THY.AP5 yeast expressing the empty pNXgate 32/33-3HA (NubG) vs. THY.AP5 expressing HMT-1::NubG. We first established that THY.AP5 cells expressing the empty vector were sensitive to 50 µM $CdCl_2$ and their sensitivity increased with increasing Cd concentration in the culture medium (Figure 2 D). In contrast, THY.AP5 cells expressing HMT-1::NubG were more tolerant to Cd and were able to grow at a concentration of Cd (75 µM), that blocked growth of yeast cells expressing vector without HMT-1 cDNA

insert (Figure 2 D). These findings show that: first, HMT-1::NubG construct is functional because it increases Cd tolerance in *S. cerevisiae*; second, the ability of *Ce*HMT-1 to increase heavy metal tolerance in *S. cerevisiae*, whose genome lacks PC synthase homologs, complements our previous findings and observation of others that HMTs act independently of PC synthases, reinforcing the remarkable conservation of HMTs' function in metal detoxification.

The N-terminal Extension Domain (NTE) is essential, but not sufficient for HMT-1-HMT-1 interactions

Since the N-terminal extension domain (NTE) is a conserved structural feature of HMT-1 proteins, unique to this half transporter family, we expected that it may be critical for HMT- 1 function. Therefore, we used the mbSUS approach to test if deletion of the NTE domain would affect the ability of HMT-1 to interact with itself. Truncated HMT-1, lacking NTE (designated ΔNTE) or possessing NTE only (designated NTE), were fused at their C-termini with NubG of pXNgate21-3HA vector (ΔNTE-HMT-1::NubG, NTE::NubG, respectively, Figure 3 A) and co-expressed with HMT-1-CubPLV as described above. Interactions were assayed by monitoring colony formation of serially-diluted cell inocula on SC medium lacking adenine and histidine, or by β-galactosidase activity. Interactions were suppressed by supplementing SC medium with methionine (Figure 3 C). We found that regardless of the approaches used for the analysis, interactions occurred only when a full-length HMT-1:: NubG or -CubPLV fusions were co-expressed in diploid yeast cells. Interactions were significantly suppressed when a full-length HMT-1::CubPLV was co-expressed with HMT-1::NubG lacking NTE (Figure 3 C). Minimal, methionine-repressible cell growth relative to the negative control (HMT-1::CubPLV + NubG) was observed when ΔNTE-HMT-1::NubG prey construct was co-expressed with the full-length HMT-1::CubPLV bait. However, the β-galactosidase activity was detectible only when a full-length bait and prey constructs were co-expressed (Figure 3 C). Cell growth and the β-galactosidase activity assays can be interpreted to mean that the full-length HMT-1 and HMT-1 lacking NTE do not interact, or that interactions are very weak and

are at the limit of detection. Failure to detect HMT-1 self-association was not due to decreased expression or stability of the truncated HMT-1 since it was detected in microsomal membranes by immunoblot analysis (Figure 3 B). However, it was possible that the lack of interactions was due to fact that the NTE domain was necessary for targeting, but not for interactions. Therefore, HMT-1 without NTE and full length HMT-1 might localize to different subcellular compartments. If the latter suggestion is correct, and NTE is dispensable for interactions, than co-expressed in yeast ΔNTE-HMT-1::NubG and ΔNTE-HMT-1::CubPLV constructs might interact since both would be in the same subcellular compartment. However, the interactions occurred only in cells co-expressing a full-length HMT-1::NubG or -CubPLV fusions, but not in cells co-expressing HMT-1::CubPLV and HMT-1::NubG constructs lacking NTE (Figure 4 A).

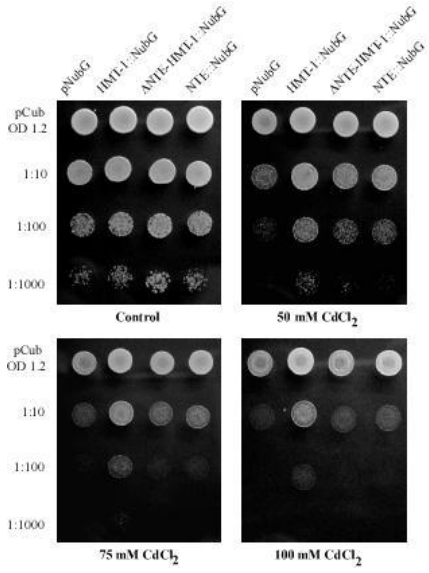

Figure 4. NTE is essential, but not sufficient for the ability of HMT-1 to confer Cd tolerance. Dilution series of THY.AP5 cells expressing different constructs are indicated at the top of the Figure. See legend to Figure 3 for the identity of the constructs. Yeast cells were grown at the indicated concentrations of $CdCl_2$. Note the striking growth difference at 75 and 100 μM $CdCl_2$.

These results further support our suggestion that the NTE domain is necessary for interactions, but do not rule out the possibility that it is also important for targeting. Interactions were not observed when a full-length HMT-1::CubPLV was co-expressed with NTE::NubG construct (Figure 3 C). Failure to detect HMT-1 self-association was not due to decreased expression or stability of the NTE domain since it was detected

in microsomal membranes by immunoblot analysis (Figure 3 B). Since the NTE alone did not interact with the full-length HMT- 1, we concluded that the NTE domain is not sufficient for HMT- 1-HMT-1 interaction, and that other structural feature(s) must associate to form a functional transporter.

NTE and Oligomerization are essential for HMT-1 function in Cd detoxification

Since formation of at least a four-domain structure is a prerequisite for the activity of half-molecule ABC transporters [13,14,16,21], and truncated HMT-1 does not self-associate, we expected that truncated HMT-1 would not confer Cd tolerance in *S. cerevisiae*. Consistent with this prediction, the *C. elegans* HMT-1 deletion mutant, *gk155*, lacks two cytosolic loops and a transmembrane domain of the NTE and is hypersensitive to heavy metals [7]. To test our hypothesis we compared Cd sensitivity of THY.AP5 yeast expressing the empty pNXgate32/33-3HA (NubG) vector, the full-length HMT-1::NubG, the HMT-1-NubG lacking the NTE domain, or the NTE domain fused to NubG. Cd sensitivity was monitored as described above. We found that only the fulllength HMT-1 conferred Cd tolerance of yeast cells (Figure 4 B). Since only a full-length HMT-1 is capable of interacting with itself in mbSUS (Figure 3 C), we concluded that self-association is essential for HMT-1 functional activity and that the NTE domain plays a structural role, preserving HMT-1 self-association and function in metal detoxification.

Discussion

HMTs are acutely required for heavy metal detoxification in different species, act by unknown mechanisms, and are distinct from other ABC transporters due to their unique topology: they are half-molecule ABC proteins, and are the only half-transporters with an NTE. Since functional activity of half-molecule ABC transporters requires homo- and/or hetero-oligomerization, in this manuscript we addressed two basic questions. First, does functional HMT-1 oligomerize? Second, what is the role of the NTE domain in HMT-1 function? In this manuscript we present the following observations: first, HMT-1 exists in a protein complex in *C. elegans* and, as determined by mbSUS, at least homodimerizes in *S. cerevisiae*.

Accordingly, the molecular mass of 269 kDa of PFO-extracted HMT-1::GFP, detected by gel-filtration chromatography, is consistent with its being a dimer (Figure 1B, C). Nevertheless, since higher molecular mass species were also detected (e.g. 340 kDa, Figure 1B, C), it is also possible that HMT-1 trimerizes, or that HMT-1 homodimers associate with other cellular protein(s). Future studies will discriminate between these possibilities and will establish the identity of proteins present in the HMT-1-associated protein complex. Second, the NTE domain plays a structural role and is necessary, but is not sufficient for HMT-1 homomerization, suggesting that other structural components must associate with HMT-1 to form a functional transporter. Third, the ability of HMT-1 to homomerize is needed for its function in Cd detoxification. Since the presence of NTE and heavy metal detoxification function of HMTs are conserved across species, we speculate that in addition to serving a structural role, the NTE domain possesses transport activity, and directly contributes to heavy metal detoxification. The functional significance of the NTE has been studied in some full-molecule ABC transporters of the ABCC subfamily [22, 28, 29]. For instance, the NTE domain of a full-molecule ABC transporter, *S. cerevisiae* YCF1, is needed for vacuolar membrane trafficking and transport [28]. In contrast, the NTE domain of ABCC1/MRP1 has redundant trafficking signals with the COOH-region [29], but regulates its homodimerization [22]. Unlike *Ce*HMT-1, the NTE of ABCC1/MRP1 is both essential and sufficient for oligomerization. We do not know whether the NTE domain of CeHMT-1 is required only for self-association or, as shown for full-molecule ABC transporters of ABCC subfamily, is also involved in membrane trafficking and transport activities. The prominence of heavy metals as environmental toxins and the remarkable conservation of HMT-1 structural architecture and function in different species reinforce the value of continued studies of HMT-1 in model systems for identifying functional domains in HMTs of humans.

Materials and methods

C. elegans strains and growth conditions

C. elegans strains used in this study are listed in Table 1. Worms were maintained at 20 degree

Celsius on solid Nematode Growth medium (NGM) using the *E. coli* OP50 strain as a food source [30]. *S. cerevisiae* Strains and Growth Condition THY.AP4 (*MATa leu2-3,112 ura3-52 trp1-289 lexA::HIS3 lexA::ADE2 lexA::lacZ*) and THY.AP5 (*MATa URA3 leu2-3,112 trp1-289 his3-D1 ade2D::loxP*) were obtained from the Dr. Wolf B. Frommer lab (Stanford University) depository at Arabidopsis Biological Resource Center (ABRC) http://www.arabidopsis. org/abrc/index.jsp. Yeast were cultured at 30 degree Celsius on YPAD media [26, 27]. Yeast cells were transformed with bait and prey constructs using the LiOAc/polyethylene glycol method [31]. Transformants were selected for leucine or tryptophan prototrophy on synthetic complete (SC) media as described below and in [26, 27]. For evaluation of cadmium tolerance, the SC media was supplemented with $CdCl_2$ at the indicated concentrations.

Generation of transgenic worms expressing HMT-1::GFP

A ten kb genomic fragment, consisting of the promoter (*phmt-1*) and genomic sequence of *C. elegans hmt-1*, was PCR-amplified and fused at the C-terminus of the translated polypeptide with GFP of the pPD117.01 vector [32]. Transgenic animals expressing HMT- 1::GFP were generated by co-injecting the engineered construct (80 ng/ml) and the selectable marker, a plasmid carrying a functional gene (unc-119+ , 100 ng/ml) into the gonadal syncytium of severely paralyzed, uncoordinated (uncoordinated, Unc) *unc- 119(ed-3)* adult hermaphrodites [33,34]. Non-Unc transgenic animals exhibiting GFP-mediated fluorescence were selected using a Leica MZ16FA automated fluorescence stereo zoom microscope with a Leica EL6000 metal halide illuminator as described previously [7]. Given that DNA introduced into the germline via micro-injection rarely integrates into chromosomes, but generally is organized into extrachromosomal DNA arrays that are frequently lost during mitosis, we integrated HMT-1::GFP of one line, VF10.1, by ɤ-ray-induced integration and isolated eighteen independently-derived stable transgenic lines showing the same GFP expression pattern [34]. One of the resulting worm lines (VF11.1) was crossed into *hmt-1(gk161)* [7] to generate the *hmt-1* mutant strain (VF12) expressing HMT-1::GFP under the control of *hmt-1* promoter *(hmt-1(gk161)III;gfIs1[phmt-1-hmt- 1::GFP,unc-119+])*. Since HMT-1::GFP rescued

the Cd sensitivity of *hmt-1(161)* allele (not shown), we concluded that the construct is functional. Therefore, we used VF12 strain in subsequent studies.

Preparation of microsomal and soluble proteins from *C. elegans*

Worms (VF1 and VF12 strains, expressing transcriptional *phmt- 1*::GFP [7] or translational *phmt-1-hmt*-1::GFP constructs) were cultured at 20 degree Celsius on NGM agar plates seeded with *Escherichia coli* OP50. Age-synchronized (young adults) worms were used for protein isolation and fractionation [35]. To generate sufficient age synchronized worms, 60 young adults were placed per each of four 150615 mm NGM agar plates with OP50, and cultured at standard condition for 3.5 days (until the progeny of inoculated worm were egg-laying adults and sufficient embryos were visible on the plates). Young adult hermaphrodites were collected from plates with M9 medium and washed free from *E. coli* OP50 by two rounds of centrifugation (3,500 g for 2 min) and resuspension in M9 medium. To replace M9 medium with lysis buffer, the worm pellet from the second centrifugation was resuspended in lysis buffer containing 50 mM TRIS-HCl, pH 7.6, 2 mM 2-mercaptoethanol, 1 mM phenylmethylsulfonyl fluoride (PMSF), and 1 mg/ml each of leupeptin, aprotinin, and pepstatin. After centrifugation at 3,500g for 2 min, the final worm pellet was resuspended in the same lysis buffer (1/1.5 of V worms/V buffer ratio) and transferred into eppendorf tubes. Worms were broken by sonication at 4 degree Celsius in lysis buffer and worm debris was cleared by low-speed centrifugation at 3,500g for 10 min. The supernatant, containing microsomal and soluble proteins, was collected and subjected to ultracentrifugation at 115,000 g for 1 h using a Beckman bench-top ultracentrifuge. The supernatant, containing soluble proteins was collected, frozen in liquid N2 and kept at -80 degree Celsius for subsequent studies. The microsomal pellet (membranebound vesicles of total cellular membranes), was washed, repelleted at 115,000g, resuspended in the same lysis buffer, frozen in liquid N2 and kept at -80 degree Celsius for subsequent studies.

Gel-filtration FPLC

Membrane proteins isolated from VF12 strains were solubilized prior to gel-filtration chromatography using either non-denaturing detergent perfluorooctanoate (PFO), which preserves interactions within protein oligomers [23,24], or with SDS, a strong ionic detergent which disrupts protein interactions [25]. Briefly, aliquots of membrane proteins (150 µg) were suspended in a buffer containing 50 mM Tris-HCl, pH 7.4, 150 mM NaCl and PFO or SDS at a final concentration of 4% or 1%, respectively, and solubilized for 1 h at room temperature. The insoluble material was cleared by centrifugation at 11,000 g at 4 degree Celsius for 10 min before 500 ml aliquots of the supernatants were injected onto Superose 6HR column (GE Healthcare) equilibrated with 50 mM Tris-HCl, pH 7.4, 150 mM NaCl and PFO (0.5%) or SDS (0.1%). The column was developed with the same buffer at a flow rate of 0.3 ml/min, 250 ml fractions were collected and proteins were precipitated with trichloracetic acid (TCA, to a final concentration of 10%) at 4 degree Celsius overnight. After collecting the precipitated proteins by centrifugation at 11,000g at 4 degree Celsius for 10 min, proteins were washed-free from TCA by 3 rounds of resuspension with ethanol and centrifugation at 11,000g at 4 degree Celsius for 10 min. The protein pellet was air-dried and reconstituted in 100 mM Tris-HCl (pH 8.0). The distribution of HMT-1::GFP in collected fractions was then analyzed by SDS-PAGE and immunoblot analysis. The elution profiles of protein markers, including ovalbumin (45 kDa), conalbumin (75 kDa), aldolase (158 kDa), ferritin (440 kDa) and thyroglobulin (669 kDa) (GE Healthcare) were analyzed and detected in collected fractions using the UV detector of the FPLC system (AKTA purifier, GE Healthcare).

Construction of HMT-1 Split-Ubiquitin plasmids and detection of HMT-1 protein interactions using Mating- Based Split-Ubiquitin System (mbSUS)

The homomerization of HMT-1 was tested using the mbSUS approach [26, 27]. The NubG and CubPLV vectors, KAT1- CubPLV and NubG-KAT1 constructs and THY.AP4 and THY.AP5 were obtained from the Dr. Wolf B. Frommer lab (Stanford University) depository at Arabidopsis Biological Resource Resource Center (ABRC) http://www.arabidopsis.org/abrc/index. jsp. The cDNAs corresponding

to the full-length open reading frame (ORF) and partial cDNAs were amplified from *C. elegans* N2 strain RNA by reverse transcription (RT) PCR to generate constructs by in vivo cloning in yeast [26,27]. Briefly, cDNAs were flanked with B1 and B2 linkers by PCR using the following primer pairs (Table 2). For NubG fusions, pNXgate32/33-3HA or pXNgate21-3HA vectors were cleaved with EcoRI/SmaI, whereas pMetYCgate vector was cleaved with PstI/HindIII. Gel-purified PCR products and linearized vectors were co-transformed into THY.AP4 or THY.AP5 strains for creating CubPLV bait and NubG prey clones, respectively. THY.AP4 cells expressing CubPLV bait constructs were selected on SC medium for leucine prototrophy, whereas THY.AP5 cells expressing NubG-prey constructs were selected for tryptophan prototrophy. Several clones from each THY.AP5 and THY.AP4 transformation were incubated on appropriate SC medium with or without G418. Plasmids were extracted from cultures grown without G418 (cells carrying vectors with inserts did not grow on G418) and inserts were sequenced. THY.AP4 and THY.AP5 cells carrying bait or prey constructs, respectively, were mated and diploids, co-expressing bait and prey, were selected on SC medium lacking leucine, tryptophan and uracil, but containing adenine and histidine. Interactions were selected in diploid cells on SC medium lacking adenine and histidine. Interactions were suppressed by methionine (75 mM) [26, 27]. Growth was monitored for 2–9 days. Interactions were also verified using β-galactosidase assays as described [26, 27].

Subcellular fractionation of *S. cerevisiae*

Membrane proteins were isolated and fractionated using modified procedures [36, 37]. Briefly, *S. cerevisiae* THY.AP5 cells expressing different HMT-1::NubG-fused constructs, or the empty NubG vector were converted to spheroplasts with Zymolyase 20T (ICN) in a buffer that also contained 1% (w/v) yeast extract, 2% (w/v) Bacto-Peptone) 0.7 M sorbitol, 1% (w/v) dextrose, 5 mM dithiothreitol, and 100 mM Tris-Mes (pH 7.5). Spheroplasts were disrupted by homogenization in a Dounce homogenizer in a medium containing 50 mM Tris-HCl, pH 7.6, 2 mM dithiothreitol, 1 mM EGTA, 1 mM phenylmethyl sulfonylfluoride and 1 mg/ml each of leupeptin, pepstatin, and aprotinin. The crude lysate was cleared by

centrifugation at 4,000g for 10 min. The lysate was then spun at 100,000 g for 30 min to pellet total microsomal membranes. Membranes were reconstituted in the same buffer containing 10% glycerol, frozen in liquid nitrogen and stored at -80 degree Celsius.

SDS-PAGE and western blot analyses

Aliquots of proteins (30 µg/lane) were subjected to SDS-PAGE on 7% (w/v) gels and electrotransferred to nitrocellulose filters for 18 h at 4 degree Celsius at a constant current of 60 mA in Towbin buffer containing 0.05% SDS [38]. For immunodetection of GFP epitope, the nitrocellulose blots were probed with the primary goat polyclonal anti-GFP antibody (1:1,000 dilution, Rockland Immunochemicals), and with the secondary HP-conjugated antigoat IgG antibody (1:2,500, Rockland Immunochemicals). For immunodetection of influenza hemagglutinin-HA epitope, microsomal membrane proteins were de-lipidated in TCA prior to SDS-PAGE and immunoblot analysis [39]. The nitrocellulose blots were probed with the primary rabbit polyclonal anti-HA antibody (1:2,000 dilution, Sigma) and secondary, an HR-conjugated antirabbit IgG antibody (1:10,000 dilution GE Healthcare). In both cases, immunoreactive bands were visualized with ECL using the LumiGLO system (KPL).

REFERENCES

1. Dean M, Rzhetsky A, Allikmets R (2001) The Human ATP-Binding Cassette (ABC) Transporter Superfamily. Genome Res 11: 1156–1166.
2. Vatamaniuk OK, Bucher EA, Sundaram MV, Rea PA (2005) CeHMT-1, a putative phytochelatin transporter, is required for cadmium tolerance in Caenorhabditis elegans. J Biol Chem 280: 23684–23690.
3. Rea PA (2007) Plant ATP-binding cassette transporters. Annu Rev Plant Biol 58: 347–375.
4. Ortiz DF, Kreppel L, Speiser DM, Scheel G, McDonald G, et al. (1992) Heavy metal tolerance in the fission yeast requires an ATP-binding cassette-type vacuolar membrane transporter. EMBO J 11: 3491–3499.
5. Hanikenne M, Matagne RF, Loppes R (2001) Pleiotropic mutants hypersensitive to heavy metals and to oxidative stress in Chlamydomonas reinhardtii. FEMS Microbiol Lett 196: 107–111.
6. Jalil YA, Ritz V, Jakimenko A, Schmitz-Salue C, Siebert H, et al. (2008) Vesicular localization of the rat ATP-binding cassette half-transporter rAbcb6. Am J Physiol Cell Physiol 294: C579–590.
7. Schwartz MS, Benci JL, Selote DS, Sharma AK, Chen AG, et al. (2010) Detoxification of multiple heavy metals by a half-molecule ABC transporter, HMT-1, and coelomocytes of Caenorhabditis elegans. PLoS One 5: e9564.
8. Ortiz DF, Ruscitti T, McCue KF, Ow DW (1995) Transport of Metal-binding Peptides by HMT1, A Fission Yeast ABC-type Vacuolar Membrane Protein. Journal of Biological Chemistry 270: 4721–4728.
9. Sooksa-Nguan T, Yakubov B, Kozlovskyy VI, Barkume CM, Howe KJ, et al. (2009) Drosophila ABC transporter, DmHMT-1, confers tolerance to cadmium. DmHMT-1 and its yeast homolog, SpHMT-1, are not essential for vacuolar phytochelatin sequestration. J Biol Chem 284: 354–362.
10. Preveral S, Gayet L, Moldes C, Hoffmann J, Mounicou S, et al. (2009) A common highly conserved cadmium detoxification mechanism from bacteria to humans: heavy metal tolerance conferred by the ATP-binding cassette (ABC) transporter SpHMT1 requires glutathione but not metal-chelating phytochelatin peptides. J Biol Chem 284: 4936–4943.
11. Paterson JK, Shukla S, Black CM, Tachiwada T, Garfield S, et al. (2007) Human ABCB6 Localizes to Both the Outer Mitochondrial Membrane and the Plasma Membrane. Biochemistry 46: 9443–9452.
12. Sanchez-Fernandez R, Davies TG, Coleman JO, Rea PA (2001) The Arabidopsis thaliana ABC protein superfamily, a complete inventory. J Biol Chem 276: 30231–30244.
13. Rees DC, Johnson E, Lewinson O (2009) ABC transporters: the power to change. Nat Rev Mol Cell Biol 10: 218–227.
14. Rees DC, Johnson E, Lewinson O (2009) ABC transporters: the power to change. Nat Rev Mol Cell Biol 10: 218–227.
15. Jones PM, George AM (1999) Subunit interactions in ABC transporters: towards a functional architecture. FEMS Microbiol Lett 179: 187–202.
16. Abele R, Tampe R (2004) The ABCs of immunology: structure and function of TAP, the transporter associated with antigen processing. Physiology (Bethesda) 19: 216–224.
17. Chloupkova M, Reaves SK, LeBard LM, Koeller DM (2004) The mitochondrial ABC transporter Atm1p functions as a homodimer. FEBS Lett 569: 65–69.
18. Liu LX, Janvier K, Berteaux-Lecellier V, Cartier N, Benarous R, et al. (1999) Homo- and heterodimerization of peroxisomal ATP-binding cassette halftransporters. J Biol Chem 274: 32738–32743.
19. Russ G, Esquivel F, Yewdell JW, Cresswell P, Spies T, et al. (1995) Assembly, intracellular localization, and nucleotide binding properties of the human peptide Transporters TAP1 and TAP2 expressed by recombinant vaccinia viruses. J Biol Chem 270: 21312–21318.

20. Taylor JC, Horvath AR, Higgins CF, Begley GS (2001) The multidrug Resistance P-glycoprotein. Oligomeric state and intramolecular interactions. J Biol Chem 276: 36075–36078.
21. Graf GA, Yu L, Li WP, Gerard R, Tuma PL, et al. (2003) ABCG5 and ABCG8 are obligate heterodimers for protein trafficking and biliary cholesterol excretion. J Biol Chem 278: 48275–48282.
22. Yang Y, Liu Y, Dong Z, Xu J, Peng H, et al. (2007) Regulation of function by dimerization through the amino-terminal membrane-spanning domain of human ABCC1/MRP1. J Biol Chem 282: 8821–8830.
23. Xu J, Liu Y, Yang Y, Bates S, Zhang JT (2004) Characterization of oligomeric human half-ABC transporter ATP-binding cassette G2. J Biol Chem 279: 19781–19789.
24. Ramjeesingh M, Huan LJ, Garami E, Bear CE (1999) Novel method for evaluation of the oligomeric structure of membrane proteins. Biochem J 342: 119–123.
25. Seddon AM, Curnow P, Booth PJ (2004) Membrane proteins, lipids and detergents: not just a soap opera. Biochim Biophys Acta 1666: 105–117.
26. Kittanakom S, Chuk M, Wong V, Snyder J, Edmonds D, et al. (2009) Analysis of membrane protein complexes using the split-ubiquitin membrane yeast twohybrid (MYTH) system. Methods Mol Biol 548: 247–271.
27. Obrdlik P, El-Bakkoury M, Hamacher T, Cappellaro C, Vilarino C, et al. (2004) K+ channel interactions detected by a genetic system optimized for systematic studies of membrane protein interactions. Proc Natl Acad Sci USA 101: 12242–12247.
28. Mason DL, Michaelis S (2002) Requirement of the N-terminal extension for vacuolar trafficking and transport activity of yeast Ycf1p, an ATP-binding cassette transporter. Mol Biol Cell 13: 4443–4455.
29. Westlake CJ, Cole SP, Deeley RG (2005) Role of the NH2-terminal membrane spanning domain of multidrug resistance protein 1/ABCC1 in protein processing and trafficking. Mol Biol Cell 16: 2483–2492.
30. Brenner S (1974) The genetics of Caenorhabditis elegans. Genetics 77: 71–94.
31. Gietz RD, Schiestl RH (1991) Applications of high efficiency lithium acetate transformation of intact yeast cells using single-stranded nucleic acids as carrier. Yeast 7: 253–263.
32. Fire A, Kondo K, Waterston R (1990) Vectors for low copy transformation of *C. elegans*. Nucleic Acids Res 18: 4269–4270.
33. Maduro M, Pilgrim D (1995) Identification and cloning of unc-119, a gene expressed in the Caenorhabditis elegans nervous system. Genetics 141: 977–988.
34. Mello C, Fire A (1995) DNA transformation. Methods Cell Biol 48: 451–482.
35. Tian C, Sen D, Shi H, Foehr ML, Plavskin Y, et al. (2010) The RGM protein DRAG-1 positively regulates a BMP-like signaling pathway in Caenorhabditis elegans. Development: 137: 2375–2384.
36. Rieder SE, Emr SD (2001) Isolation of subcellular fractions from the yeast Saccharomyces cerevisiae. Curr Protoc Cell Biol Chapter 3: Unit 3 8.
37. Vatamaniuk OK, Mari S, Lu YP, Rea PA (1999) AtPCS1, a phytochelatin synthase from Arabidopsis: isolation and in vitro reconstitution. Proc Natl Acad Sci USA 96: 7110–7115.
38. Towbin H, Staehelin T, Gordon J (1979) Electrophoretic transfer of proteins from polyacrylamide gels to nitrocellulose sheets: procedure and some applications. Proc Natl Acad Sci USA 76: 4350–4354.
39. Parry RV, Turner JC, Rea PA (1989) High purity preparations of higher plant vacuolar H+-ATPase reveal additional subunits. Revised subunit composition. J Biol Chem 264: 20025–20032.
40. Bradford MM (1976) A rapid and sensitive method for the quantitation of microgram quantities of protein utilizing the principle of protein-dye binding. Anal Biochem 72: 248–254.

CHAPTER 4

THE ROLE OF THE N-TERMINAL EXTENSION DOMAIN OF THE *C. ELEGANS* HALF-MOLECULE ABC TRANSPORTER, HMT-1, IN THE FUNCTION OF CADMIUM RESISTANCE

Introduction

The adverse health effects of heavy metals and metalloids (*e.g.* cadmium [Cd], mercury [Hg], lead [Pb] and arsenic [As]) are well established [1-3]. Despite this knowledge, exposure to heavy metals continues, and even increases in some areas, due to their sustained production and emission into the environment [4]. Members of the highly conserved and ubiquitous family of ATP-binding cassette (ABC) transporters have been shown to contribute to heavy metal detoxification in different species [5-10]. For example, in humans, HsABCC1 and HsABCC2 efflux Asconjugated to the ubiquitous tripeptide glutathione (GSH) from cells [11]. The *Saccharomyces cerevisiae* vacuolar membrane-localized ABC transporter, Ycf1p (**y**east **C**d **f**actor 1) is aHsABCC1 and HsABCC2 homolog, and detoxifies heavy metals including Cd, by sequestering metal-GS complexes into the vacuole [12-14]. Finding that heavy metal-ligand complexes are sequestered into the vacuole/lysosome in different species highlights the important role of this compartment in toxic metal inactivation. HsABCC1/2 and YCF1p are classified as "full-molecule" ABC transporters consisting of four domains: two transmembrane domains (TMD) and two ATP-binding domains (NBD) [14]. Another member of the ABC transporter family, HMT-1 (**h**eavy **m**etal **t**olerance factor 1, *alias* ABCB6), is acutely required for resistance to heavy metals including Cd, in different species [9, 15, 16]. However, unlike HsABCC1/2 and Ycf1p, HMT-1/ABCB6 is a half molecule ABC transporter. Evidence from the X-ray structure analysis of bacterial ABC proteins shows that at least two NBD are required for the functional ABC transporter [17, 18]. This configuration appears to be necessary for binding and hydrolysis of ATP to mediate ATP-powered translocation of substrates through the lipid bilayer [17, 18]. Therefore, two TMD and two NBD are required for the functional ABC transporter. Consistent with this suggestion was our recent finding that HMT-1/ABCB6 of *C. elegans*, at a minimum

homodimerizes [7]. In addition to the four-domain structure, some ABC transporters also possess a hydrophobic N-terminal extension domain termed NTE (or TMD_0). The NTE domain consists of 5 to 6 membrane spans (TMD_0) and a cytosolic linker (L_0), which connects the NTE domain with core domains of ABC transporters (TMDs or NBDs) [16]. Several research groups have revealed that the NTE has an important role in the ABC transporter function. For example the NTE domain of HsABCC1 (*alias* MRP1), is involved in cellular localization of the protein, and the NTE of Ycf1p plays an important role in Cd detoxification as well as in protein trafficking [19, 20]. However, not all ABC transporters have the NTE domain. In this regard, the topology of HMT-1 is unique: it is the only known half-molecule ABC transporter that contains an NTE domain. These features distinguish HMT-1/ABCB6 proteins from other ABC transporter family members and allow the identification of their homologs in diverse organisms including humans [16]. We showed recently that the NTE domain of *C. elegans* HMT-1/ABCB6 is essential for its ability to form homodimers and HMT-1 function in Cd resistance in heterologous system [7]. Whether it is important for cellular localization of HMT-1/ABCB6 is unknown. The subcellular localization of HMT-1/ABCB6 in *C. elegans* is unknown as well. In this regard, data on the cellular localization of HMT-1/ABCB6 in mammals yielded conflicting results: an HMT-1/ABCB6 homolog in rodents, MTABC3, is localized to the mitochondria, while HsABCB6 was found in endosomes [21, 22].

Here, in collaboration with Drs. Olena Vatamaniuk and Anuj Sharma, I show that *C. elegans* HMT-1/ABCB6 localizes to apical recycling endosomes in intestinal cells, and that the NTE domain is essential but not sufficient for trafficking of HMT-1/ABCB6 to correct endomembrane as evidenced by mislocalzation of the truncated HMT-1/ABCB6 and its targeting to other membranes including plasma membrane. We also found that while the NTE domain is essential for localization for HMT-1/ABCB6, it functions redundantly with the C-terminal region in the ability of the transporter to form homodimers. Together, this work furthers our understanding of the role of the functional domains of HMT-1/ABCB6 in its subcellular localization and ability to confer Cd tolerance

Results

HMT-1 resides on apical recycling endosomes in intestinal cells of *C. elegans*

To study the subcellular localization of HMT-1, we generated *hmt-1(gk161)* mutant worms expressing the translational fusion HMT-1::GFP under control of the *HMT-1* promoter (HMT-1::GFP). We found that while *HMT-1* was expressed in multiple tissues of *C. elegans* including head neurons, intestinal cells and coelomocytes [23], HMT-1::GFP was mainly present in intestinal cells and was located at the periphery of vesicular structures (Figure 1A-C).

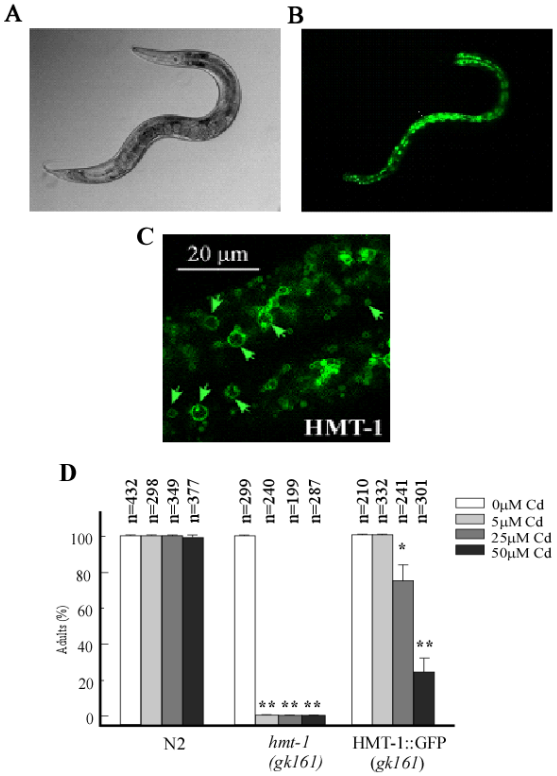

Figure 1. Localization pattern and Cd sensitivity assays of HMT-1::GFP in *hmt-1* mutant worms. A. DIC image of a *HMT-1::GFP*-expressing worm **B.** Image of fluorescence signal of HMT-1::GFP expressed in intestinal cells. **C.** Confocal microscopy analysis of the *hmt-1* mutant worm expressing HMT-1::GFP shows that HMT-1 is expressed in intestinal cells; arrow heads indicate that HMT-1::GFP localizes to the periphery of vesicular compartments. **D.** HMT-1::GFP rescues Cd sensitivity of the *hmt-1(gk161)* mutant allele. The adult hermaphrodites of indicated strains were placed on NGM plates containing the indicated $CdCl_2$ concentration. Worms were counted after wild-type worms reach the adult stage on 0 µM $CdCl_2$, (approximately after 3 days). The total number of worms tested (n) is written above each bar. The asterisks represent statistically significant differences between the mean values of positive control, at 0 µM $CdCl_2$ and Cd treated conditions (*$p<0.05$, **$p<0.01$).

To establish the identity of HMT-1::GFP expressing subcellular compartments, we co-expressed HMT-1::GFP with marker proteins for different endocytic compartments [24, 25]. Transgenic worms expressing RAB-5::RFP (an early endosomal marker), RAB-7::RFP (the late and early endosomal marker), RME-1::RFP (a marker for basolateral recycling endosomes) and RAB-11:mCherry (a marker apical recycling endosomes marker) from the intestinal-specific *vha-6* promoter [26] were crossed into *hmt-1(gk161)* mutant worms expressing HMT-1::GFP and the resulting transgenic worms were analyzed by confocal microscopy. Confocal studies of these strains revealed that HMT-1::GFP did not co-localize with RME-1 (Figure 2 Q-T) and only a minor fraction of HMT-1::GFP co-localized with RAB-7 and RAB-5 (Figure 2 I-L & M-P).

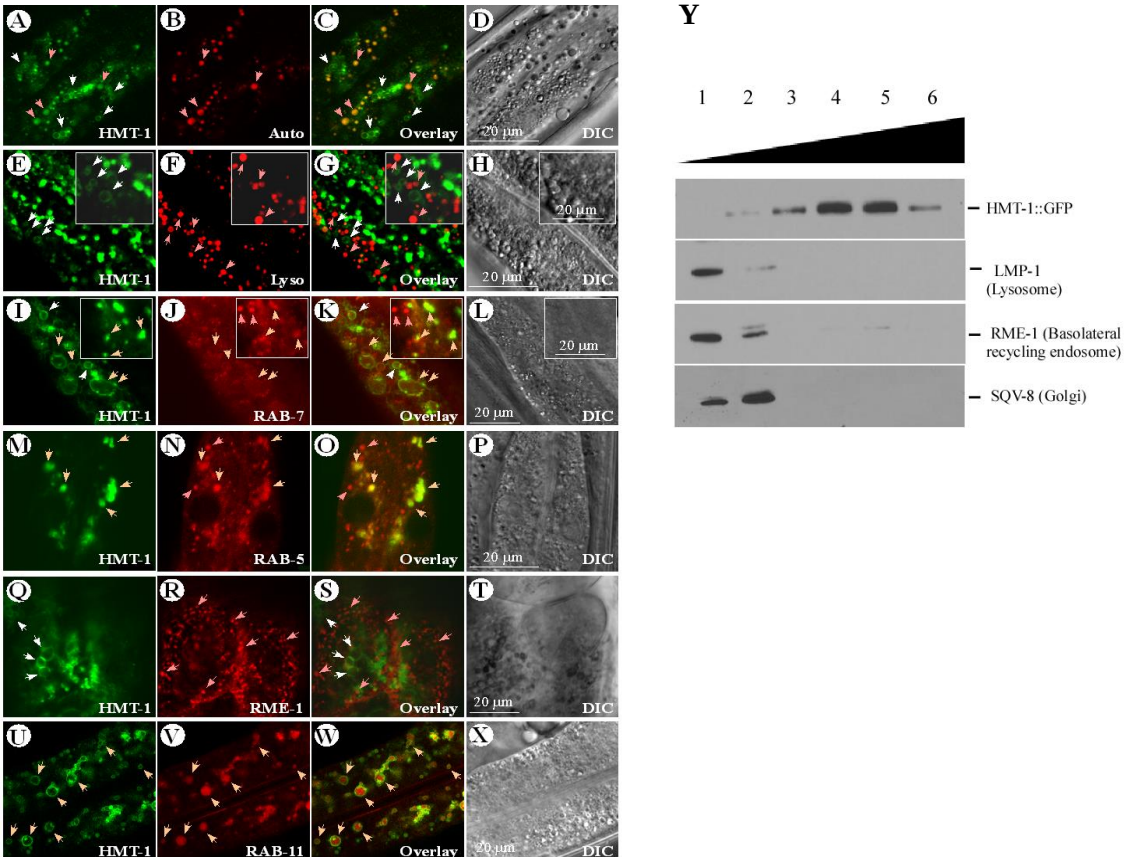

Figure 2. HMT-1::GFP resides on apically-localized recycling endosomes of intestinal cells of *C. elegans*. A-D. Confocal microscopy analysis of HMT-1::GFP (GFP) and autofluorescence signals (Auto) in intestinal cells of HMT-1::GFP expressing worms. HMT-1::GFP-mediated fluorescent does not co-localize with the lysosome-related gut granules accumulating birefringent and autofluorescent material (Overlay). White arrow heads indicate the membrane-bound vesicles with HMT-1::GFP-mediated fluorescence; pink arrow heads indicate the lysosomal-related autofluorescent granules. E-H. HMT-1::GFP

expressing *hmt-1(gk161)* were stained with the lysosomal dye, LysoTracker Red. Overlay image (Overlay) shows that the HMT-1::GFP fluorescence signal (GFP) does not co-localize with the lysotracker-signal in lysosomes (Lyso). I-L. Analysis of HMT-1 localization in *hmt1(kg161)* strain co-expressing HMT-1::GFP with a marker for early and late endosomes, RAB-7::RFP. Expression of RAB-7::RFP in intestinal cells was driven by the *vha-6* promoter. Overlay microphotograph (Overlay) shows that HMT-1::GFP fluorescence signal (GFP) partially co-localizes with the RAB-7::RFP signal (RAB-7). M-P. Analysis of HMT-1 localization in the *hmt1(kg161)* strain co-expressing HMT-1::GFP with a marker for early endosomes, RAB-5::RFP. Overlay microphotograph (Overlay) shows that HMT-1::GFP fluorescence signal (GFP) partially co-localizes with RAB-5::RFP signal (RAB-5). Q-T. Analysis of HMT-1 localization in the hmt1(kg161) strain co-expressing HMT-1::GFP with a marker of basolateral recycling endosomes, RME-1::RFP. Overlay microphotograph (Overlay) shows that HMT-1::GFP fluorescence signal (GFP) does not co-localize with RME-1::RFP signal (RME-1). U-X. Analysis of HMT-1 localization in the *hmt1(kg161)* strain co-expressing HMT-1::GFP with a marker of apically-located recycling endosomes, RAB-11::mCherry. Overlay microphotograph (Overlay) shows that HMT-1::GFP signal (GFP) co-localizes with RAB-11::mCherry signal (RAB-11). A DIC microphotograph shows a section of the analyzed intestinal cells (DIC). Y. Western blot analyses of fractioned *C. elegans* membranes. Total membranes, isolated from *hmt-1(gk161)*; *phmt-1;hmt-1*::GFP worms were fractioned by sucrose density gradient. Fractions were collected and subjected to SDS-PAGE and western blot analyses using the monoclonal anti-GFP primary and the anti-mouse secondary antibody. Note that HMT-1::GFP did not co-fraction with the marker for lysosomes or basolateral recycling endosomes, or Gogi apparatus.

On the other hand, we observed a strict superimposition of the fluorescence from HMT-1::GFP and RAB-11::mCherry suggesting that HMT-1::GFP resides on the apical recycling endosomes (Figure 2 U-X).

HMT-1 interacts with itself in *C. elegans*.

Our recent findings revealed that HMT-1 at least dimerizes to confer Cd resistance in yeast [7]. Here, we substantiated these findings using co-imunoprecipitation and co-localization assays in *C. elegans*. To do so, we generated *hmt-1(gk161)* mutant worms expressing HMT-1::RFP, and *hmt-1(gk161)* mutant worms co-expressing HMT-1::GFP and HMT-1::RFP. We then evaluated whether the HMT-1::RFP construct is functional by testing Cd-resistance capabilities of *hmt-1(gk161)* worms. Consistent with previous findings, *hmt-1(gk161)* mutant worms exhibited hypersensitivity to 5 µM $CdCl_2$, *hmt-1(gk161)* mutant co-expressing HMT-1::GFP or HMT-1::RFP expressing worms became tolerant to Cd up to 25 µM $CdCl_2$ suggesting that HMT-1::RFP construct is functional as well. Therefore, worms expressing HMT-1::RFP or worms co-expressing HMT-1::RFP with HMT-1::GFP were used for subsequent studies. We then investigated the localization of HMT-1 constructs in these strains using confocal microscopy and found,

that, as expected HMT-1:: GFP and HMT-1::RFP signals co-localized (Figure 3 B).

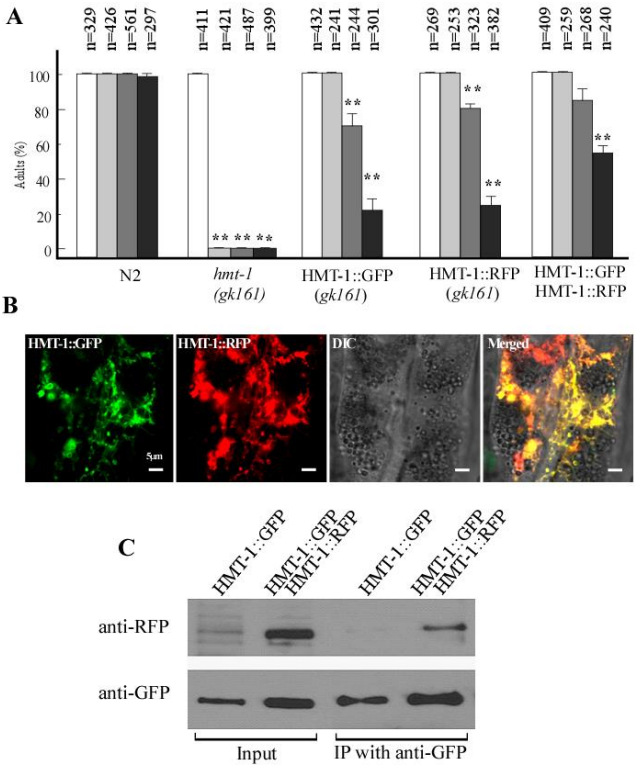

Figure 3. **HMT-1 interacts with itself in *C. elegans*. A.** Cd sensitivityof wild-type, *hmt-1 (gk161), hmt-1 (gk161)* expressing HMT-1::GFP, *hmt-1 (gk161)* expressing HMT-1::RFP, *hmt-1 (gk161)* co- expressing HMT-1::GFP and HMT-1::RFP. The total number of worms tested is written (n) above each bar. The asterisks represent statistically significant differences between the mean values of the positive control, at 0 µM CdCl2 and Cd treated conditions(*p<0.05, **p<0.01) **B.** Fluorescence microscopy image of *hmt-1 (gk161)* worms co-expressing HMT-1::GFP and HMT-1::RFP. It showed that they co-localized. **C.** Co-Immunoprecipitation assay showed that HMT-1::GFP interact with HMT-1::RFP.

Furthermore, both HMT-1::GFP and HMT-1::RFP were co-precipitated with the anti-GFP antibody. Thus, HMT-1 interacts with itself in *C .elegans* as it does in the heterologous system (Figure 3 C and [7]).

The NTE domain is essential for HMT-1 function in cadmium resistance in *C. elegans*

The NTE domain was previously shown to play a critical role in Cd resistance of *S. cerevisiae* ABC transporter, Ycf1p [19]. Also, our studies in yeast showed the important role of the NTE in the function of HMT-1 in Cd resistance [7]. Here we tested the role of the NTE domain in HMT-1 function and localization in *C. elegans*. To do so, we generated several constructs (Figure 4 A): a construct containing HMT-1::GFP

that lacks the NTE domain (ΔNTE-HMT-1::GFP) and a construct containing only the NTE domain (NTE::GFP), both expressed under the control of the *HMT-1* promoter.

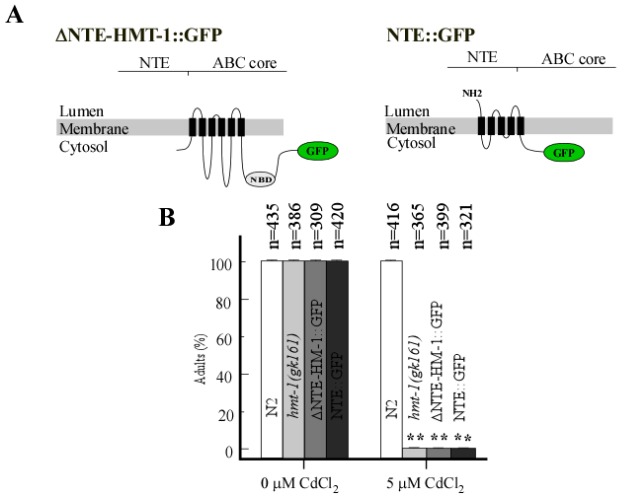

Figure 4. Cd sensitivity assay of *hmt-1(gk161)* mutant worms expressing HMT-1::GFP, ΔNTE-HMT-1::GFP, NTE::GFP. A. The predicted topology of truncated HMT-1s; ΔNTE-HMT-1::GFP, NTE::GFP**. B.** ΔNTE-HMT-1::GFP, NTE::GFP constructs do not rescue Cd sensitivity of *hmt-1(gk161)* mutant worms. In contrast, the full-length HMT-1::GFP rescues Cd sensitivity of *hmt-1(gk161*) worms at 5 μM $CdCl_2$ The total number of worms tested (n) is written above each bar. Asterisks represent statistically significant differences between the mean values of positive control, at 0 μM $CdCl_2$ and Cd treated conditions (*p<0.05, **p<0.01).

These constructs were then expressed in *hmt-1(gk161)* mutant worms (Figure 4 A). We first determined the ability of truncated HMT-1 proteins to rescue Cd sensitivity of the *hmt-1(gk161)* mutant. We found that while wild-type and *hmt-1* mutant worms expressing HMT-1::GFP were not sensitive to 5 μM $CdCl_2$ (Figure 4 B), *hmt-1(gk161)* mutant worms expressing truncated HMT-1 constructs were sensitive to 5 μM $CdCl_2$ to the same degree as the *hmt-1(gk161)* mutant worms (Figure 4 B). These results are consistent with our past studies in *S. cerevisiae*, showing that yeast heterologously expressing truncated HMT-1 proteins do not confer Cd tolerance [7] and substantiate our conclusion that the NTE domain is essential for the function of HMT-1in Cd resistance.

The NTE domain is essential but not sufficient for subcellular localization of HMT-1

Since the NTE domain was previously shown to play a critical role in membrane trafficking of ABC transporter family members such as Ycf1p and MRP1/ABCC1 in mammalian cells [19, 20], it is possible that inability of truncated HMT-1 protein to confer Cd tolerance was due to its mislocalization in the *hmt-1(gk161)* mutant worms. To test our hypothesis we compared the localization pattern of the full-length functional HMT-1::GFP with ΔNTE-HMT-1::GFP and NTE::GFP, which were individually expressed in the *hmt-1(gk161)* mutant worms. As shown in Figure 5 A, the localization pattern of ΔNTE-HMT-1::GFP was diffuse but concentrated towards the plasma membrane in intestinal cells. To ensure that diffuse distribution of fluorescence was not due to degradation of ΔNTE-HMT-1::GFP and resultant cytosolic localization of GFP, total cellular lysates from the *hmt-1* mutant expressing HMT-1::GFP, or ΔNTE-HMT-1::GFP, or NTE::GFP were fractioned into soluble and membrane protein fractions and subjected to SDS-PAGE and immunoblot analysis.

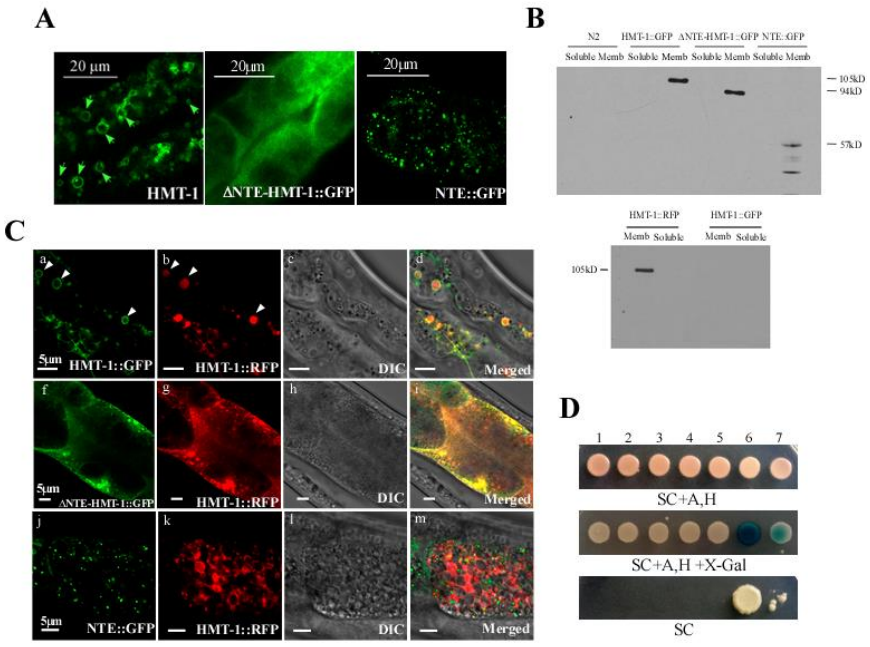

Figure 5. Localization pattern of HMT-1::GFP, ΔNTE-HMT-1::GFP and NTE::GFP in *hmt-1(gk161)* mutant worms. A. The Figure shows the GFP-mediated fluorescence in *hmt-1(gk161)* mutant worms expressing the full-length HMT-1::GFP, HMT-1 lacking the NTE domain (ΔNTE-HMT-1::GFP), and NTE fused to GFP (NTE::GFP). **B.** Western blot analysis of HMT-1::GFP, ΔNTE-HMT-1::GFP, NTE::GFP, HMT-1::RFP. **C.** Full length HMT-1::GFP co-localizes with HMT-1::RFP (a-d). The majority of HMT-1::RFP co-localized with ΔNTE-HMT-1::GFP toward plasma membrane (f-i). NTE::GFP did not co-localized with HMT-1::RFP (j-m). **D.** The yeast two hybrid assay shows that HMT-1 lacking NTE interacts

with full length HMT-1 but the interaction is weaker than interactions of full length HMT-1– HMT-1. The number above the Figures indicate the following combination of constructs 1. Ev (Empty vector)::Cub + ΔNTE-HMT-1::NubG 2. KAT-1::Cub + ΔNTE-HMT-1::NubG 3. KAT-1::Cub + NTE::NubG 4. KAT-1-Cub +HMT-1::NubG 5. HMT-1::Cub + NTE::NubG 6. HMT-1::Cub + HMT-1::NubG 7. HMT-1::Cub + ΔNTE-HMT-1::NubG.

These studies showed that all constructs were associated with the membrane fraction of proteins and thus, the ΔNTE-HMT-1::GFP construct does not degrade (Figure 5 B). In contrast to the diffuse localization of ΔNTE-HMT-1::GFP-mediated fluorescence, NTE::GFP-mediated fluorescence was associated with internally located vesicular structures. However, these structures did not resemble the localization pattern of full-length HMT-1::GFP (Figure 5 A). Furthermore, I co-expressed truncated HMT-1::GFP constructs with a marker of apical recycling endosomes, RAB-11::mCherry and found that GFP-mediated and mCherry-mediated fluorescence did not overlap (Figure 6).

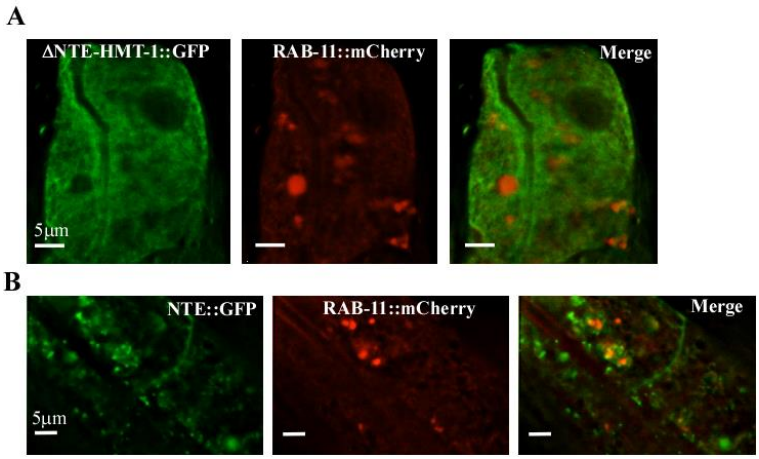

Figure 6. Neither HMT-1 lacking NTE nor NTE alone localize to apical recycling endosomes. A. A fluorescence microscopy image of *hmt-1(gk161)* mutant worms co-expressing ΔNTE-HMT-1::GFP and RAB-11::mCherry. **B.** of *hmt-1(gk161)* mutant worms co-expressing NTE::GFP and RAB-11::mCherry.

Together, these results suggested that the NTE domain is essential but not sufficient for appropriate localization of HMT-1.

ΔNTE-HMT-1 affects the localization of full-length HMT-1 and it exerts a dominant negative effect on Cd resistance of full length HMT-1

I and Dr. Anuj Sharma showed above that HMT-1 localizes to apical recycling endosomes and that the NTE domain is required for both, function and localization of HMT-1. However, although I observed different localization pattern, it was not certain whether the truncated HMT-1 proteins still reside on apical recycling endosome. Therefore, I and Dr. Anuj Sharma generated *hmt-1(gk161)* mutant worms co-expressing either HMT-1::RFP and ΔNTE-HMT-1, or HMT-1::RFP and NTE::GFP, and examined the distribution of HMT-1::RFP and the HMT-1::GFP variants in the two strains. As shown in Figure 5 C (a-d) and as shown above, HMT-1::GFP and HMT-1:: RFP co-localized in intestinal cells (white arrow heads). As expected from our analysis of NTE::GFP alone, NTE::GFP failed to co-localize with HMT-1::RFP. Although NTE seem to localize to vesicular structures, only a fraction of the GFP signal overlapped with the RFP signal. However, when ΔNTE-HMT-1::GFP was co-expressed with HMT-1::RFP, although both proteins were co-localized in the intestinal cells their localization pattern was significantly different from when they were individually expressed (Figure 5 C, f-i). This result suggests that two constructs may interact and is consistent with our finding that ΔNTE-HMT-1 weakly interacts with full length HMT-1 in the yeast two hybrid assay (Figure 5 D and [7]). If this occurs then ΔNTE-HMT-1::GFP might also affect the ability of full- length HMT-1 to confer Cd resistance. To test this hypothesis we analyzed Cd sensitivity of transgenic worms co-expressing full-length HMT-1:RFP with different truncated HMT-1::GFP variants.

Consistent with previous findings (Figure. 3 A) full-length HMT-1::GFP or HMT-1::RFP, or both constructs, rescued Cd sensitivity of the *hmt-1(gk161)* mutant at 5μM Cd, while ~ 90% and 50% of worms were able to reach the adult stage at 25 μM and 50 μM of Cd, respectively (Figure. 7).

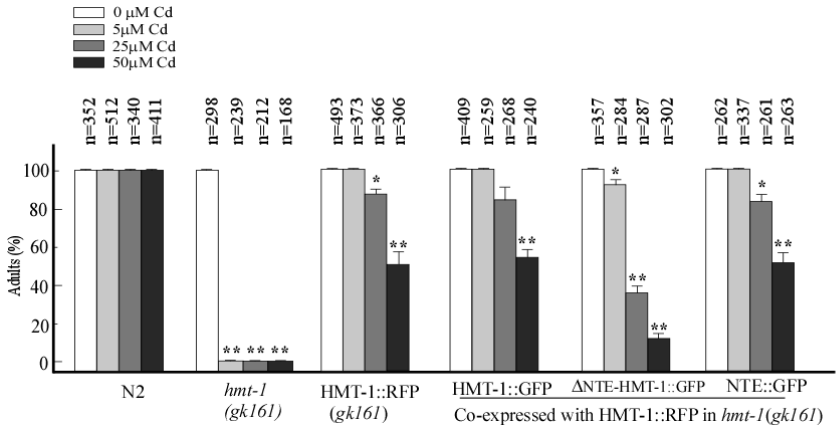

Figure 7. ΔNTE-HMT-1 showed dominant negative effect on the function of HMT-1::RFP in Cd resistance of indicated strains. Worms expressing HMT-1::RFP become highly sensitive to 25 μM $CdCl_2$ when the cnstruct is co-expressed with ΔNTE-HMT-1::GFP. This is opposite to what I observed in worms co-expressing HMT-1::RFP with HMT-1::GFP or NTE:GFP. The total number of worms tested is written (n) above each bar. The asterisks represent statistically significant differences between the mean values of positive control, at 0 μM $CdCl_2$ and Cd treated conditions (*$p \leq 0.05$, **$p \leq 0.01$).

This pattern was maintained in worms co-expressing HMT-1::RFP with NTE::GFP. In contrast, co-expression of the ΔNTE-HMT-1::GFP construct with the full-length HMT-1::RFP significantly altered the ability of the latter to confer Cd resistance in the *hmt-1(gk161)* mutant background (Figure 7). Compared to *hmt-1* mutant worms co-expressing full-length HMT-1::RFP and HMT-1::GFP or NTE::GFP, only 38±3.5%, or 8.3±1.5% of the *hmt-1* mutant co-expressing the ΔNTE-HMT-1::GFP construct with the full-length HMT-1::RFP have reached the adult stage under 25 μM and 50 μM $CdCl_2$, respectively. Therefore, I conclude that NTE plays an important but not sufficient role for HMT-1 trafficking and HMT-1 lacking NTE inhibits the appropriate localization of full length HMT-1 to apical recycling endosomes and ΔNTE-HMT-1::GFP exerts a dominant negative effect on the ability of HMT-1 to confer Cd resistance.

To confirm its dominant negative effect on HMT-1 function, I and Dr. Anuj Sharma examined if the ΔNTE-HMT-1::GFP construct still exert against native HMT-1 in wild-type. We generated transgenic worms expressing HMT-1::GFP or ΔNTE-HMT-1::GFP, or NTE::GFP in wild-type background and performed Cd sensitivity assays. Expression of the full-length HMT-1, NTE in wild-type background did not significantly alter Cd sensitivity of worms (Figure 8A).

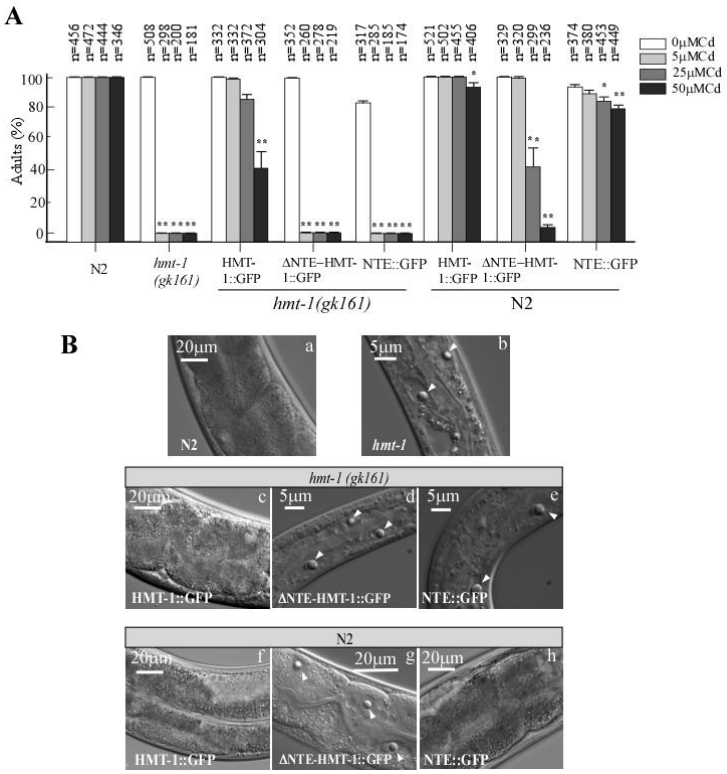

Figure 8. ΔNTE-HMT-1 exhibits a dominant negative effect on the ability of endogenous HMT-1 to detoxify Cd. A. The full-length HMT-1::GFP or ΔNTE-HMT-1::GFP, or NTE::GFP were transformed into wild-type worms and *hmt-1(gk161)* mutant worms and resulting worms were examined for Cd sensitivity. Only half of wild-type worms expressing ΔNTE-HMT-1::GFP reached the adult stage when grown at on 25 μM $CdCl_2$ in contrast to wild-type worms expressing full-length HMT-1::GFP or NTE::GFP. The total number of worms tested (n) is written above each bar. Asterisks represent statistically significant differences between the mean values of positive control, 0 μM $CdCl_2$ and Cd treated conditions (*$p \leq 0.05$, **$p \leq 0.01$). **B.** A DIC image of *hmt-1* mutant worms exhibiting refractile inclusions caused by Cd toxicity. This phenotype also appears on *hmt-1* mutant worms expressing truncated HMT-1s and wild-type worms expressing HMT-1 lacking NTE as well. The refractile inclusions are indicated with white arrows. All the worms shown in the figures are grown for 3 days on culture media containing 25μM $CdCl_2$.

However, consistently, wild-type worms expressing ΔNTE-HMT-1 exhibit highly reduced rescuing ability suggesting that HMT-1 lacking NTE domain also exhibit dominant negative effect on native HMT-1 function in Cd resistance (Figure 8 A).

Our past studies have shown that the *hmt-1(gk161)* mutant exhibits unique characteristic morphological phenotypes manifested by the formation of refractile inclusions in intestinal cells when the worms are grown with Cd [16]. This phenotype is not observed in any other Cd-sensitive mutant. Therefore,

I expected that if ΔNTE-HMT-1 exerts a dominant negative effect on HMT-1, but not another Cd detoxification protein that is not associated with the HMT-1-detoxification pathway, then wild-type worms expressing ΔNTE-HMT-1::GFP would develop refractile inclusion in intestinal cells in the presence of Cd. Consistent with our previous data, refractile inclusions appeared in intestinal cells of *hmt-1(gk161)* and *hmt1(gk161)* worms expressing truncated HMT-1 constructs but not the full-length HMT-1, all grown on Cd-containing medium (Figure 8 B b, d, e, c respectively). I found that refractile inclusions also appeared in wild-type worms expressing ΔNTE-HMT-1::GFP but not in wild-type worms expressing the full-length HMT-1 or NTE only (Figure 8 B g, f, h respectively). This result may imply that function of HMT-1 in the wild-type was inactivated due to the co-expression of ΔNTE-HMT-1 since the phenotype of refractile inclusion is highly specific to *hmt-1* mutants. Furthermore, I showed that these refractile inclusion might be associated with the nucleus since they seem to reside within the LMN-GFP marker that labels the nuclear envelop(Figure 9).

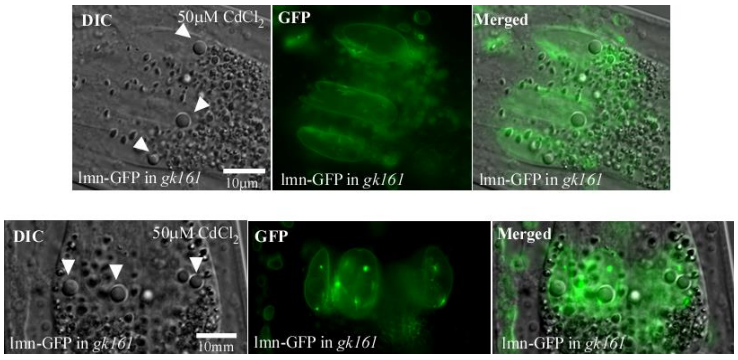

Figure 9. *hmt-1* specific morphological phenotype co-localizes with the nuclear envelope marker, LMP1-GFP. White arrow heads in the left panel indicate the refractile inclusion. Middle panel shows GFP image of nuclear lamina protein fused with GFP in *hmt-1 (gk161)* mutant worms.

Taken together, I conclude that HMT-1 function is inhibited by ΔNTE-HMT-1 and that HMT-1 lacking NTE interacts directly with HMT-1 pathway.

The C-terminus is important for HMT-1 oligomerization but not for localization

I and Dr. Anuj Sharma established that NTE of HMT-1 is critical for HMT-1 interaction,

localization and function in Cd resistance (Figure. 5, 7, 8). NTE by itself, however, is not sufficient for interaction or co-localization with full-length HMT-1 [7]. Therefore, I hypothesized that an additional protein motif(s) in the ABC core may be required for protein interaction and localization. To investigate this, I tested the function of the C-terminal end, in particular, the 43 amino acid region beyond the Walker A motif, an ATPase motif, because this part was essential for localization of HsMRP1/ABCC1 [20]. I deleted 43 amino acids from the C-terminus of HMT-1 and then generated two transgenic worm strains expressing HMT-$1^{\Delta 43}$::GFP alone and co-expressing HMT-$1^{\Delta 43}$::GFP and HMT-1::RFP in *hmt-1* mutant background (Figure 10 B). Then I tested if HMT-$1^{\Delta 43}$::GFP would co-localize with HMT-1-RFP and would rescue Cd sensitivity of *hmt-1(gk161)* mutant worms. As shown in the Figure 10 C, HMT-$1^{\Delta 43}$::GFP and HMT-1::GFP co-localized. Further, I found thatwhile *hmt-1(gk161)* mutant worms expressing HMT-$1^{\Delta 43}$::GFP by itslef were acutely sensitive to Cd, HMT-$1^{\Delta 43}$::GFP did not alter the ability of the full length HMT-1::RFP or the endogenous HMT-1 to confer Cd resistance (Figure 10 D).

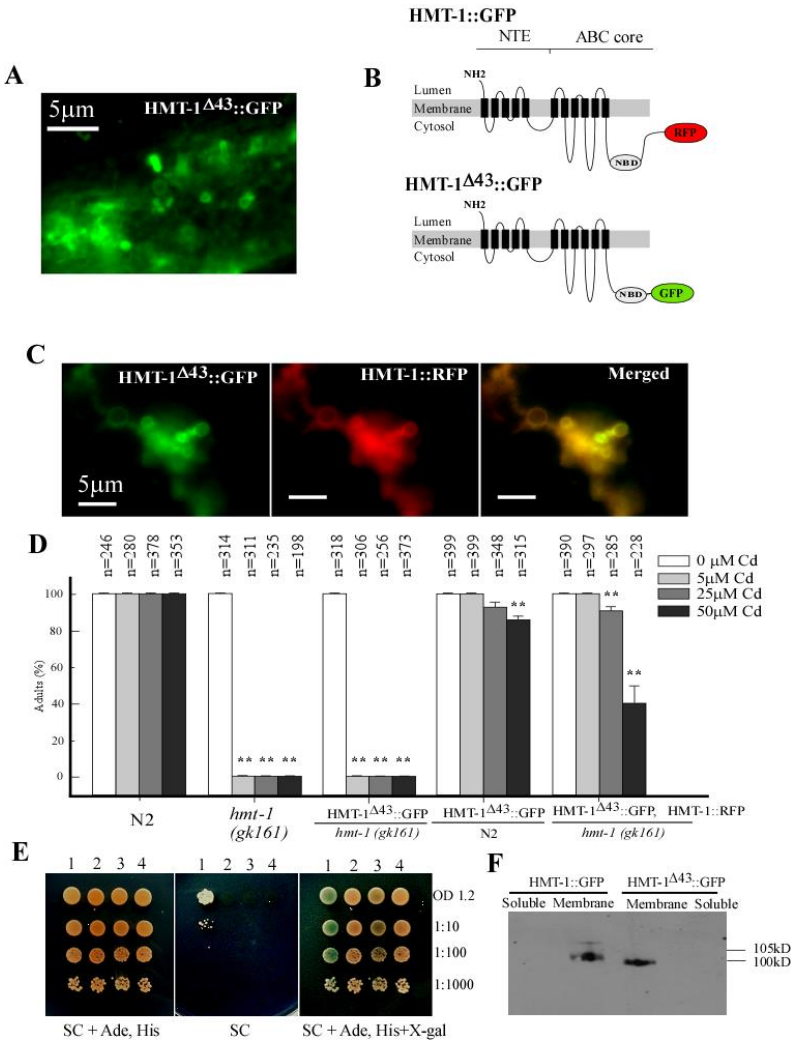

Figure 10. The C-terminus of HMT-1 contains protein motif(s) for HMT-1 interaction. A. Fluorescence microscopy image of *hmt-1(gk161)* mutant worm expressing HMT-$1^{\Delta 43}$::GFP **B.** The predicted topology of HMT-1::RFP and HMT-$1^{\Delta 43}$::GFP **C.** A fluorescence microscopy image of *hmt-1(gk161)* mutant worms co-expressing HMT-$1^{\Delta 43}$::GFP and HMT-1::RFP. **D.** The Cd sensitivity assay for wild-type, *hmt-1(gk161)*, the *hmt-1(gk161)* mutant expressing HMT-$1^{\Delta 43}$::GFP, the wild-type expressing HMT-$1^{\Delta 43}$::GFP, and the *hmt-1(gk161)* mutant co-expressing HMT-$1^{\Delta 43}$::GFP and HMT-1::RFP. HMT-$1^{\Delta 43}$::GFP could not confer Cd tolerance of *hmt-1(gk161)* worms. The total number of worms tested (n) is provided above each bar. Asterisks represent statistically significant differences between mean values of positive control, at 0 μM $CdCl_2$ and Cd treated conditions (*$p \leq 0.05$, **$p \leq 0.01$). **E.** Yeast two hybrid assay shows that HMT-$1^{\Delta 43}$ does not interact with full length HMT-1. Yeast cells co-expressing HMT-$1^{\Delta 43}$::NubG and full-length HMT-1::Cub could not grow on SC interaction selective media and turn into blue by X-gal staining meanwhile positive control, yeast cells co-expressing full-length HMT-1::NubG, full-length HMT-1::Cub grew on the selective media and turned blue. **F.** Western blot analysis of HMT-$1^{\Delta 43}$::GFP and full-length HMT-1::GFP. It showed that HMT-$1^{\Delta 43}$ expressed and reside on the membrane fraction.

These findings suggest that HMT-1$^{\Delta 43}$::GFP localized to apical recycling endosome as does native HMT-1, but unlike ΔNTE-HMT-1::GFP, does not exert a dominant negative effect on the HMT-1 pathway.

To test whether the inability of HMT-1$^{\Delta 43}$::GFP to confer Cd resistance of the *hmt-1(gk161)* mutant was due to a loss of HMT-1 homo-oligomerization, I conducted the yeast two-hybrid assay. The results revealed that HMT-1$^{\Delta 43}$ does not interact with full-length HMT-1(Figure 10 E). These results lead us to conclude that although the 43 amino acid region of HMT-1 is important for HMT-1 interaction. Taken together, I further confirm that HMT-1 homo-oligomerization is essential for HMT-1 function in Cd resistance.

Discussion

HMT-1 belongs to the ABCB6 family of ABC transporter superfamily, and is the only half ABC transporter that possess an N-terminal extension domain (NTE). Because numerous ABC transporters comprising only the "ABC core" (two TMDsand two NBDs) are fully capable of essential transporter functions such as trafficking, substrate transport, and ATP hydrolysis [17], the function of NTE is not well established. One exception is the ABCC subfamily. Structure–function analyses of MRP (**m**ulti drug **r**esistance **p**rotein), a full ABC transporter from the ABCC subfamily possessing the NTE domain, have shown that the NTE domain plays a key role in MRP localization and that lack of the NTE reduced the protein's substrate transport ability [19, 20, 27]. Also, ABC transporter protein family has been associated with variety of functions that mainly depend on their localization to specific biological membranes. There have been conflicts regarding the localization and function of ABCB6 protein in mammals claiming it to be mitochondrial or lysosomal membrane resident and functioning in either porphyrin metabolism or transition metal homeostasis [6, 28-30]. Therefore, in this study, I and Dr. Anuj Sharma examined the localization of HMT-1 in worms and the function of NTE in HMT-1 trafficking and Cd resistance. We found that HMT-1 mainly localizes to apical recycling endosome and partially to early and late endosomes

and that NTE is involved in HMT-1 localization and function in Cd resistance, while the C-terminus is involved in HMT-1-HMT-1 interactions.

Also, we established that NTE is necessary but not sufficient for localization to apical recycling endosomes suggesting a requirement of another region of HMT-1 for appropriate localization to apical recycling endosomes.

Unexpectedly, HMT-1 does not localize to the lysosome. Previous work in yeast has shown that HMT-1 of *S. pombe* as well as another ABC transporter, YCF-1 of *S. cerevisiae* and *Drosophila* HMT-1 all of which confer Cd tolerance localize to vacuole in yeast where Cd or Cd-protein complexes are sequestered [9, 13, 15]. Our result raises the possibility that in *C. elegans* Cd or Cd-associated complexes are transported into apical recycling endosomes by HMT-1. However, considering some exceptions such as the *Sp*HMT-1 homolog of algae, *Cr*CDS1 in *Chlamydomonas reinhardtii* confers heavy metal tolerance yet localizes to the mitochondria [31] and Human MRP1 and MRP2 that detoxify As yet localize to plasma membrane [11], it is also possible that apical recycling endosomes are an important reservoir for *C. elegans* HMT-1 and may also serve as sites for Cd detoxification

In addition to HMT-1, several mutated forms of half ABC transporters were discovered to be dominant negative. Co-expression of truncated human ABCG2, another half ABC transporter showed a dominant negative effect on the function of wild-type ABCG2 in drug efflux [32, 33]. This implies that, mutated form of interacting counterparts inhibits function of the protein complex.

I found that NTE is important but not sufficient for HMT-1 localization and HMT-1 homo-oligomerization. This result raised our curiosity that there reside other protein motifs for either localization or interaction in the ABC core of HMT-1 leading us to test the C-terminal 43 amino acids of HMT-1. I found that HMT-1$^{\Delta 43}$ co- localize with full length HMT1-1 However, interestingly, HMT-1$^{\Delta 43}$ could not interact with full length HMT-1. This result may explain our data that *hmt-1* mutant worms expressing HMT-1$^{\Delta 43}$ are hypersensitive to Cd, since failure to oligomerize would render HMT-1 non-functional[7]. Therefore, we conclude that HMT-1 possess HMT-1-HMT-1 interaction motifs within the NTE as well as

the 43 amino acids from the end of the C-terminal region and that both NTE and C-terminal end must be present to allow oligomer formation.

To conclude, I substantiated my past findings that HMT-1 forms at a minimum a homo-dimer. Further, I showed that HMT-1 resides at the apical recycling endosome and that the NTE domain is essential for HMT-1 trafficking. I also found that the NTE and C-terminus serve redundant functions in the ability of HMT-1 to interact with itself.

Methods and Materials

C. elegans strains and growth culture condition.

C. elegans were maintained at 20ºC on solid NGM (Nematode Growth Medium) 60mm x15mm plates supplemented with OP50 *E. coli* bacteria. *C. elegans* strains used in this study are listed in Table 1.

Table 1. List of worm strains used in this study

Strains	Relevant genotype	Source/ Reference
N2	Wild-type	[23]
VF3	*hmt-1(gk161)III*	[23]
VF12	*hmt-1(gk161)III;gfIs1[phmt-1-hmt-1::GFP, unc-119(+)]*	[7, 23]
VF13	*hmt-1(gk161), unc-119(ed3); gfIs1[hmt-1p-HMT-1::GFP, UNC119], pwIs428[vha-6-RFP-rab-11, Cbunc-119(+)]*	In this study
VF23	*hmt-1(gk161)III; gfIs2[hmt-1p-no-NTE-HMT-1::GFP]*	In this study
VF24	*hmt-1(gk161)III; gfEx4[hmt-1p-NTE::GFP]*	In this study
VF 25	*hmt-1(gk161)III; gfIs2[hmt-1p-no-NTE-HMT-1::GFP], pwIs428[vha-6-RFP-rab-11, Cbunc-119(+)]*	In this study

VF 26	*hmt-1(gk161)III; gfEx4[hmt-1p-NTE::GFP],pwIs428[vha-6-RFP-rab-11, Cbunc-119(+)]*	In this study
VF31	*N2; gfIs1[hmt-1p-HMT-1::GFP, UNC119]*	In this study
VF32	*N2; gfEx4[hmt-1p-NTE::GFP]*	In this study
VF33	*N2; gfIs2[hmt-1p-no-NTE-HMT-1::GFP]*	In this study
VF37	*hmt-1(gk161)III; gfEx5[hmt-1p-hmt-1::RFP]*	In this study
VF38	*hmt-1(gk161)III; gfIs1[hmt-1p-HMT-1::GFP, UNC119];gfEx5[hmt-1p-hmt-1::RFP]*	In this study
VF39	*hmt-1(gk161)III; gfIs2[hmt-1p-no-NTE-HMT-1::GFP];gfEx5[hmt-1p-hmt-1::RFP]*	In this study
VF40	*hmt-1(gk161)III; gfEx4[hmt-1p-NTE::GFP]; gfEx5[hmt-1p-hmt-1::RFP]*	In this study
VF46	*hmt-1(gk161)III; gfEx6[hmt-1p-Δ758-801-hmt-1::GFP]*	In this study
VF48	*hmt-1(gk161)III; gfEx6[hmt-1p-Δ758-801-hmt-1::GFP]; hmt-1(gk161)III; gfEx5[hmt-1p-hmt-1::RFP]*	In this study
VF50	*N2; gfEx6[hmt-1p-Δ758-801-hmt-1::GFP]*	In this study
VF 57	*hmt-1(gk161)III ;[lmn-1p::lmn-1::GFP::lmn-1 3'utr + pMH86; dpy-20(+)]*	In this study

Plasmid construction

The translational reporter proteins, truncated HMT-1::GFP variants and HMT-1::RFP were created by PCR-amplification from the *C. elegans* genomic using primers attached with Gateway attB linkers listed in Table 1. The length of PCR products for HMT-1, ΔNTE-HMT-1, NTE, HMT-1Δ[43] are 8240, 4774, 3616, 7380 bp respectively. The *att*B sites are displayed in lower case. All PCR reactions used in this study were performed using the Phusion High Fidelity DNA polymerase kit (New England Biolabs, Beverly, MA). Each DNA sequence was confirmed by sequencing analysis (Core sequencing facility in Cornell

University). The entry clone for Gateway cloning is created by insertion of a PCR product of the *att*B flanked genomic *hmt-1* into the pDOR222 vector by the BP reaction. The gateway final destination vector pPD117.01-RfA (reading frame cassette A) was generated according to Gateway® Vector Conversion System (Invitrogen) instructions. Briefly, insertion of 1.7 kb of gateway Cassette A was performed into multi cloning sites digested with Age I before the 5' GFP sequence of *C. elegans* expression vector pPD117.01 used in our previous study [23]. The pPD117.01 plasmid contains 2.1 kbp of *hmt-1* promoter. The final *C. elegans* expression vector with ORF was then generated by the LR reaction between the entry clone and the destination vector. After each BP and LR reaction the plasmid construct was sequenced to avoid the codon frame shift. The destination vector pPD117.01-RfA-RFP was generated by deletion of GFP from the pPD117.01 plasmid using AgeI and NheI restriction enzymes. The RFP DNA fragment was PCR-amplified and inserted to replace GFP in the pPD117.01 vector. The primer sequences for RFP cDNA amplification are listed in Table 2.

Table 2. Primer list used in this study

Variants	Primer sequence
HMT-1	FW: **5'-** aca agt ttg tac aaa aaa gca ggc tct cca acc acc ATG GGC TTT TCA CCA TTT CTC GA **-3'**
	RV: **5'-** tcc gcc acc acc aac cac ttt gta caa gaa agc tgg gta CGG AAG CTC CTC GCC GAG TTC AA - **3'**
ΔNTE-HMT-1	FW: **5'-** aca agt ttg tac aaa aaa gca ggc tct cca acc acc ATG CAA CTT CGC GTC GTT TTT TG -**3'**
	RV: **5'-** tcc gcc acc acc aac cac ttt gta caa gaa agc tgg gta CGG AAG CTC CTC GCC GAG TTC AA - 3'
NTE	FW: **5'-** aca agt ttg tac aaa aaa gca ggc tct cca acc acc ATG GGC TTT TCA CCA TTT CTC GA - **3'**
	RV: **5'-** tcc gcc acc acc aac cac ttt gta caa gaa agc tgg gta GAGGGAAATTGATTTTGTCG **-3'**
HMT-1$^{\Delta 43}$	FW: **5'-** aca agt ttg tac aaa aaa gca ggc tct cca acc acc ATG GGC TTT TCA CCA TTT CTC GA **-3'**
	RV: 5'- tcc gcc acc acc aac cac ttt gta caa gaa agc tgg gta ATC AAG AAC AAG AAT AAG GTC -3'

RFP	FW: 5’- CCG ACCGGT ATGGCCTCCTCCGAGGACGT-3’
	RV: 5’- GTAGCTAGC TTAGGCGCCGGTGGAGTGGC-3’
gk161 allele genotype	FW: 5’- AAATGGCGTAATCAACCGAG- 3’
	RV: 5’-TGAGCGGTGTGTAGAGTTGG-3’

The LR reaction between entry clone, pDONR222-*hmt-1* and pPD117.01-RfA-RFP was conducted to generate HMT-1::RFP expression vector.

Generation of transgenic worms

The transgenic worm strains expressing ΔNTE-HMT-1::GFP, NTE, HMT-1$^{\Delta 43}$::GFP were designated VF23,VF24, VF46, respectively. Strains were generated by injecting 100 ng/µl of pPD117.01 carrying the corresponding constructs into the gonadal syncytium of adult hermaphrodites of *hmt-1*(*gk161)* mutant worms, while vector pPD117.01-*phmt-1;*HMT-1::RFP was injected to create VF37 worms expressing HMT-1::RFP under control of *HMT-1* promoter. Wild-type worms expressing HMT-1::GFP, ΔNTE-HMT-1::GFP, NTE, HMT-1$^{\Delta 43}$-GFP,which correspond to strain VF31, VF33, VF32, VF 48 were produced by crossing males of VF12, VF23, VF24, VF46 to hermaphrodites of wild-type. The VF50 was generated by crossing VF46 with N2. VF57 was generated by crossing wild-type worms expressing LMN-1::GFP with VF3 (the *hmt-1(gk161)*). The resulting progeny was then screened on Cd containing plates to obtain *gk161* allele background genotype. Crosses were done 6 times and the genotype was confirmed by worm PCR. Briefly, 20 worms were incubated with PCR lysis buffer (60g/ml proteinase K, 10mM Tris-Cl, pH 8.2, 50mM KCl, 2.5mM MgCl2, 0.45% Tween-20, 0.05% gelatin) in PCR tubes then frozen at -80 for 10 min. to release DNA by freeze-cracking of worms. A drop of mineral oil was placed on the top of the buffer and heated for 1 hour at 65º C followed by 95º C for 15mins. Then worms and DNA mixture were used as a temple for worm PCR. The primers used to determine the genotype of wild-type versus *gk161* allele are listed in the Table 2. The resulting transgenic worms were screened by GFP or RFP mediated

fluorescence using Leica MZ16FA automated fluorescence stereozoom microscope with Leica EL6000 metal halide illuminator. The injected plasmids were integrated into genome to maintain stable inheritable expression by γ-irradiation described in our previous study [23].

Cadmium sensitivity assays

Cd sensitivity assays were performed based on the procedures described in our previous study [23]. Briefly, 2 adult hermaphrodites were placed on solid NGM plates supplemented with indicated concentrations of $CdCl_2$ andseeded with OP50 *E. coli* bacteria. Th Worms were allowed to lay eggs for 4 to 5 hours. After 4 to 5 hours, adult worms were removed to remain only several dozens of eggs. The hatched worms were grown until the progeny of the worms in positive control conditions reached the adult stage, which takes approximately 3 to 4 days. Then we counted and analyzed the percentage of reaching adult stage of the progeny and morphological phenotype caused by Cd toxicity. The graph of Cd sensitivity represents the result of the mean values of three independent experiments each of which had three replicates. The total number of worms tested (n) is presented above each graph bar. T-test: two samples assuming unequal variance was utilized to manifest the statistical significance of our data.

Imaging for subcellular localization of HMT-1 constructs

Worms were immobilized in a drop of 20 mM NaN_3 and mounted on the 2% agarose glass pad. Confocal microscopy Zeiss 63x (1.40 oil, DIC) lens and Zeiss Axio Imager M2 microscope were used to image GFP or RFP fluorescence in worms. Images were captures with AxioCam MR Camera and the Zeiss AxioVision 4.8 software. FITC and Texas Red filter sets were utilized to image GFP and RFP mediated fluorescence respectively. The signal of HMT-1::GFP was collected at 517 nm which exclude contributions of autofluorescence and 2-channel fast line-by-line multitracking technique was utilized to remove autofluorescent signal.

Preparation of microsomal and soluble proteins from *C. elegans*

Worms expressing translational *phmt-1-hmt-1::GFP* variants and *phmt-1-hmt-1::RFP* were synchronized at the adult stage for protein extraction. To synchronize worms I grew, 100 adult worms on ten 100 mm x15 mm NGM plates (10 worms/ plate) seeded with sufficient OP50 *E. coli* until their progeny reach to fully gravid worms. The resulting progeny worms are collected and bleached with synchronization solution containing 0.2 N NaOH, 20% bleach (5% solution of sodium hypochlorite, Chlorox) to prepare large quantities of eggs. Eggs were hatched and synchronised at the n early larva stage 1(L1) in M9 buffer overnight. Aproximately 10,000 L1s were placed on 150 mm x 10 mm NGM plates seeded with plenty of OP50, grown to the adult stage and about 1 ml of pellet of resulting worms were collected in M9 buffer. I washed the collected worms in M9 buffer 3 times, after each wash step worms were incubated in M9 buffer for 10 min. to release the bacteria from worms gut. Then M9 buffer was replaced with worm lysis buffer containing 50 mM TRIS-HCl, pH 7.6, 150mM $NaCl_2$, 1mM EGTA, 2 mM DTT, 2 mM 2-mercaptoethanol, 1 mM phenylmethylsulfonyl fluoride (PMSF), and 1 mg/ml each of leupeptin, aprotinin, and pepstatin. Worms in lysis buffer were broken by sonication at 4ºC until all the fractures of worm body were disappeared. After sonication, total worm crude extract was collected by removal of cell debris by centrifugation at 3500 x g for 10 min. The crude extract was then fractionized into microsomal and soluble protein by ultra centrifugation at 100,000 x g for 40 mins using Beckman bench-top ultra centrifuge. The supernatant, soluble protein was kept into microtubes followed by plunge into liquid N2 and kept in -80ºC. The microsomal vesicle pellets containing membrane proteins were resuspended with the same lysis buffer and frozen with liquid N2, stored in -80C. The protein concentration was measured by Bradford assay (Bio-rad). Subcellular fractionation of microsomal membrane protein was performed by sucrose density gradient. 16%, 22%, 28%, 34%, 40% of sucrose solutions prepared in the same lysis buffer were made separately. The different concentrations of sucrose solution were loaded very carefully not to disrupt the density layer into the microcentrifuge tube sequentially from the higher concentration. About 500 µg of total microsomal membrane protein were then loaded onto the top layer and subjected to ultracentrifugation

for 2.5 hours at 100,000 x *g* using Beckman SW41Ti rotor. Each protein sections between layers were then collected with micropipettor and wash 3 times with lysis buffer to remove remaining sucrose. The resulting fractionized proteins were frozen with liquid N_2, stored in -80ºC.

Immunoblot assay

SDS-PAGE and immunoblot assays were done based on the procedures described in our previous study [7]. Briefly, for each HMT-1 constructs, 5 µg of protein were resolved by 7% SDS-PAGE gel and wet-electrotransferred to 0.2 µm nitrocellulose membrane for 18 h at 4ºC at a constant current of 60 mA in Towbin buffer containing 0.05% SDS. 1:1000 dilution of monoclonal anti-GFP (Covance), anti-RME-1, anti-LMP-1, polyclonal anti-RFP (Pierce) were used as a primary antibody. 1:10,000 dilution of HRP-linked anti-mouse for anti-GFP, anti-RME-1, anti-LMP-1 and anti-Rabbit (GE healthcare) for anti-RFP were used as secondary antibody. The immunoreactive protein bands were visualized with Chemiluminescent Substrate (KPL).

Yeast two hybrid assay

Yeast two hybrid assay to detect HMT-1 interactions in this study were prepared as described previously [7]. Briefly, *hmt-1* lacking 132 bp at three prime end, which designated as HMT-$1^{\Delta 43}$, was obtained by PCR amplification from wild-type cDNA using attB linker flanked primers as listed in the Table 1. . For NubG constructs, pXNgate21-3HA vector was linearized with EcoRI/SmaI digestion while pMetYCgate vector was cleaved with PstI/HindIII. The linearized pXNgate21-3HA, pMetYCgate vectors and the *hmt-1* PCR products were co-transformed into THY. AP4 (MATa leu2-3,112 ura3-52 trp1-289 lexA::HIS3lexA::ADE2 lexA::lacZ), THY. AP5 (MATa URA3 leu2-3,112 trp1-289 his3-D1 ade2D::loxP) yeast strains respectively by lithium acetate yeast transformation method to produce NubG prey and CubPLV bait clones. Transformed THY. AP4 yeast cells expressing CubPLV bait were selected on SC for leucine prototrophy, while THY.AP5 expressing NubG prey were selected for tryptophan prototrophy.

Mating was performed between both yeast strains expressing CubPLV bait or NubG to create diploid yeast cells co-expressing CubPLV bait and NubG prey, which were screened on the SC plates containing adenine and histidine but without leucine and tryptophan. Interaction between bait and prey constructs were detected by growing on selectable SC medium lacking adenine, histidine, leucine, tryptophan. In addition, β-galactosidase assay was conducted to further confirm the interaction.

This is a manuscript in preparation.

*Sungjin Kim[a,b] , *Anuj K Sharma[a], Olena K Vatamaniuk[a]

[a]Department of Crop and Soil Sciences, Cornell University, Ithaca, New York 14853

[b]Graduate Field of Environmental Toxicology, Cornell University, Ithaca, New York 14853

* These authors contributed equally to this work

REFERENCES

1. Waalkes, M.P., *Cadmium carcinogenesis.* Mutat Res, 2003. **533**(1-2): p. 107-20.
2. Waalkes, M.P., T.P. Coogan, and R.A. Barter, *Toxicological principles of metal carcinogenesis with special emphasis on cadmium.* Crit Rev Toxicol, 1992. **22**(3-4): p. 175-201.
3. Baron, S., J. Carignan, and A. Ploquin, *Dispersion of heavy metals (metalloids) in soils from 800-year-old pollution (Mont-Lozere, France).* Environ Sci Technol, 2006. **40**(17): p. 5319-26.
4. Cooksey, C., *Health concerns of heavy metals and metalloids.* Sci Prog, 2012. **95**(Pt 1): p. 73-88.
5. Broeks, A., et al., *Homologues of the human multidrug resistance genes MRP and MDR contribute to heavy metal resistance in the soil nematode Caenorhabditis elegans.* EMBO J, 1996. **15**(22): p. 6132-43.
6. Jalil, Y.A., et al., *Vesicular localization of the rat ATP-binding cassette half-transporter rAbcb6.* Am J Physiol Cell Physiol, 2008. **294**(2): p. C579-90.
7. Kim, S., D.S. Selote, and O.K. Vatamaniuk, *The N-terminal extension domain of the C. elegans half-molecule ABC transporter, HMT-1, is required for protein-protein interactions and function.* PLoS One, 2010. **5**(9): p. e12938.
8. Ortiz, D.F., et al., *Heavy metal tolerance in the fission yeast requires an ATP-binding cassette-type vacuolar membrane transporter.* EMBO J, 1992. **11**(10): p. 3491-9.
9. Sooksa-Nguan, T., et al., *Drosophila ABC transporter, DmHMT-1, confers tolerance to cadmium. DmHMT-1 and its yeast homolog, SpHMT-1, are not essential for vacuolar phytochelatin sequestration.* J Biol Chem, 2009. **284**(1): p. 354-62.
10. Preveral, S., et al., *A common highly conserved cadmium detoxification mechanism from bacteria to humans: heavy metal tolerance conferred by the ATP-binding cassette (ABC) transporter SpHMT1 requires glutathione but not metal-chelating phytochelatin peptides.* J Biol Chem, 2009. **284**(8): p. 4936-43.
11. Leslie, E.M., A. Haimeur, and M.P. Waalkes, *Arsenic transport by the human multidrug resistance protein 1 (MRP1/ABCC1). Evidence that a tri-glutathione conjugate is required.* J Biol Chem, 2004. **279**(31): p. 32700-8.
12. Li, Z.S., et al., *The yeast cadmium factor protein (YCF1) is a vacuolar glutathione S-conjugate pump.* J Biol Chem, 1996. **271**(11): p. 6509-17.
13. Li, Z.S., et al., *A new pathway for vacuolar cadmium sequestration in Saccharomyces cerevisiae: YCF1-catalyzed transport of bis(glutathionato)cadmium.* Proc Natl Acad Sci U S A, 1997. **94**(1): p. 42-7.
14. Paumi, C.M., et al., *ABC transporters in Saccharomyces cerevisiae and their interactors: new technology advances the biology of the ABCC (MRP) subfamily.* Microbiol Mol Biol Rev, 2009. **73**(4): p. 577-93.
15. Ortiz, D.F., et al., *Transport of metal-binding peptides by HMT1, a fission yeast ABC-type vacuolar membrane protein.* J Biol Chem, 1995. **270**(9): p. 4721-8.
16. Vatamaniuk, O.K., et al., *CeHMT-1, a putative phytochelatin transporter, is required for cadmium tolerance in Caenorhabditis elegans.* J Biol Chem, 2005. **280**(25): p. 23684-90.
17. Rees, D.C., E. Johnson, and O. Lewinson, *ABC transporters: the power to change.* Nat Rev Mol Cell Biol, 2009. **10**(3): p. 218-27.

18. Smith, P.C., et al., *ATP binding to the motor domain from an ABC transporter drives formation of a nucleotide sandwich dimer.* Mol Cell, 2002. **10**(1): p. 139-49.
19. Mason, D.L. and S. Michaelis, *Requirement of the N-terminal extension for vacuolar trafficking and transport activity of yeast Ycf1p, an ATP-binding cassette transporter.* Mol Biol Cell, 2002. **13**(12): p. 4443-55.
20. Westlake, C.J., S.P. Cole, and R.G. Deeley, *Role of the NH2-terminal membrane spanning domain of multidrug resistance protein 1/ABCC1 in protein processing and trafficking.* Mol Biol Cell, 2005. **16**(5): p. 2483-92.
21. Jalil, Y.A., Ritz, V., Jakimenko, A., Schmitz-Salue, C., Siebert, H., Awuah, D., Kotthaus, A., Kietzmann, T., Ziemann, C., Hirsch-Ernst, K. I., *Vesicular localization of the rat ATP-binding cassette half-transporter rAbcb6.* Am J Physiol Cell Physiol, 2008. **294**(2): p. C579-90.
22. Mitsuhashi, N., Miki, T., Senbongi, H., Yokoi, N., Yano, H., Miyazaki, M., Nakajima, N., Iwanaga, T., Yokoyama, Y., Shibata, T., Seino, S., *MTABC3, a Novel Mitochondrial ATP-binding Cassette Protein Involved in Iron Homeostasis.* J. Biol. Chem., 2000. **275**(23): p. 17536-17540.
23. Schwartz, M.S., et al., *Detoxification of multiple heavy metals by a half-molecule ABC transporter, HMT-1, and coelomocytes of Caenorhabditis elegans.* PLoS One, 2010. **5**(3): p. e9564.
24. Schroeder, L.K., et al., *Function of the Caenorhabditis elegans ABC transporter PGP-2 in the biogenesis of a lysosome-related fat storage organelle.* Mol Biol Cell, 2007. **18**(3): p. 995-1008.
25. Campbell, R.E., et al., *A monomeric red fluorescent protein.* Proc Natl Acad Sci U S A, 2002. **99**(12): p. 7877-82.
26. Shaner, N.C., et al., *Improved monomeric red, orange and yellow fluorescent proteins derived from Discosoma sp. red fluorescent protein.* Nat Biotechnol, 2004. **22**(12): p. 1567-72.
27. Yang, Y., et al., *Regulation of function by dimerization through the amino-terminal membrane-spanning domain of human ABCC1/MRP1.* J Biol Chem, 2007. **282**(12): p. 8821-30.
28. Kiss, K., et al., *Shifting the paradigm: the putative mitochondrial protein ABCB6 resides in the lysosomes of cells and in the plasma membrane of erythrocytes.* PLoS One, 2012. **7**(5): p. e37378.
29. Paterson, J.K., et al., *Human ABCB6 localizes to both the outer mitochondrial membrane and the plasma membrane.* Biochemistry, 2007. **46**(33): p. 9443-52.
30. Tsuchida, M., et al., *Human ABC transporter isoform B6 (ABCB6) localizes primarily in the Golgi apparatus.* Biochem Biophys Res Commun, 2008. **369**(2): p. 369-75.
31. Hanikenne, M., et al., *A comparative inventory of metal transporters in the green alga Chlamydomonas reinhardtii and the red alga Cyanidioschizon merolae.* Plant Physiol, 2005. **137**(2): p. 428-46.
32. Xu, J., et al., *Characterization of oligomeric human half-ABC transporter ATP-binding cassette G2.* J Biol Chem, 2004. **279**(19): p. 19781-9.
33. Xu, J., et al., *Oligomerization domain of the multidrug resistance-associated transporter ABCG2 and its dominant inhibitory activity.* Cancer Res, 2007. **67**(9): p. 4373-81.

CHAPTER5

FUTURE WORK

Achieving an integrated understanding of how organisms detoxify noxious heavy metals for developing remedies against metal-caused diseases, require the identification of detoxification pathways and analyses of their components. In this regard, HMT-1, a half-molecule ATP-binding cassette (ABC transporter) in the nematode *Caenorhabditis elegans* is prominently required for heavy metal detoxification and has homologs in diverse organisms including humans[1-5]. The research described in this dissertation focuses on the function of HMT-1 in Cd detoxification and the effect of Cd on the ionome/metalome in *C. elegans*. Given the facts that CeHMT-1- defective worms are acutely sensitive to even micromolar concentrations of Cd; that CeHMT-1 has homologs in higher organisms including humans; and that CeHMT-1 renders a much higher Cd-tolerance than other ABC transporters including PGP-1, PGP-3 PGP-5 and MRP-1 in *C. elegans* [6, 7], it is critical to understand how HMT-1 operates. In this thesis I showed that HMT-1 interacts with itself to detoxify Cd. It is possible, however, that HMT-1 also interacts with other ABC transporters and/or other cellular proteins, forming a hetero-oligomer. It was established that yeast protein YCF-1, an ortholog of mammalian MRP-1, physically interacts with CKA1 kinase and small GTPase Tus1 protein, both regulating the function of YCF-1[8]. Furthermore, analyses of the Cd-transcriptome identified Cd effect on the expression of genes from the putative metal-responsive and stress-response pathways including Jun N-terminal kinase (JNK)/mitogen-activated protein kinase (MAPK), p38, and extracellular signal-regulated kinase (ERK) pathways [9, 10]. Considering that function of YCF-1 is regulated by phosphorylation, HMT-1 may be also regulated by phosphorylation by these or similar kinases. This suggests that Cd detoxification pathways are regulated at multiple levels, raising the possibility that HMT-1 mediated heavy metal detoxification mechanism may be controlled by these signal transduction pathways.

I also found that Cd exposure disrupts the *tbc-2*-dependent endocytic pathway which affect the Cd tolerance of *C. elegans*. This result confirms the earlier finding that environmental toxicant can inhibit the secretory pathway resulting in abnormal maturation of endosomes [11]. Therefore, future studies will involve: 1) screens for putative interactors of HMT-1 and its physiological substrate; 2) analyses of factors that regulate HMT-1 transport activity (e.g. phosphorylation); 3) screens for key proteins involved in the endocytic pathway, which are affected by Cd toxicity.

Another set of studies in this thesis was dedicated to the analyses of the effect of Cd on the metallome/ionome of *C. elegans.* Using inductively coupled plasma mass spectrometry (ICP-MS) and synchrotron based X-ray fluorescence microscopy (SXFM), I showed that Cd decreases internal concentrations of several essential trace elements, while it increases the accumulation of toxic elements. Also, I showed that Cd accumulates mainly throughout the intestine and Cd induces Fe re-distribution:from being diffuse in intestinal cells of worms grown under control conditions, Fe moves to discrete spots near the center of intestinal cells after Cd exposure. However, we do not know whether this ionome signature of Cd toxicity is a mechanism of Cd detoxification or a consequence of Cd toxicity in the animal. Furthermore, we don't know the identity of the punctate structures of intestinal cell containing Cd and Fe. Moreover, the study of the function of HMT-1 in Cd distribution and the distribution of other biologically-relevant elements is also very intriguing. In this consideration, subsequent studies will include building anatomical maps of elemental distribution in wild-type and *hmt-1* mutant worms grown with or without Cd for SXFM studies. Since the disadvantage of cyro-fixation used in this study for SXFM analysis is that fluorescent marker proteins (e.g. GFP) expressed in worms lose the ability to emit fluorescence, we cannot use various subcellular fluorescent markers to identify the area where Cd and Fe accumulate in Cd-treated worms. However, among great advantages of the XFM technology is that it allows using fully hydrated samples and thus conserves cellular structures intact. Therefore, the next step in these investigation will include using hydrated samples together with fluorescent vital dyes or transgenic animals expressing fluorescent makers with hydrated samples. This would mean that we can identify the area where Cd and Fe are

accumulated more accurately. Therefore, future studies will involve: 1) performing SXFM with *hmt-1* mutant worms to investigate whether the ionome signature I found in this study is a defensive system against Cd toxicity, 2) generating different transgenic worms expressing various subcellular maker, and 3) setting up a novel procedure for scanning hydrated *C. elegans* samples.

REFERENCES

1. Vatamaniuk, O.K., et al., *CeHMT-1, a putative phytochelatin transporter, is required for cadmium tolerance in Caenorhabditis elegans.* J Biol Chem, 2005. **280**(25): p. 23684-90.
2. Schwartz, M.S., et al., *Detoxification of multiple heavy metals by a half-molecule ABC transporter, HMT-1, and coelomocytes of Caenorhabditis elegans.* PLoS One, 2010. **5**(3): p. e9564.
3. Kim, S., D.S. Selote, and O.K. Vatamaniuk, *The N-terminal extension domain of the C. elegans half-molecule ABC transporter, HMT-1, is required for protein-protein interactions and function.* PLoS One, 2010. **5**(9): p. e12938.
4. Sooksa-Nguan, T., et al., *Drosophila ABC transporter, DmHMT-1, confers tolerance to cadmium. DmHMT-1 and its yeast homolog, SpHMT-1, are not essential for vacuolar phytochelatin sequestration.* J Biol Chem, 2009. **284**(1): p. 354-62.
5. Preveral, S., et al., *A common highly conserved cadmium detoxification mechanism from bacteria to humans: heavy metal tolerance conferred by the ATP-binding cassette (ABC) transporter SpHMT1 requires glutathione but not metal-chelating phytochelatin peptides.* J Biol Chem, 2009. **284**(8): p. 4936-43.
6. Broeks, A., et al., *Homologues of the human multidrug resistance genes MRP and MDR contribute to heavy metal resistance in the soil nematode Caenorhabditis elegans.* EMBO J, 1996. **15**(22): p. 6132-43.
7. Kurz, C.L., et al., *Caenorhabditis elegans pgp-5 is involved in resistance to bacterial infection and heavy metal and its regulation requires TIR-1 and a p38 map kinase cascade.* Biochem Biophys Res Commun, 2007. **363**(2): p. 438-43.
8. Paumi, C.M., et al., *ABC transporters in Saccharomyces cerevisiae and their interactors: new technology advances the biology of the ABCC (MRP) subfamily.* Microbiol Mol Biol Rev, 2009. **73**(4): p. 577-93.
9. Hsiao, C.J. and S.R. Stapleton, *Early sensing and gene expression profiling under a low dose of cadmium exposure.* Biochimie, 2009. **91**(3): p. 329-43.
10. Song, M.O., J. Li, and J.H. Freedman, *Physiological and toxicological transcriptome changes in HepG2 cells exposed to copper.* Physiol Genomics, 2009. **38**(3): p. 386-401.
11. Matsuo, S., et al., *Influence of fluoride on secretory pathway of the secretory ameloblast in rat incisor tooth germs exposed to sodium fluoride.* Arch Toxicol, 1996. **70**(7): p. 420-9.

APPENDIX

THE EFFECT OF CADMIUM ON THE TBC2-DEPENDENT ENDOSOMAL TRAFFICKING PATHWAY.

Introduction

Localization of ABC transporters to the endocytic compartments highlights their role as cellular scavengers**.** Secretory pathways that lead to the formation of various endocytic compartments include budding and fusion of small transport vesicles, fusion and fission of large organelles, and maturation processes that change organelle identity over time. One of the pathways to form the various endosomes is initiated at the plasma membrane while the other one is initiated at the endoplasmic reticulum and proceeds via Golgi. Both pathways lead to the formation of early endosomes that can be then differentiated into recycling endosomes or multivesicular bodies/late endosomes eventually differentiated into lysosomes [1]. Many aspects of these processes are regulated by small GTPases belonging to the Rab family [1, 2] and Rab-GAPs, which are Rab GTPase activating proteins that control the activity of Rabs by inverting active form of Rab-GTP to Rab-GDP [3]. It has been shown that disruption of RAB-GAP-5 in *C. elegans* has led to abnormal maturation of early endosome [4] and *TBC-2,* Rab-5 GAP knockout worms contain enlarged vesicles that contain markers for early endosome(RAB-5), late endosomes (RAB-7) and lysosomes (LMP-1) suggesting a block occurring at the early to late endosome-lysosome transition [5]. Furthermore, environmental toxicant, fluoride, disrupts the secretory pathway of ameloblast cells resulting in disorder of Golgi stacks and accumulation of small vesicles on the secretory route between rER and Golgi, formation of abnormal large granules [6]. However, whether heavy metals affect membrane trafficking is unknown.
I also found that Cd prevents endocytic trafficking by blocking the progression of the pathway beyond the late endosomes. This conclusion was made by finding that Cd phenocopies the RAB-7-dependent *tbc-2* (-) large late endosome phenotype in the intestinal cells. Further, I showed that disruption of the TBC-2 pathway increases Cd sensitivity of worms. Together, this work furthers our understanding of the role of

the functional domains of HMT-1/ABCB6 in its subcellular localization and ability to confer Cd tolerance, and uncovers the novel aspect of Cd toxicity through its effect on the TBC2-dependent endosomal trafficking.

Results

Higher concentration or longer exposure to Cd promotes the formation of the enlarged HMT-1::GFP-positive vesicles.

I next wanted to test whether Cd would alter the HMT-1::GFP localization pattern. I grew wild-type worms expressing HMT-1::GFP in the media supplemented with 25μM or 75μM $CdCl_2$ for 5 days and analyzed the subcellular localization of HMT-1 after third and fifth day of growth with Cd. The result is that while HMT-1 localizes to apical recycling endosome when the worms were grown in the media supplemented with 25μM Cd for 3days, HMT-1 was localized to enlarged vesicles when expose at higher dose or exposed for a longer period to Cd; 75μM Cd for 3, 5 days or 25μM Cd for 5 days respectively (Figure 1 d, e, f).

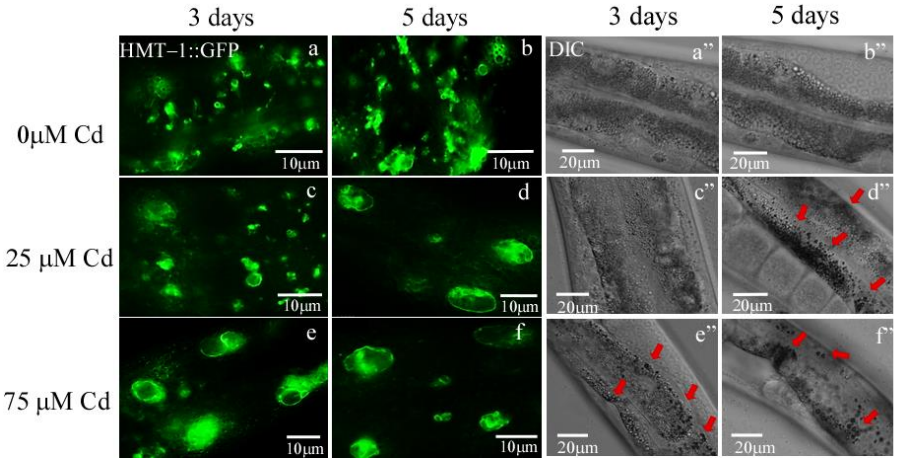

Figure 1. Higher or longer exposure of Cd induce the formation of HMT-1-loclaized, enlarged vesicle. a-f. Image of GFP fluorescence signals of the wild-type animals expressing HMT-1::GFP grown for either 3 days or 5 days on the NGM media supplemented with 0 μM $CdCl_2$, 25 μM $CdCl_2$, 75 μM $CdCl_2$ respectively. Higher or longer exposure of Cd induce the formation of HMT-1- localized, enlarged vesicle. **a"-f".** DIC image of corresponding animals of **a-f**.

These enlarged HMT-1::GFP-positive compartments also appeared when worms were grown with 300 μM $CuCl_2$, but not with 2 mM $NaAsO_2$, both of which are highly toxic to worms [7] (Figure 2).

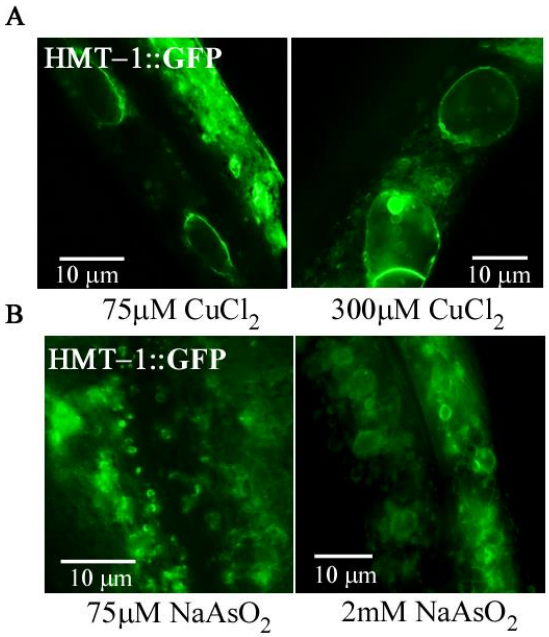

Figure 2. Cu also induce the formation of HMT-1-loclaized, enlarged vesicle but not As. Image of GFP fluorescence signals of the wild-type animals expressing HMT-1::GFP grown for either 5 days on the NGM media supplemented with **A**. 75 μM, 300 μM $CuCl_2$ and **B**. 75 μM, 2mM $NaAsO_2$.

Furthermore, the worms exhibiting enlarged HMT-1-localized vesicles were severely impaired by Cd toxicity. The tissues of these worms seemed to have been damaged forming dark and black punctas by Cd (Figure 1 d", e", f") but no, or less pronounced symptoms of the toxic effect of Cd were discovered in the worms treated with 25μM Cd for 3 days (Figure 2 c"). This suggests that too much exposure of Cd is beyond resistance capacity of worms. Also, I showed that this enlarged compartment contains LMP-1-GFP, which is a marker for lysosomes (Figure 3).

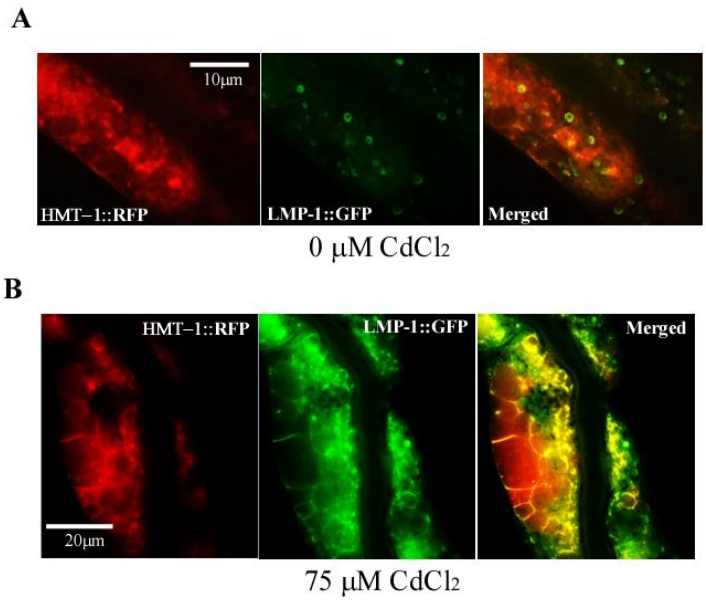

Figure 3. The Cd- induced enlarged vesicles where HMT-1 localized is lysosome or lysosome positive. **A.** Image of GFP and RFP fluorescence signals of the wild-type animals co-expressing HMT-1::RFP and LMP::GFP without Cd. The lysosomal marker is not co-localized with HMT-1::RFP without Cd. **B.** Image of GFP and RFP fluorescence signals of the wild-type animals co-expressing HMT-1::RFP and LMP::GFP with 75 μM $CdCl_2$. The lysosomal marker is co-localized with HMT-1::RFP at 75 μM $CdCl_2$.

HMT-1 and LMP-1 were co-localized when the worms co-expressing HMT-1::RFP and LMP-1::GFP were grown on 75μM Cd for 5 days (Figure 4 B) but this co-localization did not occurred when worms were grown without Cd (Figure 4 A).

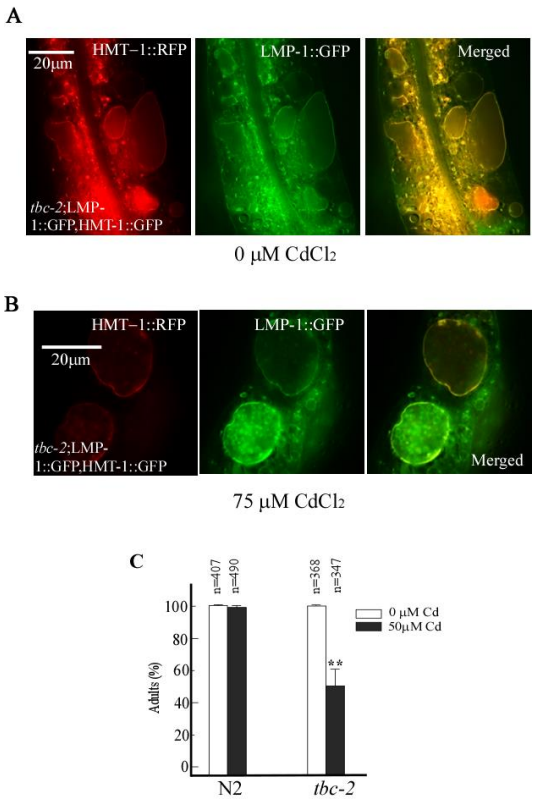

Figure 4. The membrane trafficking of HMT-1 is *tbc-2* dependent. A. Image of GFP and RFP fluorescence signals of the *tbc-2* mutant animals co-expressing HMT-1::RFP and LMP::GFP without Cd. **B.** Image of GFP and RFP fluorescence signals of the *tbc-2* mutant animals co-expressing HMT-1::RFP and LMP::GFP with 75 μM $CdCl_2$ **C.** Cd sensitivity assay of indicated strains with 50 μM $CdCl_2$ without Cd.

This result could be interpreted by at least two scenarios: First, too much Cd exposure may inhibit the proteins that are critical for the secretory pathway regulating maturation of endosomal compartments. Thus, HMT-1 may be trapped in certain endocytic vesicles resulted from the disrupted secretory pathway. Second, HMT-1 is destined to be degraded when it exceeds its resistance capacity in higher concentration of Cd thus delivered to lysosomes to be degraded.

Cd blocks the *tbc-2* dependent endosomal maturation

It has been shown that environmental toxicant, fluoride, disrupts the secretory pathway of ameloblast cells, leading to disorder of Golgi stacks and accumulation of small vesicles on the secretory

route between rER and Golgi, formation of abnormal large granules [6]. This result is consistent with our hypothesis that Cd promotes the formation of abnormal enlarged vesicles by inactivating directly or indirectly the endosome maturation pathway. To test our hypothesis I aimed to test the relationship of Cd toxicity with *tbc-2*, Rab GTPase activating protein. TBC-2 is a conserved putative Rab GTPase-activating protein (GAP), playing a role as a regulator of endosome to lysosome maturation in several tissues. It catalyzes the hydrolysis of GTP to GDP on Rab-7 GTPase, which renders it inactive. In *tbc-2* mutant *C. elegans*, it has been shown that early and late endosomes are disrupted, which results in the formation of LMP-1, RAB-7 positive-large vesicles in intestinal cells due to the hyperactivity of RAB-7 [5]. These enlarged vesicle resemble HMT-1::GFP-positive vesicles formed in Cd-treated worms.

I first tested Cd sensitivity of *tbc-2* mutant animals. The result is that although the sensitivity is not as outstanding as in *hmt-1* mutant animals, *tbc-2* mutants were more sensitive to Cd than the wild-type (Figure 4 C). Importantly, I found that HMT-1::RFP was localized to the periphery of large vesicles that were formed in the *tbc*-2 mutant and this occurred even without Cd (Figure 4 A). Furthermore, HMT-1::RFP co-localized with LMP-1::GFP, both associated at the periphery of enlarged vesicles formed in the intestinal cells of the *tbc-2* mutant even without Cd. I also found that Cd did not alter formation of these vesicles (Figure 4 B). Given that formation of these enlarged vesicles in the *tbc-2* mutant is RAB-7 dependent [5], to test whether formation of similar structures in Cd-treated worms is within the same TBC-2-dependent pathway, I performed *rab-7* RNAi assay in wild-type worms expressing HMT-1::RFP. I predicted that if the enlarged-HMT-1 positive vesicles are induced by the disruption of *tbc-2* dependent endocytic pathway, the enlarged vesicles would be diminished by *rab-7* RNAi.

In addition, I performed RNAi assay against *lgg-1*, an ortholog of mammalian autophagy gene MAP-LC3 [8] to test whether the enlarged vesicles is related to autophagy because it contains small sub-vesicles inside (Figure 6 A) as found in autophagosomes [5, 9]. First, I confirmed that the enlarged vesicles occurred in *tbc-2* mutant were removed by *rab-7* RNAi (Figure 5 B) as was shown previously [5].

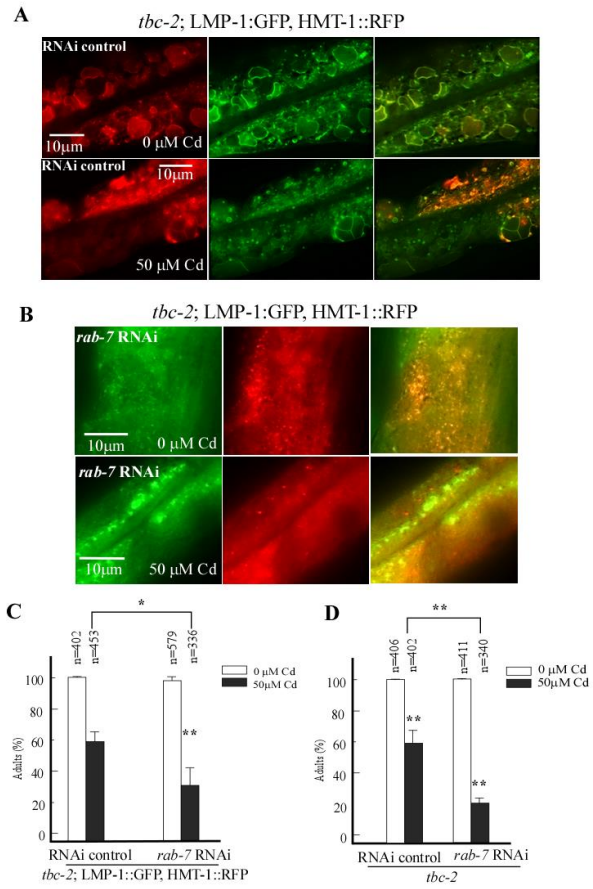

Figure 5. The phenotype of *tbc-2* mutant animals co-expressing HMT-1::RFP and LMP-1::GFP was suppressed by *rab-7* RNAi. A. Image of GFP and RFP *tbc-2* mutant animals co-expressing HMT-1::RFP and LMP-1::GFP was grown for 4 days on the NGM media seeded with HT115 bacteria containing L4440 as a control without Cd (upper panels) and with 50 μM $CdCl_2$ (lower panels). **B.** *tbc-2* mutant animals co-expressing HMT-1::RFP and LMP-1::GFP were grown for 4 days on the NGM media seeded with HT115 bacteria containing L4440-*rab-7* without Cd (upper panels) and with 50 μM $CdCl_2$ (lower panels).

The result is that as shown in the Figure 6 A, without Cd, HMT-1::GFP expressed in the wild-type worms in three different RNAi conditions (control RNAi, *rab-7* RNAi, *lgg-1* RNAi) normally localize to apical recycling endosome which size is less than 5 μm diameter.

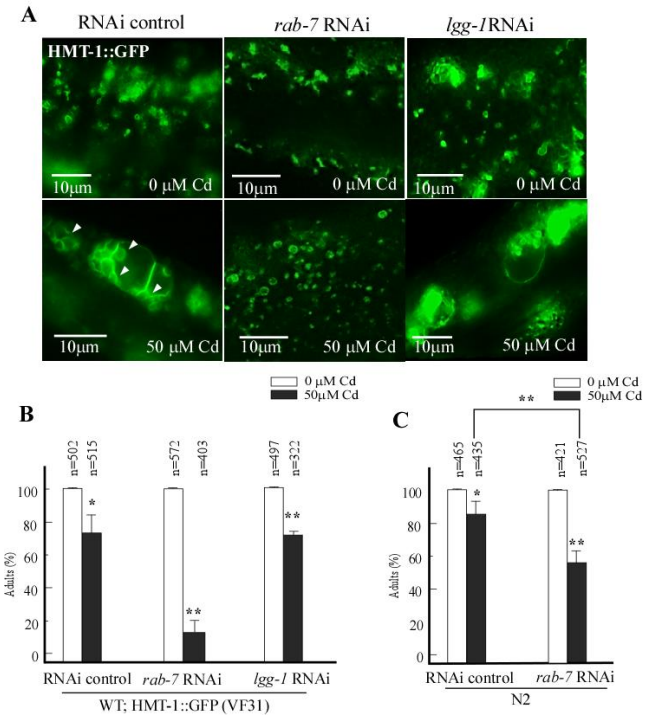

Figure 6. ***rab-7* RNAi suppresses HMT-1-positive, enlarged vesicles. A.** The left two panels shows a GFP fluorescence signal image of wild-type animals expressing HMT-1::GFP grown on the NGM media seeded with HT115 bacteria containing L4440-empty vector as a control with 50 μM $CdCl_2$ and without Cd. The middle two panels show a GFP fluorescence signal image of wild-type animals expressing HMT-1::GFP grown on the NGM media seeded with HT115 bacteria containing HT115-*rab-7* with 50 μM $CdCl_2$ and without Cd. The right two panels shows show a GFP fluorescence signal image of wild-type animals expressing HMT-1::GFP grown on the NGM media seeded with HT115 bacteria containing HT115-*lgg-1* with 50 μM $CdCl_2$ and without Cd. **B.** The wild-type animals expressing HMT-1::GFP treated with control RNAi ,*rab-7* RNAi and *lgg-1* RNAi were tested for Cd sensitivity at 0 μM $CdCl_2$ and 50 μM $CdCl_2$. The total number of worms tested is written (n) above each bar. The asterisks represent statistically significant differences between the mean values of positive control, at 0 μM CdCl2 and Cd treated conditions (*p<0.05, **p<0.01). **C.** The wild-type animals expressing HMT-1::GFP treated with control RNAi ,*rab-7* RNAi.

However, while HMT-1::GFP-positive vesicles were enlarged in the control RNAi and *lgg-1* RNAi which size is about 5μm- 20 μm at 50 μM $CdCl_2$ exposure, HMT-1-positive enlarged vesicles were suppressed by *rab-7* RNAi and its size is less than 2 μm. Furthermore, interestingly worms in which enlarged vesicles were suppressed showed increased Cd-sensitivity by *rab-7* RNAi (Figure 5 C, D and Figure 6 B, C). In the *tbc-2* mutant and *tbc-2* mutant worms co-expressing HMT-1::RFP and LMP-1::GFP both of which were treated with control RNAi, 58.86 ± 8.43 and 57.32 ± 6.72 percent of the worms reached the adult stage at 50 μM $CdCl_2$, respectively. However, only 19.39 ± 2.7 and 33.95 ± 10.53 percent of *tbc-2* mutant and *tbc-*

2 mutant co-expressing HMT-1::RFP and LMP-1::GFP reached to the adult stage when both of which were treated with *rab-7* RNAi at 50 μM $CdCl_2$ respectively (Figure 5 C, D). Consistently, compared to RNAi control and *lgg-1* RNAi, only about 20 % of *rab-7* RNAi -treated wild-type worms expressing HMT-1::GFP could reach to the adult stage at 50 μM $CdCl_2$. (Figure 6 C) Consistently *rab-7* RNAi treated wild-type animals showed increased Cd sensitivity (Figure 6 D) This result suggests that worms necessarily possess enlarged, HMT-1-positive vesicle to confer a resistance against higher exposure of Cd. That is, the HMT-1-localized vesicles may become enlarged to satisfy the large capacity to rescue animals from fatal concentration of Cd suggesting that rab-7 dependent endosomal maturation may serve as a way to resist Cd toxicity.

Taken together, I concluded that: 1) Cd blocks the *tbc-2* dependent endocytic pathway; 2) *tbc-2* plays a role in Cd-resistance; 3) the formation of enlarged, HMT-1-positive vesicles plays a role in Cd resistance.

Discussion

I have shown that higher dose of Cd results in formation of enlarged, HMT-1 positive vesicles in *C. elegans*. Also, these animals showing enlarged, HMT-1- localized vesicle have impaired cell tissues when they were treated either with higher dose or longer time with Cd. This result demonstrates that either the enlargement of HMT-1-localized vesicles is needed to maximize their capacity to rescue high dose of Cd, or that vesicles are forms as a consequence of inability of worms to resist fatal amounts of Cd. To find out this, I performed the RNAi assay and found that enlargement of HMT-1 localized vesicles is *rab-7* dependent. Also, the animals with suppressed enlarged vesicles showed increased Cd sensitivity. This may be the answer for our prior hypothesis that enlargement of HMT-1-localised vesicles is important for Cd resistance. Taken together, Cd may negatively regulate the *tbc-2* so that *rab-7* is constitutively active to induce the formation of HMT-1-localized enlarged vesicle thus the study that demonstrates the involvement of Cd on the function of *tbc-2* or its equivalent proteins need to be conducted in the future.

Methods and Materials

C. elegans strains and growth culture condition.

C. elegans were maintained at 20ºC on solid NGM (Nematode Growth medium) 60 mm x15mm plates supplemented with OP50 *E. coli* bacteria. *C. elegans* strains used in this study are listed in Table 1.

Table 1: List of worm strains used in this study

Strains	Relevant genotype	Source/ Reference
N2	Wild-type	[7]
VF37	*hmt-1(gk161)III; gfEx5[hmt-1p-hmt-1::RFP]*	In this study
VF 59	*tbc-2(tm2241); pwIs50[lmp-1::GFP + Cb-unc-119]; gfEx5[hmt-1p-hmt-1::RFP]*	In this study
VF 60	*N2; pwIs50[lmp-1::GFP + Cb-unc-119]; gfEx5[hmt-1p-hmt-1::RFP]*	In this study
tm2241	*tbc-2*	[5]

Generation of transgenic worms

VF 59, VF 60 was generated by crossing VF 37 with *tbc-2* mutant, wild-type worm expressing lmp-GFP, respectively. Crosses were done 6 times. The resulting transgenic worms were screened by GFP or RFP mediated fluorescence using Leica MZ16FA automated fluorescence stereozoom microscope with Leica EL6000 metal halide illuminator.

Cadmium sensitivity assay

Cd sensitivity assays were performed based on the procedures described in our previous study [7]. Briefly, 2 adult hermaphrodites were placed on solid NGM plates supplemented with indicated concentrations of $CdCl_2$ andseeded with OP50 *E. coli* bacteria. Th Worms were allowed to lay eggs for 4 to 5 hours. After 4 to 5 hours, adult worms were removed to remain only several dozens of eggs. The

hatched worms were grown until the progeny of the worms in positive control conditions reached the adult stage, which takes approximately 3 to 4 days. Then we counted and analyzed the percentage of reaching adult stage of the progeny and morphological phenotype caused by Cd toxicity. The graph of Cd sensitivity represents the result of the mean values of three independent experiments each of which had three replicates. The total number of worms tested (n) is presented above each graph bar. T-test: two samples assuming unequal variance was utilized to manifest the statistical significance of our data.

Worm subcellular imaging

Worms were immobilized in a drop of 20 mM NaN_3 and mounted on the 2% agarose glass pad. Confocal microscopy Zeiss 63x (1.40 oil, DIC) lens and Zeiss Axio Imager M2 microscope were used to image GFP or RFP-mediated fluorescence in worms. Images were captured with the AxioCam MR Camera and processed using the Zeiss AxioVision 4.8 software. FITC and Texas Red filter sets were utilized to image GFP and RFP mediated fluorescence, respectively.

RNAi assay

For RNAi analysis, bacterial feeding method was used [10]. 300 bp of *rab-7* cDNA from the C-terminus and 300 bp of *lgg-1* cDNA from the N-terminus was amplified with the primers (*rab-7* forward primer; ACTTACCCGGGGCTAGCCCCCGCGATCCAGACC, *rab-7* reverse primer ATTAACTCGAGTTAACAATTGCATCCCGAATTC, *lgg-1* forward primer ACTTACCCGGGATGAAGTGGGCTTACAAGGA, *lgg-1* reverse primer ATTAACTCGAGCTCGTGATGGTCCTGGTAGA) and cloned into Timmons and Fire feeding vector (L4440), with a T7 promoter on each side of the MCS inducing transcription of each DNA strand. The resulting cloned DNA was then transformed into HT115 (DE3), an RNase III-deficient *E. coli* strain with IPTG-inducible T7 polymerase activity. Then the induction of dsRNA in transformed HT115 was performed. Briefly, transformed cells was inoculated in 2-5 mL LB + antibiotics (12.5 µg/mL tetracycline

+ 75 µg/mL ampicillin), shake overnight at 37°C. Then next day the fully grown culture was diluted into 1:100 ratio with LB media with 12.5 µg/mL tetracycline + 75 µg/mL ampicillin until the culture grown to OD595 = 0.4. Induction was performed by adding sterile IPTG to 0.4 mM and grown for additional 4 hours. The resulting induced HT115 was then seeded onto the NGM plates supplemented with 12.5 µg/mL tetracycline + 75 µg/mL ampicillin and various concentration of Cd. For RNAi driven-Cd sensitivity assay, L4 animals were grown on the RNAi NGM plates until they lay enough eggs then the adult worms were removed. The hatched worms were grown until the progeny of the worms in positive control plates reach to an adult stage, which takes approximately 3 to 4 days. Then I counted and analyzed the percentage of progeny reaching the adult stage using the stereomicroscope and analyzed the morphological phenotypes caused by RNAi using the DIC microscopy.

REFERENCES

1. Sato, K., et al., *C. elegans as a model for membrane traffic.* WormBook, 2014: p. 1-47.
2. Chavrier, P. and B. Goud, *The role of ARF and Rab GTPases in membrane transport.* Curr Opin Cell Biol, 1999. **11**(4): p. 466-75.
3. Pfeffer, S., *Filling the Rab GAP.* Nat Cell Biol, 2005. **7**(9): p. 856-7.
4. Haas, A.K., et al., *A GTPase-activating protein controls Rab5 function in endocytic trafficking.* Nat Cell Biol, 2005. **7**(9): p. 887-93.
5. Chotard, L., et al., *TBC-2 regulates RAB-5/RAB-7-mediated endosomal trafficking in Caenorhabditis elegans.* Mol Biol Cell, 2010. **21**(13): p. 2285-96.
6. Matsuo, S., et al., *Influence of fluoride on secretory pathway of the secretory ameloblast in rat incisor tooth germs exposed to sodium fluoride.* Arch Toxicol, 1996. **70**(7): p. 420-9.
7. Schwartz, M.S., et al., *Detoxification of multiple heavy metals by a half-molecule ABC transporter, HMT-1, and coelomocytes of Caenorhabditis elegans.* PLoS One, 2010. **5**(3): p. e9564.
8. Melendez, A., et al., *Autophagy genes are essential for dauer development and life-span extension in C. elegans.* Science, 2003. **301**(5638): p. 1387-91.
9. Alberti, A., et al., *The autophagosomal protein LGG-2 acts synergistically with LGG-1 in dauer formation and longevity in C. elegans.* Autophagy, 2010. **6**(5): p. 622-33.
10. Kamath, R.S. and J. Ahringer, *Genome-wide RNAi screening in Caenorhabditis elegans.* Methods, 2003. **30**(4): p. 313-21.